

SOME ASPECTS OF MOLYBDENUM HALIDE CHEMISTRY

A thesis presented for the degree of
Doctor of Philosophy in Chemistry
in the University of Canterbury,
Christchurch, New Zealand.

by

G.J. GAINSFORD

1969

THESIS

200
181
.M7
G143

ABSTRACT

Chemical and X-ray crystallographic studies of molybdenum(II) halides, which are based on the well-known $(\text{Mo}_6\text{Cl}_8)^{4+}$ cluster, have been carried out.

Contrary to previous reports, the reactions of 2,2'-bipyridyl with the halides $(\text{Mo}_6\text{Cl}_8)\text{Cl}_4$ and $(\text{Mo}_6\text{Cl}_8)\text{I}_4$ yield, even under mild conditions, bipyridylium salts of chloromolybdic(II) and iodomolybdic(II) acids respectively: $(\text{BipyH})_2((\text{Mo}_6\text{Cl}_8)\text{X}_6)$ where $\text{X} = \text{Cl}, \text{I}$ and $\text{Bipy} = 2,2'$ -bipyridyl. The reactions are complicated by the formation of mixtures of products, which are mainly various crystalline forms of the bipyridylium salts. An amorphous product may be a true mono-bipyridyl complex.

An unusual oxidation occurs during the reactions of triphenylphosphine (Ph_3P) and triphenylarsine (Ph_3As) with $(\text{Mo}_6\text{Cl}_8)\text{Cl}_4$ and $(\text{Mo}_6\text{Cl}_8)\text{I}_4$. Infra-red spectral and X-ray powder photographic studies show that the oxidized ligand complexes, $(\text{Mo}_6\text{Cl}_8)\text{X}_4(\text{Ph}_3\text{ZO})_2$ ($\text{X} = \text{Cl}, \text{I}$; $\text{Z} = \text{As}, \text{P}$), are formed except under conditions in which both molecular and chemically-bound oxygen is rigorously excluded.

The conditions required to coordinate more than

two neutral unidentate ligands to the $(\text{Mo}_6\text{Cl}_8)^{4+}$ cluster have been examined. It proved possible to obtain new ionic complexes under a range of conditions. The six-fold coordination of the $(\text{Mo}_6\text{Cl}_8)^{4+}$ cluster is maintained in these compounds (e.g. $(\text{Mo}_6\text{Cl}_8)\text{I}_3(\text{triphenylphosphine oxide})_2(\text{pyridine})^+\text{I}^-$) by the ionization of one or more of the terminal halogen atoms in the molybdenum(II) halide starting material (e.g. $(\text{Mo}_6\text{Cl}_8)\text{I}_4$).

The X-ray single crystal structures of two isomorphous salts, $(\text{BipyH})_2((\text{Mo}_6\text{Cl}_8)\text{X}_6)$ ($X = \text{Cl}, \text{I}$), have been solved using the difference Patterson method. To solve another crystalline modification of the chloro-salt, the (Mo_6Cl_8) cluster was constrained to its established geometry with its centroid fixed at the origin of the unit cell. This rigid group of atoms was then rotated by the least-squares refinement of the three orientation-defining angles.

The three structures contain discrete $((\text{Mo}_6\text{Cl}_8)\text{X}_6)^{2-}$ ($X = \text{Cl}, \text{I}$) and $(\text{C}_{10}\text{H}_9\text{N}_2)^+$ (bipyridylium) ions. The anions consist of highly-symmetric (Mo_6Cl_8) clusters ($\text{Mo-Mo} = 2.606$, $\text{Mo-Cl} = 2.48 \text{ \AA}$), with six terminal halogen atoms (X) bound by single covalent bonds to the molybdenum atoms ($\text{Mo-Cl} = 2.423$, $\text{Mo-I} = 2.737 \text{ \AA}$). The bipyridylium cations are twisted from perfect cis

conformations in all three structures. The average dihedral angle between the two rings is 13 degrees. Further details of the geometries of the anion and cation are discussed.

The ionic packing in the three crystals is dominated by the bulky anions. These are arranged in expanded "hexagonal close-packed" layers with the cations centred on approximately trigonal holes in this array. The two crystalline modifications of the chloro-salt differ in the orientation of the bipyridylium cations in these layers.

ACKNOWLEDGEMENTS

The author wishes to express his deep appreciation to Professors B.R. Penfold and C.J. Wilkins, and Drs J.E. Fergusson and W.T. Robinson for their advice and help during the course of this research.

The author thankfully acknowledges the award of a Postgraduate Scholarship by British Petroleum (New Zealand) Limited and a Research Fund Fellowship by the New Zealand Universities' Grants Committee.

Finally, the author gratefully thanks his parents, Mr & Mrs A.J. Gainsford, for their support over the years.

CONTENTS

	<u>Page</u>
CHAPTER 1	
<u>A INTRODUCTION SURVEY</u>	
1. Historical Review	1
2. The Structure of the $(\text{Mo}_6\text{Cl}_8)^{4+}$ Cluster	2
3. The Chemical Nature of the $(\text{Mo}_6\text{Cl}_8)^{4+}$ Cluster	5
4. Magnetic Studies	8
5. Other $(\text{Mo}_6\text{X}_8)^{4+}$ Analogues	8
6. Bonding Theories	9
<u>B SCOPE OF THIS THESIS</u>	
7. Introduction	13
8. The Reactions of 2,2'-Bipyridyl with $(\text{Mo}_6\text{Cl}_8)\text{Cl}_4$	14
9. Triphenylphosphine and Triphenylphosphine oxide	15
10. Some Problems with $(\text{Mo}_6\text{Cl}_8)\text{Cl}_4$	17
11. Presentation	17
12. Abbreviations	19
13. Other Work	20
CHAPTER 2	
<u>THE REACTIONS OF 2,2'-BIPYRIDYL WITH THE $(\text{Mo}_6\text{Cl}_8)^{4+}$ CLUSTER SYSTEM</u>	
1. Introduction	21
2. Identification of Products	22
3. The Association of Water with Molybdenum(II) Halides	27
4. The Reactions of 2,2'-Bipyridyl with $(\text{Mo}_6\text{Cl}_8)\text{Cl}_4$ and $(\text{Mo}_6\text{Cl}_8)\text{I}_4$	30
5. Discussion	33
6. Experimental	36

	<u>Page</u>
CHAPTER 3	
<u>REACTIONS OF $(\text{Mo}_6\text{Cl}_8)\text{Cl}_4$ AND $(\text{Mo}_6\text{Cl}_8)\text{I}_4$</u>	
<u>WITH UNIDENTATE LIGANDS</u>	
A LIGAND OXIDATION	
1. Introduction	39
2. Results and Discussion	40
B OTHER MONODENTATE COMPLEXES OF $(\text{Mo}_6\text{Cl}_8)\text{Cl}_4$	
AND $(\text{Mo}_6\text{Cl}_8)\text{I}_4$	
3. Introduction	48
4. The Preparation of Ionic Complexes	48
5. Experimental Details	52
CHAPTER 4	
<u>THE SINGLE CRYSTAL X-RAY STRUCTURAL ANALYSES</u>	
<u>OF TWO ISOMORPHOUS BIPYRIDYLIUM SALTS</u>	
1. Experimental Details:	
$(\text{C}_{10}\text{H}_9\text{N}_2)_2((\text{Mo}_6\text{Cl}_8)\text{Cl}_6)$	55
2. Experimental Details:	
$(\text{C}_{10}\text{H}_9\text{N}_2)_2((\text{Mo}_6\text{Cl}_8)\text{I}_6)$	59
3. Solution and Refinement of the Structures	62
CHAPTER 5	
<u>THE X-RAY CRYSTAL STRUCTURE ANALYSIS OF A</u>	
<u>SECOND CRYSTALLINE MODIFICATION OF</u>	
<u>$(\text{C}_{10}\text{H}_9\text{N}_2)_2((\text{Mo}_6\text{Cl}_8)\text{Cl}_6)$</u>	
1. Experimental Data	71
2. Solution and Refinement	73
CHAPTER 6	
<u>DESCRIPTION AND DISCUSSION OF THE THREE</u>	
<u>STRUCTURES $(\text{BipyridylH})_2((\text{Mo}_6\text{Cl}_8)\text{X}_6)$, X = Cl, I</u>	
1. Nomenclature	78
2. The $((\text{Mo}_6\text{Cl}_8)\text{X}_6)^{2-}$ Anion	78
3. The Bipyridylum Cation	80
4. Packing of the Ions	81

	<u>Page</u>	
APPENDIX A	<u>LABORATORY PROCEDURES</u>	
1.	Standard Preparative Methods	84
2.	Analytical Procedures	85
3.	Purification of Solvents and Ligands	86
4.	Physical measurements	88
APPENDIX B	<u>THE UNIVERSITY OF CANTERBURY COMPUTING SYSTEM FOR X-RAY CRYSTAL STRUCTURE ANALYSIS</u>	
1.	Introduction	92
2.	The Computing System	92
3.	Programs Written by the Author	94
4.	Acknowledgements	95
APPENDIX C	<u>THE UNIVERSITY OF CANTERBURY SUPPER EQUI-INCLINATION DIFFRACTOMETER</u>	
1.	Introduction	96
2.	Scanning Geometry	96
3.	The Automation	97
4.	The "Dead" Time	97
5.	Operating Procedure	98
6.	Some Advantages	99
7.	Acknowledgements	100
APPENDIX D	<u>TABLES FROM CHAPTERS 4, 5 AND 6</u>	101
<u>REFERENCES</u>		122

FIGURES

		<u>Facing Page</u>
I	The $((\text{Mo}_6\text{Cl}_8)_X)_6^{2-}$ anion showing the Cl_8 cube	2
II	Bonding in the $((\text{Mo}_6\text{Cl}_8)_X)_6^{2-}$ anion	2
III	Mo_6 octahedra from $(\text{Mo}_6\text{Cl}_8)\text{Cl}_4$	4
IV	The Infra-red spectra of $(\text{Mo}_6\text{Cl}_8)_X(\text{Ph}_3\text{PO})_2$, Ph_3PO and Ph_3P	41
V	The Infra-red spectra of $(\text{Mo}_6\text{Cl}_8)_X(\text{Ph}_3\text{AsO})_2$, Ph_3AsO and Ph_3As	43
VI	Atom labels in the Bipyridylum cation	79
VII	Projection showing ions centred on the (101) plane for the Cl(A) and I structures	81
VIII	Projection showing ions centred on the (101) plane for the Cl(B) structure	82

CHAPTER 1

GENERAL INTRODUCTION

A INTRODUCTORY SURVEY

1.1 Historical Review

Investigations of the chemistry of molybdenum(II) dichloride were first reported in 1857 by Blomstrand (1). Lindner and other workers (2-9) studied further dichloride and related bromo- and iodo- derivatives through until the late 1920's but expressed their results in terms of the composition $(\text{Mo}_3\text{Cl}_4)\text{Cl}_2$ for the dichloride. This formulation resulted from the early ebullioscopic molecular weight determination (9) coupled with the reactivity found for only one-third of the chlorine present in the dichloride (1,2,3). Similarly $\frac{3}{7}$ of the chloride in the chloroacid (then formulated $\text{Mo}_3\text{Cl}_6 \cdot \text{HCl} \cdot 4\text{H}_2\text{O}$) could be removed by alkali (8).

Molybdenum(II) dihalides are involatile, resistant to oxidation to 200°C in air, stable in dilute acids and soluble in donor solvents, such as acetone and pyridine. The preparative method used, involving the high temperature break-down of higher chlorides of molybdenum (10-13) reflects these properties:

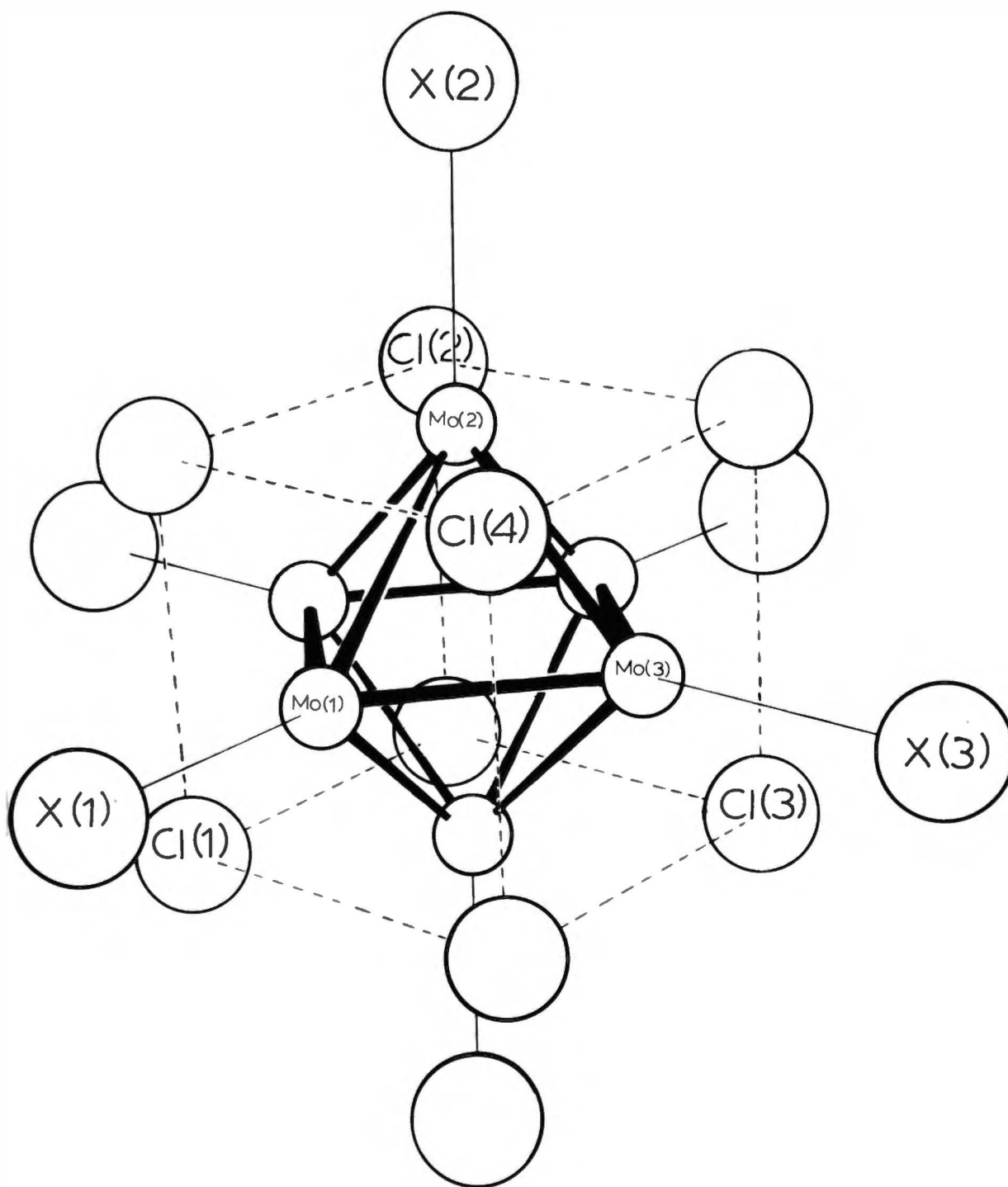


Figure I: The $((\text{Mo}_6\text{Cl}_8)\text{X}_6)^{2-}$ anion showing the Cl_8 cube

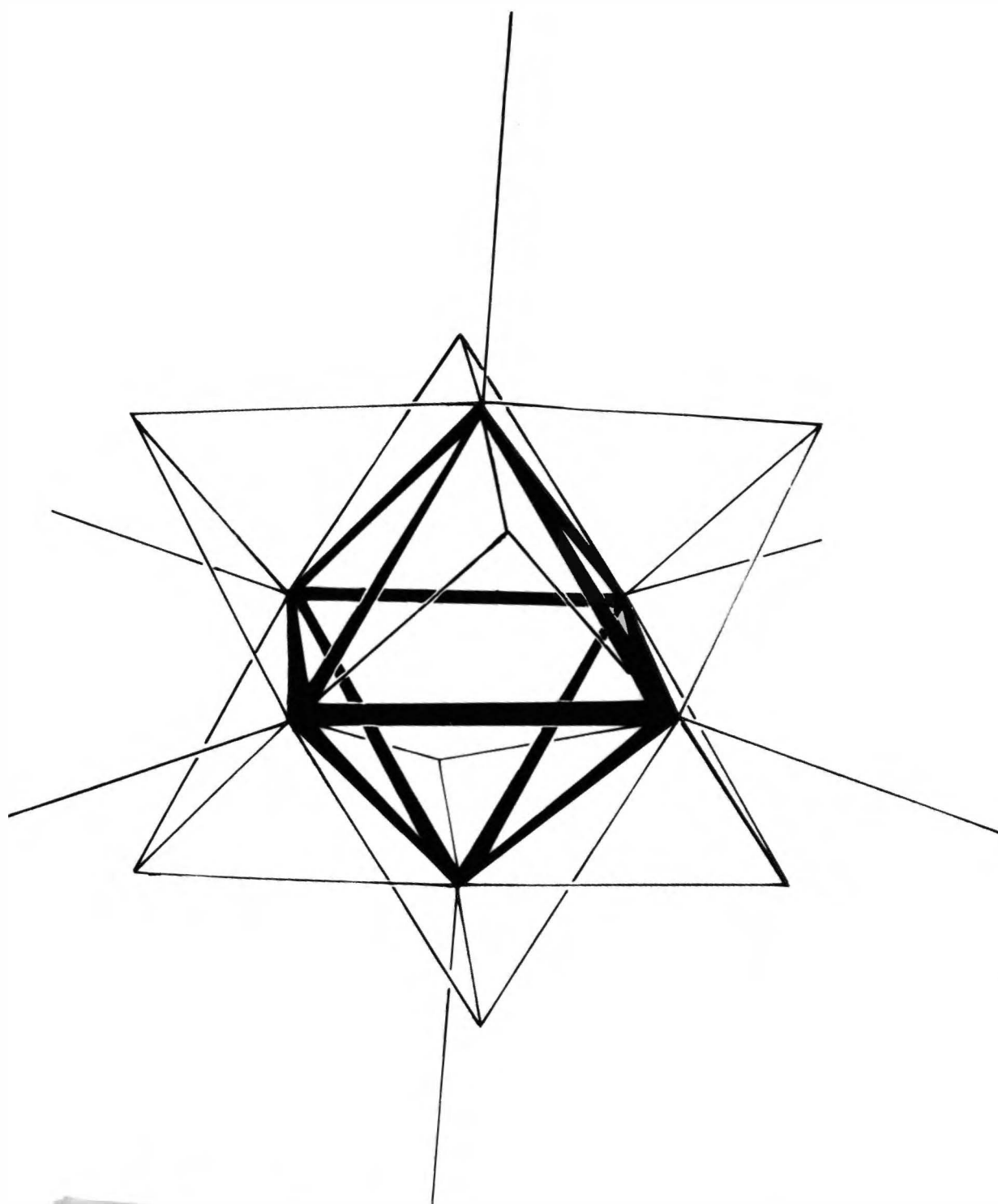


Figure II: Bonding in the $((\text{Mo}_6\text{Cl}_8)\text{X}_6)^{2-}$ anion



By 1945, when Brosset discovered the basic hexameric cluster, $(\text{Mo}_6\text{Cl}_8)^{4+}$ in the first X-ray structure analysis of an $(\text{Mo}_6\text{Cl}_8)\text{Cl}_4$ derivative, many adducts had been analysed and formulated on the above basis. Examples of such compounds are the two studied by Brosset (14,15) which he reformulated from their previously written compositions, $(\text{Mo}_3\text{Cl}_4)(\text{OH})_2 \cdot 7\text{H}_2\text{O}$ and $(\text{Mo}_3\text{Cl}_4)\text{Cl}_2 \cdot 4\text{H}_2\text{O}$ to $((\text{Mo}_6\text{Cl}_8)(\text{OH})_4(\text{H}_2\text{O})_2) \cdot 12\text{H}_2\text{O}$ and $((\text{Mo}_6\text{Cl}_8)\text{Cl}_4(\text{H}_2\text{O})_2) \cdot 6\text{H}_2\text{O}$.

1.2 The Structure of the $(\text{Mo}_6\text{Cl}_8)^{4+}$ Cluster

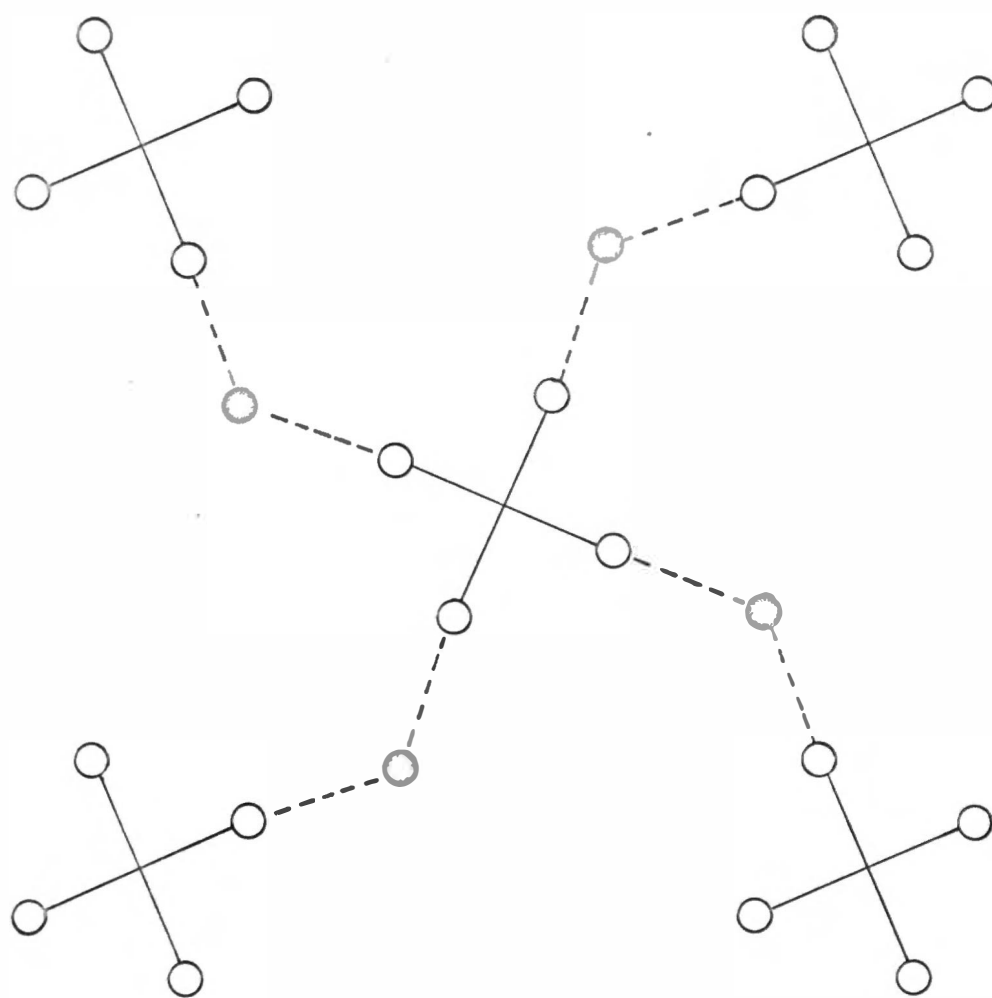
The structure of the $(\text{Mo}_6\text{Cl}_8)^{4+}$ cluster is illustrated in Figures I and II, which contain the $(\text{Mo}_6\text{Cl}_8)\text{X}_6$ group. The (Mo_6Cl_8) cluster consists of a regular octahedron of strongly-bonded molybdenum atoms (Mo), represented by the heavy lines in both figures, surrounded by a slightly distorted cube of chlorine atoms (Cl), represented by the dotted lines in Figure I. Each molybdenum atom protrudes from the appropriate cube face. In an alternative description best shown in Figure II, the chlorine atoms can be considered above the eight faces of the Mo_6 octahedron. The cluster chlorine atoms (Cl) bridge three molybdenums

while each molybdenum is bonded to four other molybdenums and four chlorines (Figure II).

The molybdenum-molybdenum bond distance found by Brosset was 2.63 Ångstroms (Å), approximately that (2.59 Å) predicted for a single Mo-Mo bond (16), but shorter than the 2.725 Å found for the distance in molybdenum metal (17). Two interesting deviations from the strict equivalence of the Mo-Mo and Mo-Cl bond lengths were found by Brosset. The Mo-Mo bonds adjacent to the bonded water were 2.62 Å, whereas those adjacent to the chloride were longer 2.69 Å. Secondly, in $(\text{Mo}_6\text{Cl}_8)\text{Cl}_4 \cdot 8\text{H}_2\text{O}$, the cluster chlorine-molybdenum bond distances (Mo-Cl, 2.6 Å) are longer than the terminal chlorine-molybdenum distances (Mo-X, 2.4 Å), which are of the order expected for a single molybdenum-chlorine bond (16). However the accuracy of Brosset's work did not justify further speculation based on these small differences.

Vaughan (18) confirmed this structure in 1950 by an X-ray radial distribution powder analysis of the ammonium salt $(\text{NH}_4)_2((\text{Mo}_6\text{Cl}_8)\text{Cl}_6)$. Brosset (19) and Vaughan et al. (20) further showed that the X-ray radial distribution curves of solutions of the chloroacid $(\text{H}_3\text{O})_2(\text{Mo}_6\text{Cl}_8)\text{Cl}_6 \cdot 6\text{H}_2\text{O}$ and some related compounds are

Figure III: Mo_6 octahedra from $(\text{Mo}_6\text{Cl}_8)\text{Cl}_4$ (13); projection showing cross-linking of (Mo_6Cl_8) clusters



Scale: 0 1 2 Å

Atoms: ○ Mo
● Cl

consistent with the hexameric cluster.

The dichloride $(\text{Mo}_6\text{Cl}_8)\text{Cl}_4$, after purification via solution in hydro-chloric acid, is amorphous to X-rays (21). Thus it was only recently (1967) that single crystals of the dichloride were prepared by Schäfer et al (13) using a temperature-gradient vacuum sublimation technique. These latter workers carried out an X-ray structure analysis of the crystals which showed that the dichloride $(\text{Mo}_6\text{Cl}_{12})$ composition is attained by the bridging of four of the six chlorine atoms bound terminally to different $(\text{Mo}_6\text{Cl}_8)^{4+}$ clusters (see Figure III). The structure, as predicted by Brosset (19), could be described formally therefore as $(\text{Mo}_6\text{Cl}_8)\text{Cl}_2\text{Cl}_{4/2}$, illustrating that six-fold coordination of each cluster is maintained.

All Mo-Mo distances are $2.61 \pm 0.01 \text{ \AA}$ in this structure; it is thus doubtful whether any significance can be placed on the different Mo-Mo lengths in Brosset's structure (p. 3). However, the molybdenum-chlorine bond lengths do vary as observed by Brosset: Mo-X (bridging clusters) = 2.50 ± 0.03 , Mo-X (not bridging) = 2.38 ± 0.03 and Mo-Cl = $2.47 \pm 0.03 \text{ \AA}$, where X = Cl (Figures I and III).

1.3 The Chemical Nature of the Chloromolybdenum(II) Ion, $(\text{Mo}_6\text{Cl}_8)^{4+}$

Research by Sheldon and others (21-32) published from 1959 onwards has shown that the chloromolybdenum(II) cluster acts as a pseudo single-atom ion, which invariably tends towards an octahedral configuration by coordination of six donor ligands. The cluster $(\text{Mo}_6\text{Cl}_8)^{4+}$ should not be considered as an independent, highly-charged ion, however. This is well illustrated by the reaction in which the ion $(\text{Mo}_6\text{Cl}_8)\text{Cl}_6^{2-}$ was heated for $1\frac{1}{2}$ hours with labelled hydrochloric acid, HCl^{36} (21). Only six chlorine atoms underwent isotopic exchange and the slow exchange rate ($k = 3.5 \times 10^{-4} \text{ sec}^{-1}$) indicated that the terminal chlorines (therefore) involved in the exchange are covalently- rather than ionically- bound.

Hence it can be appreciated why previous workers (2-8) found that only one third of the chlorine in the dichloride, $(\text{Mo}_6\text{Cl}_8)\text{Cl}_4$, is labile. The $(\text{Mo}_6\text{Cl}_8)^{4+}$ ion is stable in most chemical reactions although strongly nucleophilic anions (OH^- , F^- or NCS^-) cause partial or complete disruption of the cluster (22).

The six-fold coordination can be observed in two main ways:

(1) by the coordination of six univalent negatively-charged ligands, giving rise to adducts based on the $(\text{Mo}_6\text{Cl}_8)\text{X}_6^{2-}$ anion (Figures I,II), which are 2:1 electrolytes and crystalline to X-rays. Such compounds are easily prepared and useful because they decompose under heating (200°C) in high vacuum to give the related adducts $(\text{Mo}_6\text{Cl}_8)\text{X}_4$. For example, the chloroacid $(\text{H}_3\text{O})_2((\text{Mo}_6\text{Cl}_8)\text{Cl}_6) \cdot 6\text{H}_2\text{O}$ gives $(\text{Mo}_6\text{Cl}_8)\text{Cl}_4$; this is the basis of the standard method of purification of the latter (23).

(2) by the coordination of four univalent negatively-charged ligands and two neutral unidentate ligands (L) to give the neutral complexes $(\text{Mo}_6\text{Cl}_8)\text{X}_4\text{L}_2$, which are non-electrolytes and usually amorphous to X-rays.

Another class of compounds has recently been reported in which the six-fold coordination to the $(\text{Mo}_6\text{Cl}_8)^{4+}$ cluster is maintained by ionization of the terminal halogens in the starting material $(\text{Mo}_6\text{Cl}_8)\text{Cl}_4$. The cluster plus the coordinated ligands, in these cases, can be considered to be carrying a positive charge (e.g. $((\text{Mo}_6\text{Cl}_8)\text{Cl}_2(\text{triphenylphosphine})_3)\text{Cl}$ (33) and $((\text{Mo}_6\text{Cl}_8)\text{Cl}_2(1:10 \text{ o-phenanthroline})_2)\text{Cl}_2$ (34)).

Alkaline hydrolysis under vigorous conditions produces $\text{Mo}(\text{OH})_3$ and hydrogen (9). Adducts

$(\text{Mo}_6\text{Cl}_{8-n}(\text{OH})_n)(\text{OH})_4 \cdot n\text{H}_2\text{O}$, $n = 3-4$ produced under milder conditions are difficult to isolate as pure compounds but have been converted to more stable crystalline compounds e.g. $(\text{Et}_4\text{N})_2((\text{Mo}_6\text{Cl}_7\text{OH})\text{Cl}_6)$ (27). Subsequent reports dealt with the kinetics of alkaline hydrolysis (25,26).

At elevated temperatures, chloromolybdenum(II) derivatives are further hydrolysed by alkali to brown powders of unknown composition. Spectral studies (34,35) combined with analytical work usually are sufficient to establish whether the original (Mo_6Cl_8) cluster is intact.

In moist air, nearly all chloromolybdenum(II) compounds have a strong tendency to form hydrates (e.g. $(\text{Mo}_6\text{Cl}_8)\text{Cl}_4 \cdot 2\text{H}_2\text{O}$ (23)), some of which, on further exposure decompose and lose weight through the evolution of gaseous hydrogen halides. The nature of hydrolysis products found in aqueous solutions of the dichloride has not been fully elucidated but the proportion of products like $(\text{Mo}_6\text{Cl}_8)\text{Cl}_x(\text{OH})_{6-x} \cdot y\text{H}_2\text{O}$ increases rapidly with time and temperature (27).

Similarly, there is some evidence for $((\text{Mo}_6\text{Br}_8)(\text{H}_2\text{O})_6)^{4+}$ (36) and $(\text{Mo}_6\text{Br}_8)(\text{OH})_6^{2-}$ (24) in aqueous solutions of $(\text{Mo}_6\text{Br}_8)\text{Br}_4$ depending on the solution pH (see section

Table 1: Magnetic Measurements of Mo(II) Halides

$(10^6 \chi_m)$ (room temperature) c.g.s.u.)

<u>Compound</u>	<u>Value</u>	<u>Reference No.</u>
$(\text{Mo}_6\text{Cl}_8)\text{Cl}_4$	-230	22
	-190	38
$\text{H}_2((\text{Mo}_6\text{Cl}_8)\text{Cl}_6)8\text{H}_2\text{O}$	-360	22
$(\text{NH}_4)_2((\text{Mo}_6\text{Cl}_8)\text{Cl}_6)\cdot\text{H}_2\text{O}$	-240	22
$(\text{Mo}_6\text{Br}_8)\text{Br}_4$	-280	39
	- 60	40

1.5 below). The ion $(\text{Mo}_6\text{Cl}_8)(\text{OH})_6^{2-}$ exists in dilute alkali, $\text{pH} > 8.5$, whereas $(\text{Mo}_6\text{Cl}_8)(\text{OH})_4 \cdot n\text{H}_2\text{O}$ precipitates from solutions with pH lower than this (23).

1.4 Magnetic Studies

All compounds are diamagnetic; values measured for a range of compounds are summarised in Table 1 (36). In addition a number of compounds have been stated to be diamagnetic without quoting values for the magnetic susceptibility (22,26,29).

1.5 Other $(\text{Mo}_6\text{X}_8)^{4+}$ Analogues

Both molybdenum(II) dibromide and diiodide can be conveniently prepared by thermal decomposition of the respective trihalides but at lower temperatures than the chloride (6,32,41). A novel preparative route due to Sheldon (24) involves the fusion of molybdenum dichloride with the appropriate lithium halide; other alkali halides yield molybdenum metal and the MoX_6^{3-} ion.

While all molybdenum(II) compounds that have had structures determined are derivatives of the dichloride, there is ample chemical evidence (24) that chloro, bromo and iodomolybdenum(II) halides and their compounds contain the iso-structural cation $(\text{Mo}_6\text{X}_8)^{4+}$. The isomorphism of the hydroxides $((\text{Mo}_6\text{X}_8)(\text{OH})_4(\text{H}_2\text{O})_2) \cdot 12\text{H}_2\text{O}$,

where $X = \text{Br}, \text{Cl}$, is particularly significant as the crystal structure of the chloro compound is known to be hexameric (14).

Preparative studies of all these dihalides have been hindered by their low solubilities in unreactive solvents. Both the formation of the bis-undentate complexes (p. 6) and the possible solvolysis with suitable organic solvents such as ethanol, introduces other undesirable considerations into their reactions in solution. For example, the reactions of $(\text{Mo}_6\text{Br}_8)\text{Br}_4$ with bidentate oxy-anions, such as chromate, yield compounds that are rarely free of water (42).

Recent studies (43) in which molybdenum(II) dichloride was vigorously treated with sodium methoxide in methanol under deoxygenated, anhydrous conditions yielded $\text{Na}_2((\text{Mo}_6(\text{OCH}_3)_8)(\text{OCH}_3)_6)$, in which both terminal and cluster chloride ions are replaced by methoxy groups. This pyrophoric compound also appears to contain the analogous cluster $(\text{Mo}_6(\text{OCH}_3)_8)^{4+}$ on the basis of a range of physical measurements (e.g. conductivity, proton magnetic resonance).

1.6 Bonding Theories

Each molybdenum can employ only nine orbitals in bonding (4d,5s,5p) unless the 5d orbitals are used,

which appears to be energetically unfavourable (44). Since the effective coordination of each molybdenum is eight in the $(\text{Mo}_6\text{Cl}_8)^{4+}$ cluster, the bonding of more than one ligand to a molybdenum would not be expected. The following theories have been presented to describe the stereochemistry and energies of the cluster bonding.

Sheldon (22) proposed that each molybdenum is bonded to four chlorine atoms and one extra ligand by $d_{x^2-y^2} sp^3$ tetragonal pyramidal hybrid orbitals. Of the remaining orbitals, the d_{xy} and d_{yz} possess lobes directed exactly along the intermolybdenum axes. It is possible for each of the four coplanar molybdenum atoms to combine with one of these orbitals to give a molecular orbital system. Thus there would be three such sets of coplanar atoms each forming molecular orbitals to which each molybdenum contributes two electrons.

The assumption must be made that coupling of the remaining two electrons in the non-bonding orbitals, d_{xy} and d_{z^2} results in the observed diamagnetism of these compounds. Also, weak molybdenum-molybdenum bonding is predicted because this theory allows only twelve electrons for twelve bonds.

On the valence bond approach to bonding, each molybdenum atom is directly bonded to four other

molybdenum atoms and four halogen atoms with a square anti-prismatic stereochemistry (45), with a d_{z^2} or s-orbital excluded from the hybridisation scheme. Such a bonding scheme does imply the use of bent bonds (46) and considerable distortion from a normal square anti-prism would be required (47).

Crossman et al (48) suggested the use of hybrid molecular orbitals built up from d, s and p type of valency orbitals, about each molybdenum atom as postulated by Duffey (49). The two sets (metal-metal and metal-halogen) of calculated molecular orbitals are just filled by the 24 electrons available, leaving the empty p_z orbital available for the terminal (or centrifugal (37)) ligand bonding.

Cotton and Haas (50) used a similar but somewhat simplified molecular orbital treatment of the bonding, which did prove successful in accounting for the numbers of atoms and the net charge on this and other metal atom-cluster compounds. The p_z orbital was again totally involved with the bonding of the terminal ligand and did not interact with the d_{z^2} orbital. The other assumption made was that ligand-metal π -bonding need not be considered. Both these treatments have been criticized by Kepert and Vrieze (37), on the basis of the distortion from this model observed and the expected shifts in the

energy levels calculated on the bonding of the terminal ligands.

Kettle (51) has rationalized the bonding of the $\text{Mo}_6\text{Cl}_8^{4+}$ group in terms of a forty electron model, which he considers to be better (52) than the above theories because it is applicable to several other metal halogen clusters (e.g. $\text{Ta}_6\text{Cl}_{12}^{2+}$ (53)). Thirty-six molybdenum valence electrons and eight chlorine electrons less the four to give the cluster its charge (a total of 40) are placed in molecular orbitals defined by the twelve edges and eight faces of the metal octahedra, all electrons being paired and in bonding orbitals. The electronic properties of molybdenum(II) dichloride and its compounds therefore are typical of a d^0 rather than d^4 configuration, as observed (section 1.4).

A recent application of the electron-in-a-box theory to the bonding by Libby (54) seems useful only as a test of the stability of any postulated metal cluster systems.

B SCOPE OF THIS THESIS

1.7 Introduction

It has been well established that neutral unidentate ligands (L) react with $(\text{Mo}_6\text{Cl}_8)\text{Cl}_4$ under a variety of conditions to give the monomeric, non-electrolytes $(\text{Mo}_6\text{Cl}_8)\text{Cl}_4\text{L}_2$, thus fulfilling the six-fold coordination of the $(\text{Mo}_6\text{Cl}_8)^{4+}$ cluster (p. 6). The reactions of $(\text{Mo}_6\text{Cl}_8)\text{Cl}_4$ or the tetra-iodide $(\text{Mo}_6\text{Cl}_8)\text{I}_4$ with 2,2'-bipyridyl, o-phenanthroline and o-phenylene-bisdimethylarsine yield complexes of formulated composition $((\text{Mo}_6\text{Cl}_8)\text{X}_2\text{L}_2)\text{X}_2$ (where X is Cl, I), all of which are 2:1 electrolytes. Similarly, 2,2':6',2''-terpyridyl gives derivatives $((\text{Mo}_6\text{Cl}_8)\text{X}_3\text{terpy})\text{X}$ in which only one of the terminal halogens is ionized (33).

While the constitution of the complexes formed by unidentate ligands poses no additional bonding problem, the mode of attachment of bidentate ligands is less certain. Studies of the reactions of potentially bidentate oxy-anions, such as the sulphate (SO_4^{2-}), with $(\text{Mo}_6\text{Cl}_8)\text{Cl}_4$ and $(\text{Mo}_6\text{Br}_8)\text{Br}_4$ (42,55,56) did not confirm any of the four possibilities outlined in 1967 (33). The chemical and steric evidence for neutral bidentate ligand complexes favours one of these mechanisms in which coordination of the ligand is associated with a

displacement of a cluster halogen from its normal position. Since such a deformation might be expected to cause ionisation or labilisation of halogens it was relevant that when the complex $((\text{Mo}_6\text{Cl}_8)\text{I}_2(\text{bipy})_2)\text{I}_2$ (see p.19) is titrated with silver nitrate six halogens react (55).

One of the main aims of this research was to determine the mode of coordination of such bidentate ligands. Clearly, a single crystal X-ray structure analysis of one of the neutral bidentate complexes mentioned would yield the necessary information. Unfortunately, these complexes as normally prepared are in very fine crystalline form (i.e. powders). Considerable time was thus spent in preparation of suitable single crystals.

1.8 The Reactions of Bipyridyl with $(\text{Mo}_6\text{Cl}_8)\text{Cl}_4$

As some single crystals of $((\text{Mo}_6\text{Cl}_8)\text{Cl}_2(\text{Bipyridyl})_2)\text{Cl}_2$ had been reported by Robinson (55), much preparative work centred on reactions of $(\text{Mo}_6\text{Cl}_8)\text{Cl}_4$ with bipyridyl. However, as demonstrated in this thesis the reactions of these two compounds are much more complex than previously recorded.

Even under the relatively mild conditions of solvent reflux (65°) the reaction of $(\text{Mo}_6\text{Cl}_8)\text{Cl}_4$ and bipyridyl yields bipyridylium salts of chloromolybdic(II) acid,

$(\text{BipyridylH})_2((\text{Mo}_6\text{Cl}_8)\text{Cl}_6)$ along with other products, which are amorphous to X-rays. One of these latter products appears to be a 1:1 adduct of $(\text{Mo}_6\text{Cl}_8)\text{Cl}_4$ and bipyridyl, formulated as $(\text{Mo}_6\text{Cl}_8)\text{Cl}_4(\text{Bipyridyl})(\text{H}_2\text{O})_n$ $2 > n > 0$ as it is a non-electrolyte in dimethylformamide. In total, five different products have been identified in the ensuing study of this reaction.

Analogous reactions between $(\text{Mo}_6\text{Cl}_8)\text{I}_4$ and bipyridyl have also been observed. The reported complex " $(\text{Mo}_6\text{Cl}_8)\text{I}_2(\text{Bipy})_2\text{I}_2$ " mentioned above, for example, contains the corresponding salt of iodomolybdic(II) acid, $(\text{BipyH})_2((\text{Mo}_6\text{Cl}_8)\text{I}_6)$.

As a result of this complexity, the three crystal structure analyses carried out were of the bipyridylium salts, $(\text{BipyH})_2((\text{Mo}_6\text{Cl}_8)\text{X}_6)$, $\text{X} = \text{Cl}, \text{I}$. Although the mode of coordination of bidentate ligands to the cluster $(\text{Mo}_6\text{Cl}_8)^{4+}$ was thus not elucidated by these structure analyses, they provide precise dimensions of the $(\text{Mo}_6\text{Cl}_8)^{4+}$ cluster, which have not been previously obtained.

1.9 Triphenylphosphine and Triphenylphosphine Oxide

Contrary to a previous report (22), Fergusson and others (33) found that molybdenum(II) dichloride reacts with triphenylphosphine to form a normal bis-unidentate

complex $(\text{Mo}_6\text{Cl}_8)\text{Cl}_4(\text{Ph}_3\text{P})_2$, where Ph_3P is triphenylphosphine. Further work involving this complex yielded ionic compounds such as $((\text{Mo}_6\text{Cl}_8)\text{Cl}_2(\text{Ph}_3\text{P})_2(\text{pyridine})_2)\text{Cl}_2$, in which more than two monodentate ligands coordinate to the cluster. In a similar way to the bidentate complexes, the monomeric cluster unit is envisaged as carrying an overall positive charge (e.g. as $((\text{Mo}_6\text{Cl}_8)\text{Cl}_2(\text{Ph}_3\text{P})_2(\text{pyridine})_2)^{2+}$). A further study of triphenylphosphine reactions was thus undertaken since such ionic complexes effectively test the six-fold coordination of the $(\text{Mo}_6\text{Cl}_8)^{4+}$ cluster. As these complexes are normally powders crystalline to X-rays, suitable single crystals for an X-ray structural analysis were also anticipated.

Again, the reactions are more complex than previously suspected. An early examination of the bis-complexes of triphenylphosphine and triphenylphosphine oxide with $(\text{Mo}_6\text{Cl}_8)\text{Cl}_4$ showed they were the same compound. Infra-red studies and X-ray powder photo analysis established this compound as $(\text{Mo}_6\text{Cl}_8)\text{Cl}_4(\text{triphenylphosphine oxide})_2$. Oxidation also occurs in the analogous $(\text{Mo}_6\text{Cl}_8)\text{I}_4$ reactions.

Similarly, triphenylarsine and triphenylarsine oxide combine with $(\text{Mo}_6\text{Cl}_8)\text{Cl}_4$ and $(\text{Mo}_6\text{Cl}_8)\text{I}_4$ to give the corresponding oxide complexes under normal reaction

conditions. A study of the conditions of reaction implemented by this author was carried on by P.F. Snowden, in this department (42). He has verified that triphenylarsine and triphenylphosphine complexes can only be prepared under conditions in which oxygen is rigorously excluded; because of this restriction on solvents, the compounds prepared were rarely pure bis-adducts.

1.10 Some Problems with $(\text{Mo}_6\text{Cl}_8)\text{Cl}_4$

Further work prompted by these observations has shown that the anhydrous dichloride $((\text{Mo}_6\text{Cl}_8)\text{Cl}_4)$ is not always obtained from chloromolybdic(II) acid $(\text{H}_3\text{O})_2((\text{Mo}_6\text{Cl}_8)\text{Cl}_6) \cdot 6\text{H}_2\text{O}$, in the standard preparation (23). Insufficient emphasis has been placed, apparently, on the strongly hygroscopic nature of the dichloride and tetraiodide $(\text{Mo}_6\text{Cl}_8)\text{I}_4$. The influence of such water on the physical and chemical properties of these basic starting materials in association with their previous history may explain some of the unusual properties observed (e.g. different solubilities in the same solvents).

1.11 Presentation

The reactions of bipyridyl with the $(\text{Mo}_6\text{Cl}_8)^{4+}$ cluster system are detailed in Chapter 2. In section 2.3 of this chapter, a discussion of the problems

associated with the composition of molybdenum(II) chloride is presented.

All studies of monodentate ligand reactions with $(\text{Mo}_6\text{Cl}_8)\text{Cl}_4$ and $(\text{Mo}_6\text{Cl}_8)\text{I}_4$ including the triphenylphosphine and triphenylphosphine oxide work are contained in Chapter 3.

X-ray diffraction structure analyses of the two isomorphous bipyridylum salts, $(\text{BipyridylH})_2((\text{Mo}_6\text{Cl}_8)\text{X}_6)$, $\text{X} = \text{Cl}, \text{I}$, which were solved by the difference Patterson method, are contained in Chapter 4. The X-ray structure analysis of the other crystalline modification of $(\text{BipyridylH})_2((\text{Mo}_6\text{Cl}_8)\text{Cl}_6)$, which was solved by a novel use of rigid group least-squares refinement procedures, is presented in Chapter 5.

A review of the structural features of the three X-ray crystal structures studied is contained in Chapter 6.

Appendix A consists of a full description of the standard preparative methods, which are abbreviated in the text, followed by brief accounts of the analytical and physical techniques used.

The University of Canterbury computer programming system designed for the IBM 360/44 computer is outlined in Appendix B. The numerous calculations referred to in Chapters 4, 5 and 6 were carried out using the programs

of this system. Those programs which were the particular concern of the author are noted.

Appendix C briefly outlines the Canterbury University Supper equi-inclination Diffractometer system (CUSED). Implementation of the automation to the design of T. Zoltai (57) and consequent data handling was another facet of the X-ray research carried out by the author.

All tables referred to in the X-ray diffraction structural analyses and discussion in Chapters 4, 5 and 6 are collected in Appendix D, in order of reference in the text.

1.12 Abbreviations

As some mention will be made in succeeding chapters to several compounds with lengthy I.U.P.A.C. (58) names, the following abbreviations have been adopted:-

2,2'Bipyridine	bipyridyl	bipy
1:2 bisdiphenylphosphinoethane	diphosphine	diphos
1:10 phenanthroline	o-phenanthroline	o-phen
pyridine		py
triphenylphosphine		Ph ₃ P
triphenylphosphine oxide		Ph ₃ PO
triphenylarsine		Ph ₃ As
triphenylarsine oxide		Ph ₃ AsO
pyridine-N-oxide		pyNO
o-phenylenebisdimethylarsine	diarsine	diars

2,2':6',2"-terpyridyl	terpyridyl	terpy
ethanol		EtOH
tetrahydrofuran		T.H.F.
chloroform		CHCl ₃
dimethylformamide		D.M.F.
dimethylsulphoxide		D.M.S.O.
nitrobenzene		PhNO ₂

Similarly it will be convenient for brevity and uniformity to denote the polynuclear halides and their derivatives by their structural formulæ (e.g. octa- μ_3 -chlorohexamolybdenum(II) tetraiodide as $(\text{Mo}_6\text{Cl}_8)\text{I}_4$). It is noted that representation of the (Mo_6Cl_8) cluster as the charged species $(\text{Mo}_6\text{Cl}_8)^{4+}$, although a useful abbreviation is strictly incorrect as pointed out on page 5.

1.13 Other Work

During the course of this research, work was carried out on the final refinements of two trinuclear Re(III) structures, $\text{Cs}_3\text{Re}_3\text{Br}_{12}$ and $\text{CsRe}_3\text{Cl}_3\text{Br}_7(\text{H}_2\text{O})_2 \cdot \text{H}_2\text{O}$. Since these two structures are outside the intended scope of this work and have been described in detail elsewhere (59,60) they will not be referred to in this thesis.

CHAPTER 2

THE REACTIONS OF BIPYRIDYL WITH THE $(\text{Mo}_6\text{Cl}_8)^{4+}$ CLUSTER SYSTEM

2.1 Introduction

Investigations of the reactions of $(\text{Mo}_6\text{Cl}_8)\text{Cl}_4$ and $(\text{Mo}_6\text{Cl}_8)\text{I}_4$ with bipyridyl initially followed the preparative methods used by Robinson (55). With the assumption that higher temperatures (130°C) and pressures would not adversely affect the formation of the bis-bipyridyl complexes he had found, a series of experiments in sealed tubes were carried out. These were aimed at increasing crystallite size and thereby providing samples from which single crystals suitable for X-ray analyses could be selected.

Though bulk analyses of the products of these reactions did not indicate pure bis-bipyridyl complexes, single crystals were isolated which gave the same X-ray powder photographs as those found for the complexes $((\text{Mo}_6\text{Cl}_8)\text{X}_2(\text{Bipy})_2)\text{X}_2$, $\text{X} = \text{Cl}, \text{I}$, by Robinson (55). It came, therefore, as a surprise when the X-ray studies of these crystals showed that they were, in fact, bis-bipyridylium salts of chloromolybdic(II) and iodomoly-

Table 2 : Analysis of X-ray Powder Patterns of the Reaction Products of Bipyridyl:

(i) with $(Mo_6Cl_8)Cl_4$

<u>Reaction Number</u>	<u>Reaction Conditions</u>	<u>Crystalline Products Identified (see Table 3)</u>			
		<u>1</u>	<u>2</u>	<u>3</u>	<u>4</u>
1	Batch 1, $(Mo_6Cl_8)Cl_4$ heated under reflux ^a in EtOH	*	*		
2 ^b	Batch 2, $(Mo_6Cl_8)Cl_4$ sealed tube experiment ^a in T.H.F.	*	*		
3	$(Mo_6Cl_8)Cl_4$ prepared by Robinson ^c , heated under reflux in T.H.F.	*	*		
4	Batch 3, $(Mo_6Cl_8)Cl_4(H_2O)$; residue after heated under reflux in T.H.F.				
5(a)	Residue obtained after filtrate of 4 concentrated on water bath and cooled.		* ^w	*	*
5(b)	Dry petroleum ether added in excess to filtrate of 4	*	*		*
6	Single crystals grown in the filtrate of 5(a)			*	
7	Single crystals isolated by Robinson ^c			*	
(ii)	<u>with $(H_3O)_2((Mo_6Cl_8)Cl_6).6H_2O$, the chloroacid</u>				
8	Heated under reflux in EtOH	*	*		
9 ^d	Room temperature addition in EtOH		*		*
10	Chloroacid partially dried in vacuo, room temperature in EtOH	*	*	* ^w	*
11	Chloroacid partially dried in vacuo, heated under reflux in EtOH	*	*		
12	Heated under reflux in T.H.F. for 5 minutes				*
13	Heated under reflux in T.H.F. for 2 hours	*	*		*

KEY: a See Section A.1 of Appendix A

b Amorphous material present (by separation from crystals)

c Reference (55)

d $d = 12.6 \text{ \AA}$ (weak) line not identified

w Only strongest lines observed.

bdic(II) acids respectively: $(\text{BipyH})_2((\text{Mo}_6\text{Cl}_8)\text{X}_6)$,
 $\text{X} = \text{Cl}, \text{I}$.

Further reactions under various conditions, summarised for $(\text{Mo}_6\text{Cl}_8)\text{Cl}_4$ in Table 2(1), soon established that these salts are formed even under milder conditions as was the case in Robinson's work (heating under reflux in tetrahydrofuran, experiment 3, Table 2). As a consequence of this study, no fewer than five different products have been found (Table 3). Only two of these have been given a definite formula because the reactions usually yield mixtures of the five products.

2.2 Identification of the Products of the Reaction of $(\text{Mo}_6\text{Cl}_8)\text{Cl}_4$ with Bipyridyl

Examination of the bulk products prepared in these reactions has been carried out principally using X-ray powder photography. Single crystal X-ray diffraction studies of three of the products (numbers 1, 2 and 3) verified the distinctive X-ray powder lines indicated in Table 3.

Since the X-ray powder photographs revealed that mixtures of products were often present in what appeared to be homogeneous samples, chemical analyses are of little use for purposes of identification. Corresponding to the experiment numbers in Table 2, these analyses

Table 3 : Distinctive X-ray Powder Lines and Comments of Products Identified from the Reactions of $(\text{Mo}_6\text{Cl}_8)\text{Cl}_4$ with Bipyridyl

<u>Product Number</u>	<u>d-spacings of Distinctive X-ray Powder lines (Å)</u>	<u>Comments / Composition</u>
1	9.57, 8.16, 8.07, 7.04, 6.53, 6.20, 5.93, 5.51	$(\text{BipyH})_2((\text{Mo}_6\text{Cl}_8)\text{Cl}_6)$ from single crystal structure analysis (Cl(B), Chapter 5).
2	5.81 (medium) line to distinguish from product 1.	Also $(\text{BipyH})_2((\text{Mo}_6\text{Cl}_8)\text{Cl}_6)$ from single crystal structure analysis (Cl(A), Chapter 4).
3	13.8, 11.8, 9.2	Single crystals isolated give distorted diffraction pattern; probably a Bipyridylum salt of the chloroacid.
4	10.0 (broad, strong), 7.4-6.9 (strong, broad).	Isolated by X-ray powder photography only; high carbon analysis (see Expt. 12).
5	amorphous product(s)	Some evidence to a formulation of $(\text{Mo}_6\text{Cl}_8)\text{Cl}_4(\text{Bipy})(\text{H}_2\text{O})_n$, $0 < n < 2$.

are presented in Table 4.

Also, infra-red spectral analyses ($4000-230\text{ cm}^{-1}$) are uninformative of the nature of the products in these reactions. Schilt and Taylor (61) have reported approximately the same characteristic shifts are observed for the infra-red spectra of bipyridyl coordinated to protons or to metals. Many absorption spectra of these products and related complexes, such as those with pyridine, were collected. Even the expected molybdenum-nitrogen (stretching mode) absorption could not be recognized from these. This latter observation was predicted by Cotton, Wing and Zimmerman (35) from their recent study of the complex infra-red spectra of the $(\text{Mo}_6\text{X}_8)\text{Y}_6$ system.

It should be pointed out at this stage that the presence of amorphous material in any bulk products cannot easily be confirmed by X-ray powder photography. For this reason, the fifth product in Table 3 (amorphous material) has not been included in the X-ray powder analyses contained in Table 2. In the following report, the formulations of the five distinctive products will be discussed.

Products 1 and 2 These two products are grouped together because they are two different crystalline modifications of the bipyridylium salt of chloromolybdic

Table 4: Analyses of Products of Reactions (Table 2); Bipyridyl with $(\text{Mo}_6\text{Cl}_8)\text{Cl}_4$ and $(\text{H}_3\text{O})_2((\text{Mo}_6\text{Cl}_8)\text{Cl}_6) \cdot 6\text{H}_2\text{O}$

<u>Experiment Number</u>	<u>Additional Information</u>	<u>Bulk Chemical Analyses (%)</u>				<u>Conductivity</u>
		<u>C</u>	<u>H</u>	<u>Cl</u>	<u>Mo</u>	<u>Λ_m ($\Omega^{-1} \cdot \text{cm}^2$)</u>
1		14.6	1.4	33.0		
2	Single crystal Preparation	12.2	1.2	32.2 ^{aa}	47.4	44.7 ^c
3	X-ray Powder Photo (55)					
4	Amorphous to X-rays	11.9	1.5	34.5		7.5 - 15.3 ^d
5(a)	Density 2.1 - 2.4 g cm ⁻³	21.3	2.4	(31 ± 2) ^b		109 ^d
7	Product 3 (55)	18.3	1.9	32.7		112 ^e , 118 ^d
8	Immediate precipitate	18.0	1.5	35.8 ^{aa}	40.8	131 ^d
12	Product 4 (Table 3)	20.5	2.0			94 ^{d, f}
14	Product 1 (from Expt.2)	17.1	1.5			

Theoretical Analyses

$(\text{Mo}_6\text{Cl}_8)\text{Cl}_4(\text{Bipy})(\text{H}_2\text{O}) \cdot \text{H}_2\text{O}$	10.0	1.0	35.7	48.3	0-50 ^d , <15 ^c
$(\text{Mo}_6\text{Cl}_8)\text{Cl}_4(\text{Bipy})$	10.4	0.7	36.8	49.6	" "
$(\text{Mo}_6\text{Cl}_8)\text{Cl}_2(\text{Bipy})_2\text{Cl}_2$	18.3	1.2	32.4	43.9	110-130 ^d , 35-50 ^c
$(\text{BipyH})_2((\text{Mo}_6\text{Cl}_8)\text{Cl}_6)$	17.3	1.4	35.9	41.7	" "
$(\text{BipH})_2((\text{Mo}_6\text{Cl}_8)\text{Cl}_6) \cdot (\text{BipyH} \cdot \text{Cl})_{0.5}$	20.2	1.8	34.7	38.8	" "

KEY: a = see Appendix A

aa = average two measurements

b = Estimated value (incomplete decomposition)

c = in PhNO_2

d = in D. M. F.

e = in D. M. S. O.

f = based on molecular weight of 1387.

(II) acid as mentioned above: $(\text{BipyH})_2((\text{Mo}_6\text{Cl}_8)\text{Cl}_6)$. Single crystals of both of these forms suitable for X-ray diffraction analyses were isolated from experiment 2, a sealed tube preparation (see Section A.1 of Appendix A). The unusual occurrence of these two modifications, and their structural features as determined by the single crystal X-ray diffraction analyses (Chapters 4 and 5) are dealt with in Chapter 6.

Products 3 and 4 Both products 3 and 4 were identified by their X-ray powder photographs (Table 3) before single crystals of the latter were grown and studied (experiment 6, Table 2). Since these products are also formed during the reactions of the chloroacid, $(\text{H}_3\text{O})_2((\text{Mo}_6\text{Cl}_8)\text{Cl}_6) \cdot 6\text{H}_2\text{O}$ and bipyridyl (Table 2 (11)), they are most probably bipyridylium salts of the chloroacid. This is further borne out by their conductivities in dimethylformamide (experiments 5(a) and 12, Table 4), which have the expected values for 2:1 electrolytes.

However, in both cases, the analytical figures for carbon are significantly higher than required for the pure bis-bipyridylium salt formulation (see experiments 5(a) and 12, Table 4). Since the two products were prepared from the chloroacid and bipyridyl in both ethanol and tetrahydrofuran (experiments 9 and 12, Table 2), the possibility that these products are solvated

bipyridylium salts can be excluded. Also the infra-red spectra of these two compounds show only bands corresponding to those expected for the bipyridylium cation.

These high carbon analyses may be due to the presence of amorphous material, which cannot be distinguished from the crystalline product(s) in the bulk yields (e.g. in experiment 12, Tables 2 and 4). However, some evidence suggests that the readily identifiable amorphous material formed in the reactions of bipyridyl and $(\text{Mo}_6\text{Cl}_8)\text{Cl}_4$ has lower carbon analyses than the bipyridylium salt formation corresponding to a 1:1 $(\text{Mo}_6\text{Cl}_8)\text{Cl}_4$: bipyridyl adduct (see Product 5 below).

All the products of the reactions summarised in Table 2 were washed free of ligand and dried under vacuum (Appendix A). Also, it is now apparent that hydrogen chloride is present and involved in both the reactions of $(\text{Mo}_6\text{Cl}_8)\text{Cl}_4$ and the chloroacid with bipyridyl. Thus, in the light of the X-ray powder photographic (Table 2) and infra-red evidence, the presence of small amounts of bipyridylium hydrochloride(s) cannot be ruled out as an explanation of these high carbon analyses.

In fact, the preliminary single crystal study carried out on product 3, the details of which are presented in Section 2.6 of this chapter, indicates a

formulation of higher molecular weight than the bis-bipyridylium salt composition, $(\text{BipyH})_2((\text{Mo}_6\text{Cl}_8)\text{Cl}_6)$. These crystals of product 3 give X-ray patterns typical of one-dimensionally-disordered compounds (62); thus, it seems at least possible that bipyridyl (and hydrogen chloride) may be enclosed in some random fashion within the crystal lattice of the single crystals of product 3. Because of their most probable composition (bipyridylium salts) and the disorder problem, further X-ray study of these single crystals was not undertaken.

From its association with product 3 in the identified mixtures (see Table 2), the crystalline material designated as product 4 is most likely to be of similar type.

Product 5 - Amorphous Material In addition to the crystalline products described, material amorphous to X-rays (section A.4 (iv), Appendix A) was obtained. As indicated on p. 23, it is not easy, in general, to establish whether amorphous compounds are present in the mixtures found. However, after careful separation of visibly crystalline material from the yield of experiment 2 (Tables 2 and 4), it was confirmed that the residual powder was amorphous. The X-ray photograph of the latter showed only very faint traces of powder lines.

In only one experiment (number 4) was an amorphous

product obtained free from all crystalline material. The infra-red spectrum of this product showed that it definitely contained water. However, moisture was not found in all samples of amorphous material which have been isolated. The bands used in this identification were the stretching ($\nu(\text{O-H})$) and bending ($\delta(\text{H-O-H})$) absorptions for water (63). A further broad absorption at 520 cm^{-1} was also observed in these spectra. This latter band has recently been tentatively assigned to the (Mo-OH_2) stretching frequency in these systems (42).

As a result of the difficulty of interpreting analytical data of mixtures, it is not possible to give a confident formulation for the amorphous products but one analysis did approximate to a 1:1 complex, $((\text{Mo}_6\text{Cl}_8)\text{Cl}_4(\text{Bipy})(\text{H}_2\text{O})_n)$ $2 > n > 0$ (experiment 4, Table 4). In view of the hydration that may also be affecting these reactions, a note on the susceptibility of $(\text{Mo}_6\text{Cl}_8)\text{Cl}_4$ to moisture is appropriate before proceeding with a closer examination of the reactions studied.

2.3 The Association of Water with Molybdenum(II) Halides

It has been established (23, 42) and further confirmed in this work that molybdenum(II) halides, which are amorphous to X-rays, rapidly absorb moisture from the air (up to 10% by weight in a 24 hour period). They

then lose weight slowly, as if decomposing to give off some volatile material, presumably hydrogen chloride gas (for $(\text{Mo}_6\text{Cl}_8)\text{Cl}_4$). All the products of this exposure show some X-ray powder lines.

Recent preparations of $(\text{Mo}_6\text{Cl}_8)\text{Cl}_4$, under standard experimental conditions involving purification via the thermal decomposition of the chloroacid in vacuo (23), however, showed that product can be seriously "contaminated" with water, even after repeated heating (in vacuo) up to 350°C . Further heating above this temperature causes degradation to greenish products, presumably Mo(III) or Mo(IV) oxides. This has not been reported previously. This behaviour contrasts with the stability of pure, anhydrous $(\text{Mo}_6\text{Cl}_8)\text{Cl}_4$ which has been shown to be stable up to 800° in vacuo (22).

The water contained in these yields (Batch 3) is apparently coordinated to the cluster (p.27). Such coordination seems reasonable since any water of crystallization (as in the chloroacid starting material, $(\text{H}_3\text{O})_2((\text{Mo}_6\text{Cl}_8)\text{Cl}_6).6\text{H}_2\text{O}$) bound by only "long-range" forces (Van der Waals, hydrogen-bonding) would most probably be driven off under these extreme conditions.

When water is associated with $(\text{Mo}_6\text{Cl}_8)\text{Cl}_4$, two strong characteristic X-ray powder lines are observed (d values 7.4 and $7.0 \overset{\circ}{\text{A}}$) provided the preparation is

carried out below 300°C. Above this temperature, further distinct lines appear. Irrespective of the temperature of preparation, these compounds are non-electrolytes in dimethylformamide. On the basis of one chlorine analysis of a yield prepared at 300°C these compounds are empirically formulated as $(\text{Mo}_6\text{Cl}_8)\text{Cl}_4(\text{H}_2\text{O})$.

As yet, the experimental differences between this, and previous preparations in which water was not found, (Batches 1 and 2) have not been elucidated. Use of chloroacid supplied by an independent worker, Kepert (64), also yielded the water-coordinated product. It is concluded that any difference must arise during the heating of the acid and might therefore relate to the speed at which the maximum temperature is attained.

Certain other anomalous properties have been observed (65). These can also be related to the history of the $(\text{Mo}_6\text{Cl}_8)\text{Cl}_4$ or $(\text{Mo}_6\text{Cl}_8)\text{I}_4$ used. For example, whereas one yield (Batch 1) of $(\text{Mo}_6\text{Cl}_8)\text{I}_4$ was of very low solubility in both dry (Appendix A) and wet (solvent grade) chloroform, another preparation (Batch 2) of apparently the same compound was quite soluble in both these solvents. Another striking example was observed when two different samples of the hydrated dichloride (" $(\text{Mo}_6\text{Cl}_8)\text{Cl}_4(\text{H}_2\text{O})$ "), prepared, it is believed, under

identical conditions, showed markedly different solubilities in the same dry tetrahydrofuran. Again, the cause of such behaviour has not been found.

Although attempts were made to understand these anomalies, it appears that $(\text{Mo}_6\text{Cl}_8)\text{Cl}_4$ and $(\text{Mo}_6\text{Cl}_8)\text{I}_4$ of slightly different compositions can result from very similar experimental conditions.

The following brief examination of the reactions of bipyridyl with the $(\text{Mo}_6\text{Cl}_8)^{4+}$ system, summarised in Tables 2, 4 and 5, is presented with some reference to the particular preparation of $(\text{Mo}_6\text{Cl}_8)\text{Cl}_4$ or $(\text{Mo}_6\text{Cl}_8)\text{I}_4$ used. The tables are summaries and should be used in conjunction with the complete details of the standard methods described in Section A.1 of Appendix A.

2.4 The Reactions of Bipyridyl with $(\text{Mo}_6\text{Cl}_8)\text{Cl}_4$ and $(\text{Mo}_6\text{Cl}_8)\text{I}_4$

Depending on the previous history of the $(\text{Mo}_6\text{Cl}_8)\text{Cl}_4$ used, different reactions of bipyridyl and the dichloride can be distinguished. Even when anhydrous $(\text{Mo}_6\text{Cl}_8)\text{Cl}_4$ (Batches 1 and 2) was heated under reflux with bipyridyl in dry ethanol or dry tetrahydrofuran (experiments 1 - 3), the bulk product obtained was a mixture of bipyridylium salts (products 1 and 2) and some amorphous material

(p.26).

By contrast, the initial precipitate on heating the hydrated dichloride (" $(\text{Mo}_6\text{Cl}_8)\text{Cl}_4(\text{H}_2\text{O})$ ") with bipyridyl in tetrahydrofuran, consisted of amorphous compound alone (experiment 4, Tables 2 and 4). This adduct was filtered off and the filtrate concentrated on a water bath in anticipation of bipyridylium salt formation. Orange-red crystalline plates separated on cooling this concentrate. These contained a mixture of products 3 and 4 with small amounts of product 2 (experiment 5(a)). This is surprising since these products are water-free bipyridylium salts of the chloro-acid (pp. 23). Large crystals of product 3 were grown by further concentration of the mother liquor and seeding with a few of the orange plates above.

The comparative behaviour of some impure molybdenum (II) chloride is also of interest. This "crude" dichloride, obtained directly from the initial reaction of molybdenum and chlorine in the combustion tube (23), is always amorphous and, necessarily, anhydrous. It showed no reaction with bipyridyl dissolved in tetrahydrofuran until the reaction solution was heated under reflux. A yellow product amorphous to X-rays was deposited along with the crystalline impurities (viz. Mo and MoCl_3) originally contained in the "crude"

Table 5: Analyses of Products of Experiments of Bipyridyl with $(\text{Mo}_6\text{Cl}_8)\text{I}_4$

Expt. No.	Reactants + Bipyridyl ^a	Conditions of Reaction	Bulk Chemical Analyses (%)					Conductivity Λ_m ($\Omega^{-1}\text{cm}^2$)	To X-rays	Isomorphous to Table 3 product?; spectra
			C	H	Cl	Mo	I			
15	Batch 2, $(\text{Mo}_6\text{Cl}_8)\text{I}_4$	Sealed Tube under nitrogen in T.H.F., 130°C, 4 hours ^a	7.7	0.8		37.6		31.7 ^d	Amorphous	Product 5; 800 cm^{-1} band in infra-red spectrum
16	Filtrate of 20	Addition pet. ether and standing	14.8	1.2		32.6		121 ^d	Crystalline	Products 3,4 d-spacings, see KEY below
17	Batch 2, $(\text{Mo}_6\text{Cl}_8)\text{I}_4$	Sealed tube under nitrogen, in EtOH, 130°C, 4 hours ^a	13.2	1.2	16.7		34.0, 29.1	47.1 ^c	Crystalline	Isomorphous single crystals studied (Product 2) isolated from this expt.
18	Filtrate of 17	Pet. ether and standing	10.6	1.0					Crystalline	-

Theoretical Analyses

$(\text{Mo}_6\text{Cl}_8)\text{I}_4(\text{bipy})$	7.88	0.53	18.6	37.8	33.2	0-50 ^d , <15 ^c
$((\text{Mo}_6\text{Cl}_8)\text{I}_2(\text{bipyridyl})_2)2\text{I}$	14.3	0.95	16.9	34.3	30.3	110-130 ^d , 35-50 ^c
$(\text{BipyH})_2((\text{Mo}_6\text{Cl}_8)\text{I}_6)$	12.4	0.9	14.7	29.8	39.4	"
$(\text{BipyH})_2((\text{Mo}_6\text{Cl}_8)\text{I}_6).2(\text{T.H.F.})$	16.2	1.5	13.6	27.7	36.7	"
$(\text{Mo}_6\text{Cl}_8)\text{I}_4(\text{bipy}).2(\text{EtOH})$	10.4	1.2	17.6	35.7	31.4	?

KEY The KEY to this Table is the same as that used in Table 4.
 Isomorphous d-spacings (Experiment 16); \circ 10.6 - 9.6 (strong),
 8.6, 7.5 - 7.2 (strong), 6.3, 5.9 Å.

dichloride. Evaporation of the mother liquor under reduced pressure at room temperature gave yellow "sticky" solids. When these were extracted with tetrahydrofuran and heated in air, a mixture of crystalline products 2 and 3 (Table 3) was obtained.

The reactions of bipyridyl with the anhydrous tetraiodide $(\text{Mo}_6\text{Cl}_8)\text{I}_4$ were also examined for comparative purposes. Once again, a variety of products was obtained (see Table 5). It is significant that three of these products were isomorphous (by their X-ray powder photos) with products 2, 3 and 4 obtained from the $(\text{Mo}_6\text{Cl}_8)\text{Cl}_4$ reactions. This indicates these reactions were following similar paths. The X-ray diffraction study of the single crystals from experiment 17, isomorphous with product 2, is described in Chapters 4 and 6.

In one of the sealed tube experiments with $(\text{Mo}_6\text{Cl}_8)\text{I}_4$ and bipyridyl (experiment 15, Table 5), a red-orange amorphous compound, which analyzes as a mono-bipyridyl complex, was obtained. It is unlikely that this compound affords a parallel with the amorphous material obtained for the dichloride because it showed a broad infra-red absorption band at 800 cm^{-1} and this is absent from the spectra of the chloride material. This band has been ascribed recently (though tentatively) to a

Mo-O-Mo vibration in the $(\text{Mo}_6\text{Cl}_8)^{4+}$ system (42).

2.5 Discussion

It is now apparent that both the history of the dichloride and the possible presence of strongly coordinated water are important in the reactions the dichloride undergoes with bipyridyl. In most cases, there are obtained mixtures of products which are mainly various crystalline forms of bipyridylum salts of the chloroacid and an amorphous component which is perhaps a mono-bipyridyl complex. In the light of these findings it is pertinent to discuss (a) the reasons for the unexpected behaviour and (b) results previously obtained for this system.

(a) Notes on the Course of the Reactions of Bipyridyl with $(\text{Mo}_6\text{Cl}_8)\text{Cl}_4$ and $(\text{Mo}_6\text{Cl}_8)\text{I}_4$ Until the source of protons is definitely established, it is difficult to propose mechanisms for these reactions.

Studies of the decomposition of bipyridyl complexes of cobalt(II) and nickel(II) chlorides illustrate the considerable stability of the ligand (66). Nevertheless, proton lability in the phenyl rings of a coordinated triphenylphosphine complex of a cobalt (I) compound has been observed (67) and so the possibility of bipyridyl as a proton source cannot be entirely disregarded.

A more likely source of protons, particularly under the more extreme conditions, is the degradation of the solvents. Indeed, decomposition of ethanol under mild conditions (25°C) to yield the carbon monoxide found coordinated in compounds of certain transition metals (e.g. iridium, ruthenium) has been well established by Vaska (68), Chatt and Shaw (69) and others (e.g. in $\text{RuBr}_3(\text{CO})(\text{Ph}_3\text{P})_2$) (68).

Undoubtedly, small amounts of water present could also yield the protons necessary for rapid bipyridylum salt formation. Considered in retrospect, it is apparent that water in small concentrations would be present even under the milder reaction conditions (solvent under reflux, 65°) although some steps were taken to ensure dry conditions (see Appendix A).

(b) Consideration of the Results of Previous Investigations Cotton and Curtis (30) have reported a somewhat analogous reaction product, relevant to this discussion. When they added an alcohol soluble silver salt to an alcohol solution of $(\text{Mo}_6\text{Cl}_8)\text{Cl}_4$, the initial precipitate was a yellow material containing "molybdenum and silver apparently as $\text{Ag}_2\text{Mo}_6\text{Cl}_{14}\cdot n\text{ROH}$ ", where ROH was the alcohol. These workers also experienced some difficulty in preparing stoichiometrically well defined compounds of $(\text{Mo}_6\text{Cl}_8)\text{Cl}_4$.

Both elemental analyses and conductivity data on products which are clearly mixtures are of little use in compound identification. Hence, some doubt is cast on the formulations of other ionic complexes (p. 13 and 16) obtained by Fergusson and others (33) with both polydentate and unidentate ligands, since these workers used similar preparative methods to those described in this study. It follows also, from the suggested mono-bipyridyl complex, that 1:1 complexes of $(\text{Mo}_6\text{Cl}_8)\text{Cl}_4$ and $(\text{Mo}_6\text{Cl}_8)\text{I}_4$ with polydentate ligands may be more common than the two reported by Robinson (for terpyridyl and diphosphine (55)).

In addition, the two-stepped potentiometric curve (55) of " $((\text{Mo}_6\text{Cl}_8)\text{I}_2(\text{Bipy})_2)\text{I}_2$ " with silver nitrate, in which six labile halogens were obtained (p. 14) must now be explained in terms of a mixture of compounds, one of which is the bipyridylium salt $(\text{BipyH})_2((\text{Mo}_6\text{Cl}_8)\text{I}_6)$.

Clark and others (34) have reported the preparation of the complexes $((\text{Mo}_6\text{Cl}_8)\text{Cl}_2(\text{L})_2)\text{Cl}_2$, (L = o-phen or diars), by the mixing of the ethanolic solutions of the ligand and the chloroacid, $(\text{H}_3\text{O})_2((\text{Mo}_6\text{Cl}_8)\text{Cl}_6) \cdot 6\text{H}_2\text{O}$. The formulation of the complex with o-phenanthroline, at least, seems unlikely in the light of the preceding results with bipyridyl.

It is noted that the choice of bipyridyl as a representative bidentate ligand was an unfortunate one because of its ability to protonate easily and, possibly, to act as a bridging ligand. Further research with bidentate ligands should be carried out with a less basic ligand, and in this respect, the diarsine complexes prepared by Clark et al. (34) suggest some experiments with this ligand might prove enlightening.

In spite of the unusual chemical behaviour observed, the six-fold coordination of the cluster appears to be maintained. Because of the complexity of the system studied, however, no additional evidence about the mode of polydentate coordination to the $(\text{Mo}_6\text{Cl}_8)^{4+}$ cluster was obtained.

2.6 Experimental Section

Most experimental measurements can be found in the summary Tables 2- 5, which should be used in conjunction with Appendix A. The following results are presented here because they apply specifically to this Chapter.

(1) Preliminary Study of Single Crystals of Product 3

The cell dimensions of the tetragonal unit cell were obtained by a least-squares refinement of all cell parameters using eight independent distances on a 2θ h l

wet film photograph taken on a calibrated precession camera (70). The final values were $\underline{a} = \underline{b} = 13.16(3)$, $\underline{c} = 27.66(2) \text{ \AA}$, (see footnote p.56).

The length of the c axis, coupled with the one-dimensional disorder perpendicular to it, made accurate setting of Weissenberg layers around this axis difficult. The systematic absences noted for the sharp reflections (71) were for 00l, $l \neq 2n$ and for hk0, $h + k \neq 2n$. There was some evidence that 100, 010 and 210 were present, however. These above absences are unique for the tetragonal space group $P4_2/n$ (number 86 (72(a))).

The density of a mixture of this form with other crystals (experiment 5(a), Table 2) was measured by the gradient tube method (72b) - some spread was observed but all crystals were within the $2.1 - 2.4 \text{ g cm}^{-3}$ range. The calculated density for four molecules/unit cell of molecular weight 1385, $((\text{BipyH})_2((\text{Mo}_6\text{Cl}_8)\text{Cl}_6))$, is 1.91 g cm^{-3} .

A feature of this crystal form of passing interest is that its space group, cell dimensions and density are apparently similar to the structure $(\text{H}_3\text{O})_2((\text{Mo}_6\text{Cl}_8)\text{Cl}_4(\text{OH})_2) \cdot 4\text{H}_2\text{O}$ examined by Brosset (14), in spite of the great difference in the nature of this compound.

(11) The Reactions of Bipyridyl with the Chloroacid,

$(H_3O)_2((Mo_6Cl_8)Cl_6).6H_2O$ Addition of bipyridyl to non-aqueous solutions of the chloroacid gives immediate yellow precipitates of various bipyridylium salts (Table 2(11)). Boiling the solvent under reflux usually converts these mixtures to the two "pure" salt forms (products 1 and 2), $(BipyH)_2((Mo_6Cl_8)Cl_6)$.

CHAPTER 3

REACTIONS OF $(\text{Mo}_6\text{Cl}_8)\text{Cl}_4$ AND $(\text{Mo}_6\text{Cl}_8)\text{I}_4$
WITH UNIDENTATE LIGANDS

A LIGAND OXIDATION

3.1 Introduction

Interest in the reactions of triphenylphosphine (Ph_3P) with molybdenum(II) chloride ($(\text{Mo}_6\text{Cl}_8)\text{Cl}_4$) stems from the original prediction of Sheldon's (22,24) that complexes of triphenylphosphine could not be formed. As pointed out on p.10, there appear to be no suitable filled d-orbitals on the molybdenum atoms for π -bonding with ligands. Choosing to disregard the known donor properties of triphenylphosphine, Sheldon apparently accepted his unsuccessful reaction attempts with triphenylphosphine as proof that π -bonding ligands will not coordinate to the $(\text{Mo}_6\text{Cl}_8)^{4+}$ cluster.

On the contrary, Robinson (55) reported that this ligand not only formed the normal bis-unidentate complex, $(\text{Mo}_6\text{Cl}_8)\text{Cl}_4(\text{Ph}_3\text{P})_2$, but promoted the formation of tris- and tetrakis- monodentate ligand complexes with $(\text{Mo}_6\text{Cl}_8)\text{Cl}_4$ such as $((\text{Mo}_6\text{Cl}_8)\text{Cl}_3(\text{Ph}_3\text{P})_3)^+\text{Cl}^-$ and $((\text{Mo}_6\text{Cl}_8)\text{Cl}_2(\text{Ph}_3\text{P})_2(\text{py})_2)^{2+}2\text{Cl}^-$. These latter "ionic" compounds seemed to provide good testing of the six-fold

Table 7: Isomorphous Compounds from the Reactions of $(Mo_6Cl_8)I_4$ with Ph_3P and Ph_3PO

<u>Expt. No.</u>	<u>Reactants</u>	<u>Solvent</u>	<u>Conditions of Reaction</u>	<u>Conductivity</u> $\Delta_m \cdot \Omega^{-1} cm^2$	<u>Elemental Analysis (%)</u>				
					<u>C</u>	<u>H</u>	<u>Mo</u>	<u>Cl</u>	<u>I</u>
3	MI_4, Ph_3P	T.H.F. (65°C) ³	Heated under Reflux	31.0 ^a 42.5 ^a	25.29	1.9	29.2	14.9 ^c	26.5 ²
4	MI_4, Ph_3P	EtOH (78.5°C) ³	Heated under Reflux 2.5 hours	23.8 ^a	25.33	2.1	30.2		
5	MI_4, Ph_3P	$CHCl_3$ (61°C) ³	Heated under Reflux ¹ 0.75 hours	13.9 ^b 11.8 ^a	20.80	1.7			
6	MI_4, Ph_3P	$CHCl_3$	Room temperature ¹ Addition Xs Pet. Ether	14.8 ^a	20.17	2.1			
7	MI_4, Ph_3PO	$CHCl_3$	Room Temperature Addition Xs Pet. Ether	22.4 ^a	22.04	1.7			
8	MI_4, Ph_3P	EtOH	Room Temperature	9.2 ^b	19.01	1.9			
9	MI_4, Ph_3P^e	$CHCl_3$	Heated under reflux	45.3 ^b	21.60	2.0		15.7	26.8
15	MI_4, Ph_3PO	EtOH	M.R. = 1.0: 6.0 Sealed Tube ⁴	19.0 ^a	22.88	1.8	31.4 ^c	14.8	24.6
16	MI_4, Ph_3PO, Ph_3P	EtOH	M.R. = 1.0: 6.2: 2.6 Sealed Tube ⁴	19.5 ^a	22.94	1.8			

Theoretical Analysis



< 55^a, < 15^b 22.45 1.6 29.9 14.8 26.4

KEY See Table 6; e = $(MI_2(Ph_3P)_2)2I$ (reference 55).

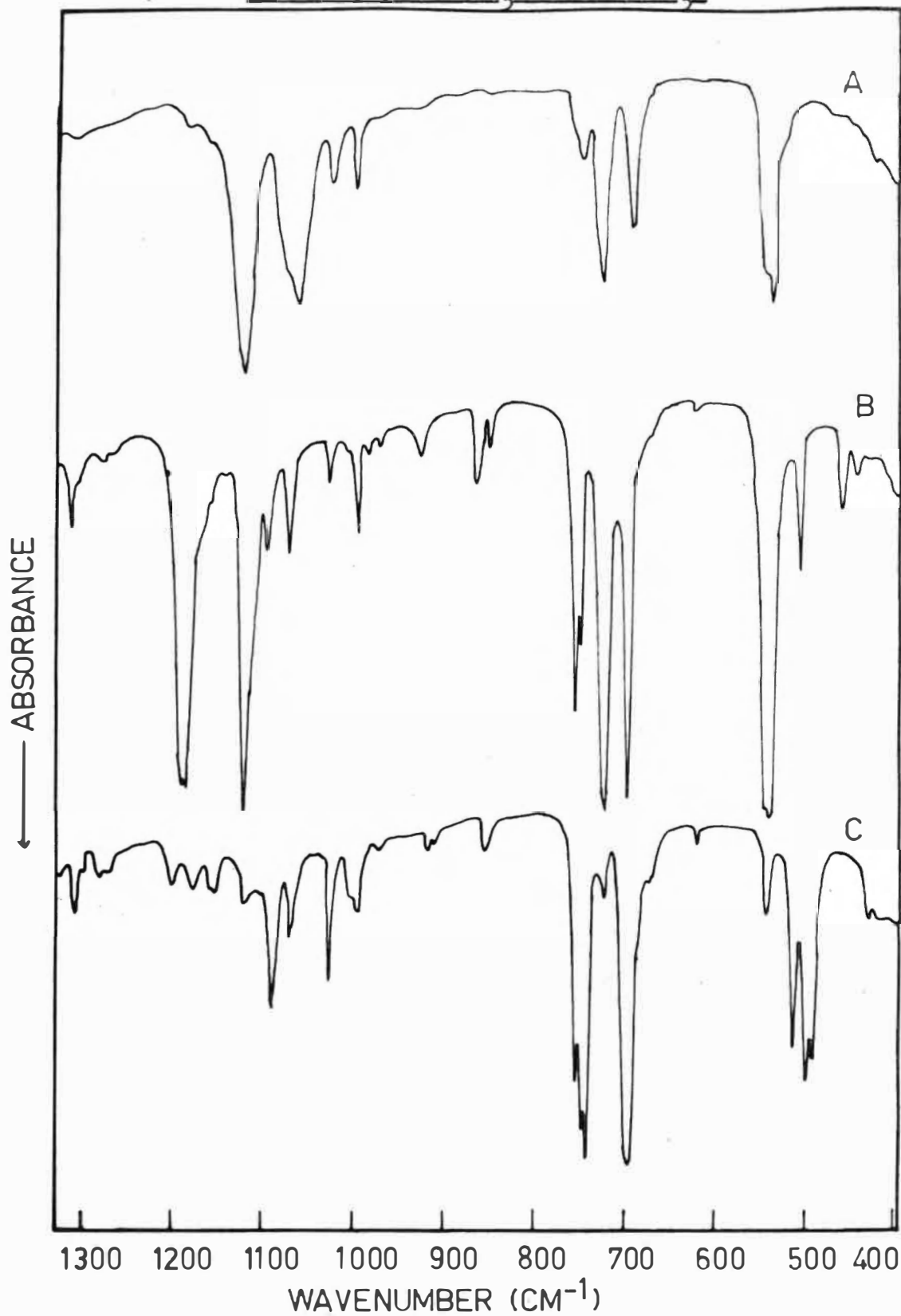
coordination of the $(\text{Mo}_6\text{Cl}_8)^{4+}$ cluster, and so a program of high temperature reactions in sealed tubes was undertaken for their preparation (as discussed in Section B of this Chapter). It was almost incidental to this plan that following an experiment in which both triphenylphosphine and triphenylphosphine oxide were present, systematic tests showed an unusual ligand oxidation had occurred.

5.2 Results and Discussion

As shown in Table 6, the reactions of $(\text{Mo}_6\text{Cl}_8)\text{Cl}_4$ with triphenylphosphine and triphenylphosphine oxide respectively yield compounds that give the same X-ray powder photograph. That is, the products are either isomorphous or identical. Further study of the reactions of $(\text{Mo}_6\text{Cl}_8)\text{I}_4$ with these two ligands (Table 7) indicated a similar pattern with again only one X-ray powder photograph resulting from all preparations. Although the quality of the X-ray powder photographs varied (presumably with the crystallite size of the products), accurate measurement of all visible lines confirmed these identifications.

Therefore, all these compounds could be either the oxidised ligand complexes $(\text{Mo}_6\text{Cl}_8)\text{X}_4(\text{Ph}_3\text{PO})_2$ or the reduced ligand complexes $(\text{Mo}_6\text{Cl}_8)\text{X}_4(\text{Ph}_3\text{P})_2$, where X =

Figure IV: Infra-red Spectra of A. $(Mo_6Cl_8)X_4(Ph_3PO)_2$
(X = Cl, I) B. Ph_3PO C. Ph_3P



Cl, I. On purely chemical grounds, both of these seemed, at that stage, equally likely. Neither the X-ray nor the analytical data served to distinguish between them. Thus it was not until the assignment of all major absorptions in the infra-red spectra ($1300-230\text{ cm}^{-1}$) of these compounds that they were identified as the oxidised ligand complexes, $(\text{Mo}_6\text{Cl}_8)_X(\text{Ph}_3\text{PO})_2$.

The reactions of triphenylarsine (Ph_3As) and triphenylarsine oxide (Ph_3AsO) with $(\text{Mo}_6\text{Cl}_8)\text{Cl}_4$ and $(\text{Mo}_6\text{Cl}_8)\text{I}_4$, summarised in Tables 8 and 9, followed an exactly analogous pattern. Again, infra-red assignments confirmed that only the oxidised ligand was present.

Infra-red Spectra Some difficulty was experienced initially in the interpretation of the unique infra-red spectrum observed for all the triphenylphosphine oxide complexes. Whereas the P-O stretching absorption ($\nu(\text{P-O})$) for the coordinated ligand is generally found between its value in the free ligand (1191 cm^{-1} (73)) and the phenyl mode vibration at 1122 cm^{-1} , no major absorption was observed in this region (see Fig. IV). Further, the Mo-O stretching band that might be expected to aid the identification of these compounds occurs in the far infra-red region ($500-200\text{ cm}^{-1}$). Metal-halogen stretching absorptions (in the cluster $(\text{Mo}_6\text{Cl}_8)^{4+}$)

Table 10 : Listing and Assignment of Major Bands of Infra-red Spectra of Ph_3P , Ph_3PO , $(\text{Mo}_6\text{Cl}_8)\text{Cl}_4(\text{Ph}_3\text{PO})_2$ and $(\text{Mo}_6\text{Cl}_8)\text{I}_4(\text{Ph}_3\text{PO})_2$ ^a

<u>Frequency Range</u>	<u>$(\text{Mo}_6\text{Cl}_8)\text{I}_4(\text{Ph}_3\text{PO})_2$</u>	<u>$(\text{Mo}_6\text{Cl}_8)\text{Cl}_4(\text{Ph}_3\text{PO})_2$</u>	<u>Assignments</u> ^b	<u>Ph_3PO</u>	<u>Ph_3P</u>
(1050-1200) cm^{-1}	1189 vw	1189 w	*		1178 w
	1163 vw	1161 w	*	1166vw	1154 vw
			*		1118 vw
	1124 vs	1124 vs	"mode q^c ", $\nu(\text{P-O})$	1122 vs	
	1097 vw		*	1095 m	1090 m
	1067 s	1067 s	$\nu(\text{P-O})$	1191 vs	-
	1056 m, sh		*	1072 m	1070 w
(680 - 800) cm^{-1}	759 w	761 w	*	752 m	745 vs
	746 m	748 m	*	747 m, sh	740 vs, 720 w
	728(s)	728 s	"mode r"	719 vs	698, 692 vs ^c
	693 m	695 m	*	695 vs	
(400 - 600) cm^{-1}	544 m	545 m, sh	$\nu_{\text{as}}(\text{C-P})$		
		538 s		541 vs	
	453 w	470 w	"mode t"	457, 451 w	433 w
		440 br, vw	$\nu_{\text{s}}(\text{C-P})$	445 w, br	423 w
	420 m, br	420 m	$\nu(\text{Mo-O})^d$		

^a See Fig. IV; Relative intensities within that particular spectrum are listed after each band.

^b See Jensen and Nielsen (73).

^c See Deacon and Green (78)

^d Tentative assignment.

m = medium

w = weak

s = strong

v = very

br = broad

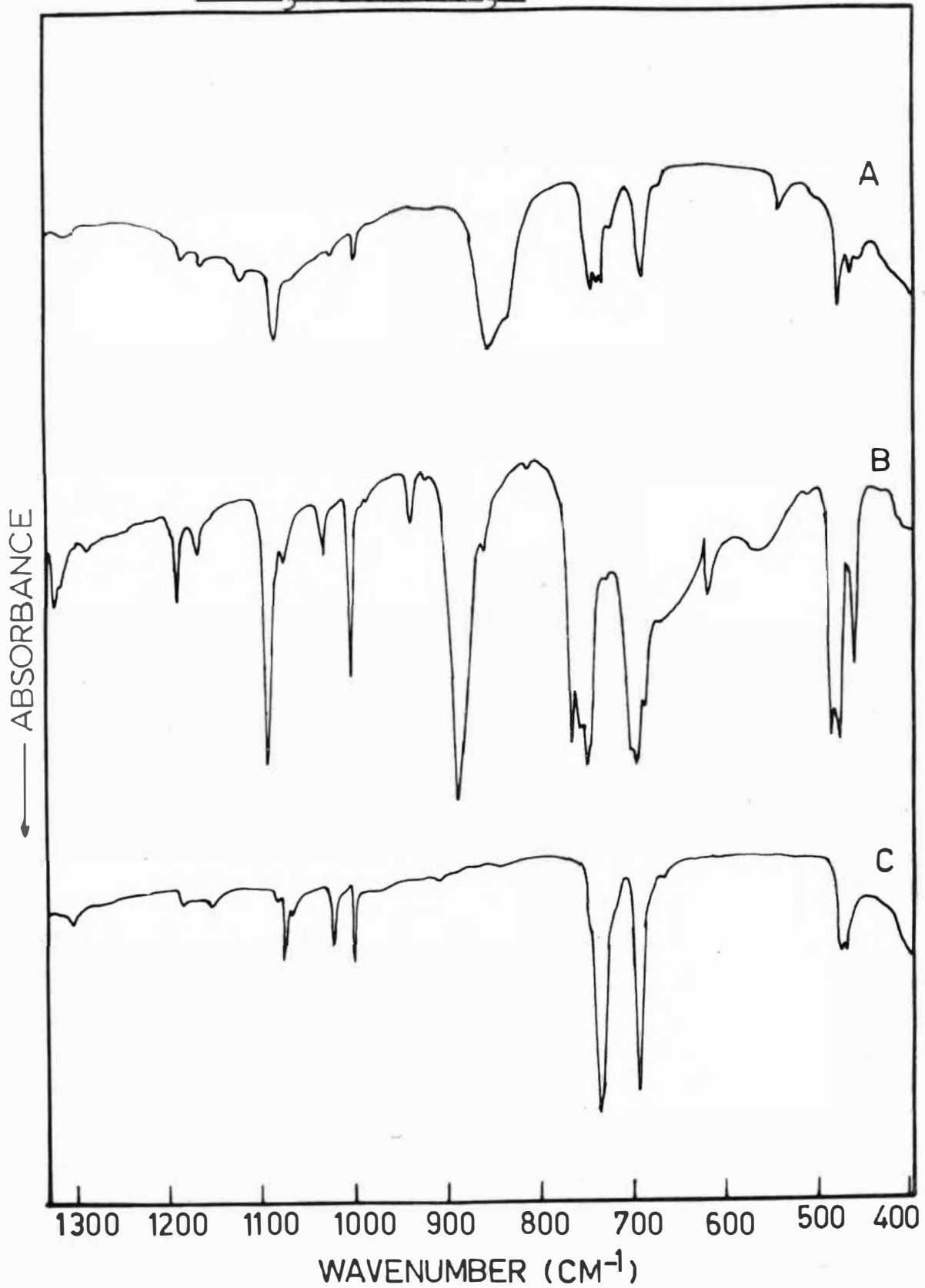
* = phenyl mode vibrations

dominate the spectra in this region (35). Some comparisons with spectra of known compounds and the clear differentiation of the phenyl vibration modes (73) was therefore necessary. The assignments (Table 10) confirmed that only triphenylphosphine oxide is present in the compounds.

Although Sheldon had assigned the $\nu(\text{P-O})$ frequency in the complex $(\text{Mo}_6\text{Cl}_8)\text{Cl}_4(\text{Ph}_3\text{PO})_2$ at 1071 cm^{-1} (26), this is considerably lower than Cotton, Barnes and Bannister (74) suggest is normal ($1121 - 1161 \text{ cm}^{-1}$). This normal displacement on coordination corresponds to strong metal-oxygen bonds (i.e. considerable reduction in P-O bond order). These latter authors also reported that broadening and splitting of the $\nu(\text{P-O})$ frequency can be caused by coupling of the vibrations (giving asymmetric and symmetric bands) or by non-equivalence in the ligand environments.

Wilkins and Haendler (76), in fact, state that the P-O frequency in the six-coordinate tin (IV) halide complexes of triphenylphosphine oxide is represented by at least two bands at 1137 cm^{-1} and 1082 cm^{-1} . A similar splitting has also been noted for the octahedral trimethylphosphine oxide complexes of tin (IV) halides (77), which are less complicated in the region in which the $\nu(\text{P-O})$ frequency occurs.

Figure V: Infra-red Spectra of A. $(\text{Mo}_6\text{Cl}_8)_4(\text{Ph}_3\text{AsO})_2$ ($X = \text{Cl, I}$)
B. Ph_3AsO C. Ph_3As



Significantly, the C-H in-plane deformation mode absorption (1122 cm^{-1}) is considerably enhanced in these compounds with its maximum at 1124 cm^{-1} . It is therefore a reasonable inference that a second component of the P-O stretching frequency is coincident with this ligand band. The other component is observed as a strong absorption at 1067 cm^{-1} . This latter band, while clearly identifiable, lies very close to two other phenyl absorptions at 1072 cm^{-1} and 1095 cm^{-1} (see Fig. IV and Table 10).

These assignments were further checked by spectral comparison with some known triphenylphosphine complexes (e.g. $\text{CdCl}_2(\text{Ph}_3\text{P})_2$ (42)). The identification of the so-called "X-sensitive" modes (labelled "q, r and s" types) as outlined by Deacon and Green (78) also confirmed that only triphenylphosphine oxide and not triphenylphosphine complexes had been prepared.

Assignments of observed absorptions in the triphenylarsine oxide spectra (see Fig. V) were more easily made since the only major difference between triphenylarsine and triphenylarsine oxide spectra is the As-O stretching frequency found at 881 cm^{-1} (73). This band in coordination compounds usually appears in a region ($800-900\text{ cm}^{-1}$) that is clear of other bands of any great strength. (74).

The compounds in this study were therefore readily identified as triphenylarsine oxide complexes from the

Table 8: Isomorphous Compounds from the Reactions of $(Mo_6Cl_8)Cl_4$ with Ph_3As and Ph_3AsO

<u>Experiment Number</u>	<u>Reactants</u>	<u>Solvent</u>	<u>Conditions of Reaction</u>	<u>Conductivity</u> $\Lambda_m, \Omega^{-1} cm^2$	<u>Elemental Analyses (%)</u>			
					<u>C</u>	<u>H</u>	<u>Mo</u>	<u>Cl</u>
10	MCl_4, Ph_3As	T.H.F.	Heated under Reflux 1.5 hours					
17	$MCl_4, Ph_3AsO,$ Ph_3P	EtOH	M.R. = 1.0: 6.0: 2.5 Sealed Tube ⁴	17 ^{a,c}	26.89	2.0	33.7	24.5
18	MCl_4, Ph_3AsO	EtOH	M.R. = 1.0: 6.2 Sealed Tube ⁴		27.01	2.0	34.7	24.8

Theoretical Analysis

$MCl_4(Ph_3AsO)_2$	$< 55^a, < 15^b$	26.25	1.8	35.0	24.7
--------------------	------------------	-------	-----	------	------

KEY See Table 6

occurrence of the $\nu(\text{As-O})$ frequency at 855 cm^{-1} (Fig. V). A similar check of other absorptions confirmed such an assignment (73).

In line with the observation of Cotton and others (74), the $\nu(\text{As-O})$ shift in frequency on coordination is smaller (26 cm^{-1}) than the $\nu(\text{P-O})$ shift ($67, 124\text{ cm}^{-1}$). A 420 cm^{-1} band is tentatively assigned to the $\nu(\text{Mo-O})$ frequency, although confirmation of this, for example by isotopic substitution, is necessary. Cotton and Curtis (30) have assigned $\nu(\text{Mo-O})$ bands in this region.

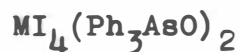
The Source of the Oxygen Three possible sources of oxygen exist: atmospheric oxygen dissolved in the solvents, the chemically bound oxygen in the solvents (e.g. in ethanol) and finally any moisture which might be present. Calculations of oxygen dissolved in the solvents used (65) indicated insufficient dissolved gas would be present for complete oxidation of the coordinated ligand. For example, in experiment 6, Table 7, just over half (2.5 cm^3) of the necessary oxygen (4.5 cm^3) would be present as dissolved gas (79). Further examination of these possibilities, discussed below, was carried out by P.F. Snowden in this department (42).

An attempted preparation of the triphenylphosphine adduct with deoxygenated tetrahydrofuran gave the oxidised ligand. The same result was obtained even when small

Table 9: Isomorphous Compounds from the Reactions of $(Mo_6Cl_8)I_4$ with Ph_3AsO and Ph_3As

<u>Expt. No.</u>	<u>Reactants</u>	<u>Solvent</u>	<u>Conditions of Reaction</u>	<u>Conductivity</u> $\Delta_m, \Omega^{-1} cm^2$	<u>Elemental Analysis (%)</u>				
					<u>C</u>	<u>H</u>	<u>Mo</u>	<u>Cl</u>	<u>I</u>
11	MI_4, Ph_3As	$CHCl_3$	Room Temperature ¹ Addition Xs Pet. Ether						
12	MI_4, Ph_3As	$CHCl_3$ (61°C) ³	Heated under reflux 1.5 hours Addition Xs Pet. Ether		21.81	1.7			
19	MI_4, Ph_3AsO	EtOH	M. R. = 1.0: 6.0 Sealed Tube ⁴	4.7 ^b	21.91	1.7	29.5	13.7	23.8
20	$MI_4, Ph_3AsO,$ Ph_3P	EtOH	M. R. = 1.0:6.4:2.5 Sealed Tube ⁴	46.0 ^a	22.07	1.6			

Theoretical Analysis



< 55^a
< 15^b

21.47 1.5 28.6 14.1 25.2

KEY See Table 6

amounts of peroxide impurity had been carefully removed from this solvent. Similarly, the use of specially dried and deoxygenated ethanol as solvent gave the oxidised ligand. It follows that the oxidation cannot be attributed to impurities containing oxygen in the solvent nor free oxygen in the system.

Snowden's general conclusion was therefore that the formation of triphenylphosphine oxide adducts is highly favoured in these systems even to the extent of abstracting oxygen from the solvent molecules. However the formation of triphenylphosphine and triphenylarsine complexes of $(\text{Mo}_6\text{Cl}_8)\text{Cl}_4$ was finally attained by the use of a dry deoxygenated solvent which did not contain any bound oxygen (trichloroethylene) in tubes sealed under an atmosphere of dry nitrogen.

Because the dichloride is not soluble in this solvent, the sealed tubes were heated to 150°C over 48 hours to give more complete reactions. Although the products so obtained did not give carbon analysis figures corresponding to the pure bis- complexes (42), they did give the infra-red absorption spectra for coordinated triphenylarsine and triphenylphosphine compounds. Corresponding reactions with $(\text{Mo}_6\text{Cl}_8)\text{I}_4$ were performed in dry deoxygenated chloroform in which

the tetraiodide was soluble. Again the triphenylarsine- and triphenylphosphine-coordinated complexes were obtained although small yields precluded complete analyses.

Identification of the Triphenylphosphine Oxide Complexes and Conditions for their Preparation

It did not always prove easy to obtain analytically-pure samples of the bis-triphenylphosphine oxide complexes of molybdenum(II) halides (see Table 7). Both the nature of the ligand oxidation (in triphenylphosphine experiments) and the difficulties of recrystallization of the products apparently work against the preparation of "pure" compounds. Nevertheless, some success was experienced in the reactions of triphenylphosphine oxide under carefully chosen conditions as indicated in Tables 6 and 7.

Conclusion This oxidation must cast serious doubt on the exact identity of all previously reported triphenylphosphine complexes (33,55). The conditions of preparation of these latter compounds suggest that the oxidised ligand would have been present at least to some extent. In particular, the crystalline product of composition $((\text{Mo}_6\text{Cl}_8)\text{I}_2(\text{Ph}_3\text{P})_2)_2\text{I}$ (55) as shown in Table 7 had the same powder photo as the $(\text{Mo}_6\text{Cl}_8)\text{I}_4(\text{Ph}_3\text{PO})_2$ samples and this must be reformulated in terms of the

oxidised ligand. Unfortunately, none of the infrared spectra of the other triphenylphosphine compounds prepared by Robinson (55) are available. Hence no more extensive corrections to their triphenylphosphine formulations can be made.

B OTHER MONODENTATE COMPLEXES OF $(\text{Mo}_6\text{Cl}_8)\text{Cl}_4$ AND $(\text{Mo}_6\text{Cl}_8)\text{I}_4$

5.3 Introduction

Mention has been made of "ionic" compounds prepared by reactions in which suitable monodentate ligands, notably triphenylphosphine, were heated under extreme conditions with $(\text{Mo}_6\text{Cl}_8)\text{Cl}_4$ (p.39). The characteristic of these preparations as interpreted by previous workers (33) is the ionization of one or more of the terminally-bound halogens to the $(\text{Mo}_6\text{Cl}_8)^{4+}$ cluster in the starting materials $(\text{Mo}_6\text{Cl}_8)\text{Cl}_4$ or $(\text{Mo}_6\text{Cl}_8)\text{I}_4$. Thus, six-fold coordination to the $(\text{Mo}_6\text{Cl}_8)^{4+}$ is maintained. These following experiments were aimed at testing the validity of this interpretation, using various oxo-ligands (viz. triphenylphosphine oxide, triphenylarsine oxide and pyridine-N-oxide).

5.4 The Preparation of "Ionic" Complexes

Although a series of reactions under extreme conditions similar to those reported by Robinson (55) were carried out only one compound of the type sought was obtained. In contrast to these conditions, two further "ionic" products were isolated for a similar reaction system under milder conditions (room temperature). The experimental results of this section are thus presented

Table 11: Further Analyses of Sealed Tube Experiment Products⁴

No.	Reactants	Molar Ratios (M.R.)	Elemental Analyses (%)				I	Conductivity $\Delta_{\text{m}}, \Omega^{-1} \text{cm}^2$	Possible Formulation
			C	H	Mo	Cl			
21	$\text{MCl}_4, \text{pyNO}$	1:8.2	12.42 ^{aa}	1.3 ^c	45.4	34.9	-	20.1 ^{a,c}	mixture $\text{MCl}_4(\text{pyNO})_{2.5}$
22	$\text{MCl}_4, \text{pyNO}, \text{Ph}_3\text{P}$	1:6.7:3.1	15.8 ^c	1.6 ^c	42.4	32.8	-	28.1 ^{a,c}	mixture $\text{MCl}_4(\text{pyNO})_{3.5}$
23	$\text{MI}_4, \text{pyNO}, \text{Ph}_3\text{P}$	1:5.2:2.7	13.88 ^a	1.3 ^c	33.4 ^{aa}	19.3	20.2	134 ^{a,c}	$(\text{MI}_2(\text{pyNO})_4)\text{I}_2$
24	MI_4, pyNO	1:10.0	11.0	1.0	41.4	19.5	15.0	33 ^{a,d}	$(\text{MI}_2(\text{pyNO})_3)\text{O}^f$

Theoretical Analyses

$\text{MCl}_4(\text{pyNO})_2$	10.07	0.8	48.3	35.7		< 55 ^a
$(\text{MCl}_3(\text{pyNO})_3)\text{Cl}$	14.00	1.2	40.9	33.1		60-80 ^a
$(\text{MCl}_2(\text{pyNO})_4)\text{Cl}_2$	17.37	1.4	38.1	30.8		110-140 ^a
$\text{MI}_4(\text{pyNO})_2$	7.70	0.6	37.0	18.2	32.6	< 55 ^a
$(\text{MI}_3(\text{pyNO})_3)\text{I}$	10.89	0.9	34.8	17.2	30.7	60-80 ^a
$(\text{MI}_2(\text{pyNO})_4)\text{I}_2$	13.71	1.1	33.0	16.2	29.1	110-140 ^a

KEY See Table 6 ; except f = contains 800 cm^{-1} broad adsorption in infra-red spectrum.

in two parts.

(a) Experiments in Sealed Tubes at Elevated Temperatures

A series of sealed tube experiments were conducted in which triphenylarsine oxide, pyridine-N-oxide, triphenylphosphine oxide and triphenylphosphine were reacted with $(\text{Mo}_6\text{Cl}_8)\text{Cl}_4$ or $(\text{Mo}_6\text{Cl}_8)\text{I}_4$ (see Appendix A). Even though the reactants were subjected to temperatures of 130° for 5-9 hours, only one "ionic" compound was prepared, $((\text{Mo}_6\text{Cl}_8)\text{I}_2(\text{pyNO})_4)_2\text{I}$. The details of these reactions and their product analyses (experiments 13-24) are contained in Tables 6-9 in the previous Section of this Chapter and Table 11 in this Section.

The above tetrakis-pyridine-N-oxide complex was a 2:1 electrolyte in dimethylformamide (experiment 23, Table 11) and was prepared from the reaction of $(\text{Mo}_6\text{Cl}_8)\text{I}_4$ and pyridine-N-oxide in the presence of triphenylphosphine. Its infra-red spectrum was normal for coordinated pyridine-N-oxide (80), with shifts of 42 cm^{-1} in the N-O stretching frequency and 11 cm^{-1} in the N-O bending frequency (to lower values).

Evidence of progressive substitution of pyridine-N-oxide was also found for the other experiments with this ligand (Table 11). Thus these latter products analyzed with compositions intermediate between bis-, tris- and tetrakis- coordination to the $(\text{Mo}_6\text{Cl}_8)^{4+}$ cluster.

It was assumed in all these sealed tube experiments that the basic cluster $(\text{Mo}_6\text{Cl}_8)^{4+}$ was intact. Positive evidence for this was difficult to find. Thus, the rather poor ultra-violet-visible reflectance spectra obtained for these products (65) could be described in terms of the general bands characterized for the $(\text{Mo}_6\text{X}_8)^{4+}$ system (33). It must be reported that, in one case, an 800 cm^{-1} broad absorption (p. 32) was found in the infra-red spectrum obtained for one product of these reactions (experiment 24). This suggests some decomposition of the starting material, $(\text{Mo}_6\text{Cl}_8)\text{I}_4$, may have occurred.

Nevertheless, the normal bis-monodentate complexes $(\text{Mo}_6\text{Cl}_8)\text{X}_4\text{L}_2$, where X is Cl, I and L is Ph_3AsO or Ph_3PO , were obtained in the sealed tube experiments (numbers 13-20) involving these ligands and the appropriate molybdenum(II) halide. These are non-electrolytes and have been dealt with in detail in Section A of this Chapter.

(b) Reactions at Lower Temperatures Two "ionic" complexes were isolated from reactions at room temperature for slightly different systems from those described above. The analytical details for these are presented in sub-section 5.4.

The complex formulated as $((\text{Mo}_6\text{Cl}_8)\text{I}_3(\text{Ph}_3\text{PO})_2^- (\text{py}))\text{I}$ was prepared by the room temperature solution of $(\text{Mo}_6\text{Cl}_8)\text{I}_4(\text{Ph}_3\text{PO})_2$ in pyridine. Both coordinated triphenylphosphine oxide (Section A of this Chapter) and pyridine (81) were observed in the infra-red spectrum of this compound. The absorption bands of the pyridine decreased in relative intensity on pumping the compound under high vacuum. Presumably the compound was losing pyridine, although it was not proved whether continuous pumping would yield the starting material, $(\text{Mo}_6\text{Cl}_8)\text{Cl}_4-(\text{Ph}_3\text{PO})_2$.

The other "ionic" product separated from saturated ethanol solutions of $(\text{Mo}_6\text{Cl}_8)\text{I}_4$, triphenylphosphine oxide and triphenylarsine oxide at room temperature. The infra-red spectral analysis of the product indicated that both these ligands were present and coordinated to the $(\text{Mo}_6\text{Cl}_8)^{4+}$ cluster. Although this product is clearly of the $((\text{Mo}_6\text{Cl}_8)\text{I}_3(\text{L})_3)^+\text{I}^-$ type (L is a unidentate ligand). by conductivity measurements, the exact proportion of the two ligands in the total product is not defined by the analytical data.

Although it is not easy to produce these "ionic" compounds, the three products prepared support the interpretation made by Fergusson and others (33) of terminal-halogen ionization (p. 39). However, it is much more difficult than these previous investigations indicated to anticipate the exact conditions in which such complexes will be formed.

In the majority of tris- and tetrakis-unidentate complexes that have been characterized, one of the ligands has been considerably smaller in physical size than the other (e.g. pyridine and triphenylphosphine oxide). Thermal dissociation related to steric hindrance effects may therefore be a factor in the high temperature reactions of large unidentate ligands with molybdenum(II) halides.

5.4 Preparative Details of the Two Ionic Complexes Prepared at Lower Temperatures

Triiodo-bis(triphenylphosphine oxide)-pyridine-octa- μ_3 -chlorohexamolybdenum(II) iodide To $\text{Mo}_6\text{Cl}_8\text{I}_4(\text{Ph}_3\text{PO})_2$ (90 mgm) was added 2 ml of dry pyridine. The yellow starting material was rapidly converted to a bright orange solid which dissolved to form an orange solution. The pyridine was removed in vacuo, washed with pet. ether and ether, and dried (5 minutes) in vacuo.

Further pumping (1 hour) under vacuum resulted in loss of pyridine (by the infra-red spectral bands). Yield estimated 80%. Found: C = 23.2, H = 2.0, Cl = 14.7, I = 23.2. $C_{41}H_{35}Cl_8I_4P_2Mo_6N$: C = 24.5, H = 1.8, Cl = 14.2 I = 25.3,%. Conductivity: In nitrobenzene, $C = 0.42 \times 10^{-3}M$, specific conductivity = $10.6 \times 10^{-5} \text{ ohm}^{-1} \text{ cm}^{-1}$, hence $\Lambda_m = 24.5 \text{ ohm}^{-1} \text{ cm}^2$. X-rays: Crystalline, but broad, $d > 8 \text{ \AA}$, powder lines only.

Triiodo-bis(triphenylarsine oxide)-triphenylphosphine oxide-octa- μ_3 -chlorohexamolybdenum(II) ^{iodide} ~~dichloride~~

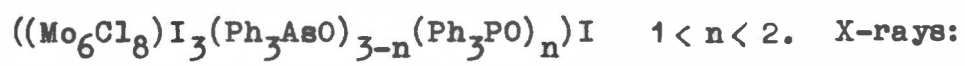
The filtrates remaining from the sealed tube experiments (numbers 15, 16, 19 and 20) were left standing in a 500 ml beaker. This compound, which settled out of the solutions, must therefore be formed by mixing of saturated ethanol solutions of $(Mo_6Cl_8)I_4$, Ph_3PO and Ph_3AsO .

The compound was soluble in dimethylsulphoxide, dimethylformamide and acetone. Found: C = 27.4, H = 2.1,

Mo = 25.3, I = 19.1, Cl = 14.5. Calculated: $Mo_6Cl_8I_4$
 $C_{54}H_{45}As_2P_1O_3$: C = 28.3, H = 2.0, Mo = 25.2, I = 22.2,
 Cl = 12.4. Calculated: $Mo_6Cl_8I_4C_{54}H_{45}As_2P_1O_3$: C =
 28.8, H = 2.0, Mo = 25.7, I = 22.6, Cl = 12.6, %.

Conductivity: In dimethylformamide, $C = 0.46 \times 10^{-3}M$, specific conductivity = $36.8 \times 10^{-3} \text{ ohm}^{-1} \text{ cm}^{-1}$, hence $\Lambda_m = 77.0 \text{ ohm}^{-1} \text{ cm}^2$.

Formulation of Bulk Product:



Crystalline; diffuse powder lines observed with
d-spacings $> 8 \text{ \AA}$.

CHAPTER 4

THE SINGLE CRYSTAL X-RAY STRUCTURAL ANALYSES OF TWO ISOMORPHOUS SALTS, $(C_{10}H_9N_2)_2((Mo_6Cl_8)X_6)$, $X = Cl, I$

4.1 Experimental Details: Bis(bipyridylium) hexachloro-octa- μ_3 -chlorohexamolybdate(II)

Yellow crystals of two forms of bis(bipyridylium) hexachloro-octa- μ_3 -chlorohexamolybdate(II), $(C_{10}H_9N_2)_2((Mo_6Cl_8)Cl_6)$, subsequently referred to as Cl(A) and Cl(B), were prepared by methods described in Chapter 2 (Experiment 2, Table 2; these are products 2 and 1 respectively, in Table 3). Preliminary X-ray and optical examinations showed that the two forms Cl(A) (3%) and Cl(B) (30%) were present in a powder matrix. Both forms exhibited the normal extinction of birefringent crystals but could be easily distinguished under the polarizing microscope. The crystal structure analysis of Cl(B) is dealt with in Chapter 5.

The cell constants a , c and β were obtained from a least-squares refinement of the setting angles of 23 strong $h0l$ reflections ($2\theta \leq 85^\circ$) accurately aligned using a pinhole collimating system on a Supper equi-inclination diffractometer. These were subsequently confirmed by a least-squares refinement of all the cell

parameters using 44 independent distances between Friedel pairs on h0l, hk0 and Okl precession photographs taken on a calibrated camera (70). Final values of cell constants were $a = 9.853(4)$, $b = 16.35(1)$, $c = 11.93(1)$ Å; $\beta = 104.12(4)^\circ$ (see Footnote below). All measurements were made at room temperature (20°C), with CuK α radiation, $\lambda = 1.5418$ Å. Unfortunately, accurate values for all these constants were not available during data collection. An incorrect b value was used to calculate equi-inclination angles and this led to errors which are discussed later in this Chapter.

Precession photographs of zero and upper reciprocal lattice levels indicated monoclinic symmetry. The cell finally chosen had systematic absences h0l when $h + l \neq 2n$ and Ok0 when $k \neq 2n$. These absences are uniquely consistent with space-group $P2_1/n$. The density of the crystals was measured as 2.39 ± 0.08 g cm $^{-3}$ using a calibrated gradient tube made up of carbon tetrachloride and bromoform (72b). The range indicated was that obtained for standard solids. For two formula units in

Footnote: Figures quoted in parentheses throughout this thesis are estimated standard deviations (esd's) in the least significant digits derived from the inverse matrix in non-linear least-squares refinement procedures.

the cell the calculated density is 2.45 g cm^{-3} . Since the general multiplicity of $P2_1/n$ is four, the formula unit must have a centre of symmetry.

All crystals were thin tabular (101), elongated along b. The specimen used for collecting intensities was of approximate dimensions $0.13 \times 0.12 \times 0.03 \text{ mm}^3$. Its shape could be geometrically defined by eight intersecting planes, measured to an accuracy of $\pm 0.015 \text{ mm}$, for absorption corrections. The mosaicity of the crystal was found to be satisfactory from the analysis of ω -scans of several reflections (82). The linear absorption coefficient for the $\text{CuK}\alpha$ radiation used was 261.2 cm^{-1} (72c); transmission coefficients ranged from 0.13 to 0.52. Intensity data were collected on a Buerger single crystal Supper diffractometer (see Appendix C). An ω -scan rate of 1.667 degrees/minute was used and corrections were made, as indicated in the appendix, to those reflections for which printout interrupted the scan. The receiving aperture size, selected to minimize extraneous background and limit the time of collection, was circular, 2.1mm in radius, positioned 64 mm from the crystal. The counter was positioned in 3 degree increments of γ , up to 93.5 degrees, for all reciprocal lattice layers h0l-h9l. The pulse height analyzer was set to pass about 85% of

the CuK α radiation for a take-off angle of 4.5 degrees.

Sixteen reflections, well separated in reciprocal space, were monitored as standards throughout the analysis. No crystal deterioration was detected in the data collection, although random drifts in the electronics were noted over periods of several days. These standards were used to internally correlate the data set.

The two accessible equivalent reflections of the monoclinic system were collected. In all, 2836 reflections were recorded; the intensity data were corrected for background and assigned standard deviations according to the formulae (83):

$$\sigma(I) = (CT + 0.5 (B_1 + B_2) + (pI)^2)^{\frac{1}{2}}$$

where CT is the total integrated count, B_1 , B_2 are the two integrated background counts, p is a factor introduced to avoid overweighting the very strong reflections, and I , the intensity, is given by $I = CT - 0.5 (B_1 + B_2)$. The absolute weighting scheme used was $w = 1/(\sigma)^2$, where w is the weight of a reflection with standard deviation, σ . The factor p was initially chosen as 0.05 but, on the basis of a statistical analysis of the agreement factors calculated for ranges of intensity, was ultimately changed to 0.09.

Values of I were next reduced to values of F^2 by application of Lorentz-polarization and absorption corrections. The intensities of equivalent reflections were then averaged to yield 1418 independent reflections. The standard deviation of an average intensity was taken as the larger of the individual estimates or the range estimate (83). When the range estimate exceeded the average estimate by more than a factor of 3.0, the individual measurements were re-examined for possible collection errors; the resulting independent set consisted of 1379 averaged reflections, plus 39 reflections observed only once. The latter reflections were down-weighted by scaling their calculated standard deviation values by $\sqrt{2}$. Only the 842 reflections with intensities greater than their standard deviations were used in subsequent analysis; the remaining 576 reflections were regarded as not above background.

4.2 Experimental Details: Bis(bipyridylum) hexaiodo-octa- μ_3 -chlorohexamolybdate(II)

Crystals of bis(bipyridylum) hexaiodo-octa- μ_3 -chlorohexamolybdate(II), $(C_{10}H_9N_2)((Mo_6Cl_8)I_6)$, hereafter I, were prepared as described in Chapter 2 (Experiment 17). The orange plates were only about 5 per cent of the yield, some of the remainder being red crystalline

powder, which gave the same X-ray powder lines. The crystals were difficult to separate from the powder.

The cell parameters, a , c and β , were obtained by the method outlined above (p.55) except 26 reflections were involved in the least-squares refinement.

Separate least-squares refinements of appropriate parameters, using distances between Friedel pairs from uncalibrated $hk0$ (10 reflections) and $0kl$ (16 reflections) precession photographs, resulted in systematically lower values. Subsequent calibration and correction for film shrinkage produced satisfactory agreement between the dimensions obtained by these two methods. All measurements were made at room temperature 20°C , using $\text{CuK}\alpha$ radiation $\lambda = 1.5418 \text{ \AA}$. Final values of cell constants were $a = 10.23(1)$, $b = 16.74(6)$, $c = 12.36(2) \text{ \AA}$; $\beta = 103.3(1)^{\circ}$.

Precession photographs ($hk0$, $0kl$) and Weissenberg photographs ($h0l$, $h1l$, $h2l$) established the same systematic absences as for Cl(A) . The observed density was found to be slightly greater than 2.9 g cm^{-3} by flotation. This is consistent with the calculated density for two formula units per cell (3.12 g cm^{-3}). All these data demonstrate that the compounds Cl(A) and I are isomorphous. This fact was not immediately obvious, even in hindsight, from their powder photographs.

An elongated plate with approximate dimensions $0.18 \times 0.08 \times 0.04 \text{ mm}^3$ was washed free of powder and mounted with the longer face parallel to the goniometer head axis. The crystal shape could be geometrically defined by nine intersecting planes, measured to an accuracy of $\pm 0.015 \text{ mm}$, for absorption corrections. The crystal habit was the same as for the Cl(A) crystal.

Reciprocal lattice levels $h0l$ - $h1l$ were collected and mechanically integrated onto multiple films using a Nonius Weissenberg camera with $\text{CuK}\alpha$ radiation at room temperature. Only reflections up to a Bragg angle of 50.0 degrees were measured. Very few reflections were observed above the diffuse background at higher angles. The plateaux of 1363 reflections, and adjacent background areas, were measured using a single beam photometer and a galvanometer calibrated to read intensities directly. A further 507 reflections, too weak to measure, were not included in the structure refinement.

Correlation data, for scaling the Weissenberg layers, were collected manually on the diffractometer described (Appendix C) using the same crystal. The data were recorded over a continuous period of 18 hours, with sample reflections used to check counter stability.

For each layer, a simple average of ratios from 5-10 measured reflections was used for the correlation. This method was quite satisfactory for most reciprocal lattice layers as shown by the final agreement factor analyses. The exception was the h11l layer for which the 5 medium to weak reflections did not give a very good scaling ratio.

The intensities were corrected for Lorentz and polarization effects and for absorption. The linear absorption coefficient was 544.7 cm^{-1} (72c) and calculated transmission coefficients ranged from 0.05 to 0.20. The weighting scheme finally used in the structure refinement was:

$$w = 1/(A + B F_0 + C F_0^2 + D F_0^3)$$

where w is the weight of a reflection with observed structure factor F_0 , $A = 147.9$, $B = -0.405$, $C = 0.0055$ and $D = -0.000002$.

4.3 Solution and Refinement of the Structures

In the full matrix least-squares refinements the function minimized for refinement on F_0 was $\sum w (|F_0| - |F_c|)^2$ and on F_0^2 was $\sum w (F_0^2 - F_c^2)^2$, where $|F_0|$ and $|F_c|$ are the observed and calculated structure amplitudes and w is the weight for each reflection. The agreement factors R_1 , R_2 and R_3 are defined as $R_1 = \sum (||F_0| - |F_c||) / \sum |F_0|$, $R_2 = (\sum w (|F_0| - |F_c|)^2 / \sum w |F_0|^2)^{1/2}$ and $R_3 =$

$$\Sigma (|F_o^2 - F_c^2|) / \Sigma F_o^2.$$

The scattering factor tables used for chlorine, nitrogen and carbon were those tabulated for self-consistent wave functions and for molybdenum and iodine for the Thomas-Fermi-Dirac Statistical model (72d). The values of $\Delta f'$ and $\Delta f''$ for molybdenum, chlorine and iodine, used for correcting for anomalous dispersion (84), were those given by Cromer (85).

Although the isomorphous replacement method was inapplicable because of the unknown positions of the replaceable atoms, the isomorphous nature of the two crystals permitted use of the difference Patterson procedure. Since this latter method is not regularly used in X-ray crystallography, it is briefly outlined.

The Difference Patterson The Patterson function, $P(u,v,w)$, can be evaluated at a series of points u,v,w filling the unit cell at regular intervals using the expression

$$P(u,v,w) = \frac{1}{V_c} \Sigma_h \Sigma_k \Sigma_l |F(hkl)|^2 \cos 2\pi(hu + kv + lw)$$

where V_c = volume of the unit cell, and $|F_{hkl}|^2$ is proportional to the observed intensity (72e). In a continuous Patterson synthesis, peaks occur at the ends of vectors from the origin which also represent inter-

atomic vectors in the crystal structure. The heights of these peaks are approximately proportional to the product of the atomic numbers of the contributing atoms.

To simplify the description of a difference Patterson, consider two isomorphous three-atom crystals NAB and MAB; M and N occupy the same positions in the two structures which are otherwise the same. Consider the simple case in which the unit cells of both structures contain only one molecular unit (NAB or MAB).

Let two capital letters AB represent the peak in Patterson space corresponding to the vector between two atoms A and B in the crystal structure. Ordinary Patterson peaks for the two crystals are tabulated:

MAB: MM, AA, BB, MA, MB, AB; MM, AA, BB, AM, BM, BA

NAB: NN, AA, BB, NA, NB, AB; NN, AA, BB, AN, BN, BA

The semi-colon divides the two centrosymmetric vector sets in each structure. Subtraction of the second Patterson from the first, a difference Patterson, gives the peaks: MM-NN, MA-NA, MB-NB (plus the centrosymmetrically related peaks).

The meaning of a term like MA-NA is that the height of this peak is the difference between the heights of peaks MA and NA. This difference is the same as $(M-N)A$. The residual peaks, therefore, can also be represented by

MM-NN, (M-N)A, (M-N)B (plus centrosymmetrically related peaks). Hence for each atom in MAB, there is a peak in the difference Patterson representing the vector from M to that atom; further, this peak has a weight exactly equal to the peak the atom would have in the electron density map of the unit cell, scaled down by (M-N).

Two other features are worth noting. Whereas the standard Patterson synthesis for a crystal of n atoms per cell has $n^2 - n$ non-origin peaks, the difference Patterson has only n non-origin peaks plus their centrosymmetrical equivalents, i.e. a total of $2n$ peaks. Secondly, to calculate the difference Patterson it is necessary to set the $|F_0|^2$'s for both crystals on the same scale.

Application to this Analysis The difference Patterson is essentially, therefore, a map of the crystal structure in which the replaceable atoms are (successively) moved to the origin. The replaceable atoms in the I and Cl(A) structures are the terminal halogens, each bonded to one molybdenum of the Mo_6 octahedral cluster with the scaling factor (M-N) above equal to 36 electrons (I-Cl). Therefore, images of the well characterized molybdenum octahedra close to the origin of the cell

were anticipated.

Both data sets were placed on an absolute scale using Wilson's method (86). The difference Patterson was then computed as a single Fourier synthesis, using appropriate Fourier coefficients:

$$P(UVW) = \frac{1}{V_c} \sum h \sum k \sum l |F''(hkl)|^2 \cos 2\pi(hU + kV + lW)$$

where $|F''(hkl)|^2 = |F_o|_I^2 - |F_o|_{Cl(A)}^2$ and subscripts I and Cl(A) indicate the intensity data from the two structures. This map was plotted in three dimensions using glass plates for each section. One of the Mo_6 octahedra was immediately obvious.

Excellent initial models, for both structures, were obtained by displacing the centroid of this cluster to a centre of symmetry in the real unit cell. A concomitant displacement of the origin from vector space produced trial coordinates for one of the three independent replaceable atoms. Refinement of the Cl(A) structure using these atoms resulted in a value for R_1 of 0.31.

Successive applications of conventional difference Fourier syntheses and least-squares refinements revealed all the non-hydrogen atoms in the Cl(A) structure and lead to a value for R_1 of 0.165. At this stage an analysis

of agreement factors for the reciprocal lattice levels $h0l$ to $h9l$ lead ultimately to the re-determination of cell constants as mentioned above (p. 56). The incorrect value of b used to calculate equi-inclination angles had introduced slight systematic errors into the data which could be accommodated by refining separate scale factors for each layer. With isotropic temperature factors and rigorously correct accounting for anomalous dispersion, the refinement converged with $R_1 = 0.116$, $R_2 = 0.092$.

These values were not as low as had been predicted on the basis of internal agreement between equivalent forms during data processing. Although this could be taken as an indication that an anisotropic thermal model was required, it was considered better to obtain evidence from the correlated data set of I before such calculations were attempted.

The fractional coordinates from Cl(A) were now used in refining the structure I. Starting from $R_1 = 0.52$ and $R_2 = 0.85$, the refinement converged normally with all atoms isotropic, to give values of 0.15 and 0.18 respectively for these agreement factors. At this point an F_0 Fourier synthesis was plotted onto glass plates for the I structure and showed the terminal iodine atoms to be vibrating anisotropically and normal to the

molybdenum-iodine bonds. By refining anisotropic temperature factors for the three terminal iodine atoms, values of R_1 and R_2 converged to 0.112 and 0.137 respectively. The chemical reasonableness of such vibrations, along with this highly significant drop in the weighted R-factor R_2 (87), were taken as justification for this thermal model.

For reasons which have been outlined by others (83) the Cl(A) structure was next refined on F_o^2 , with the terminal chlorine atoms allowed to vibrate anisotropically. The agreement factor R_3 was .151.

The two lowest isotropic temperature factors for atoms in each bipyridyl ring of each structure, indicated chemically reasonable nitrogen atoms. Refinement of both models resulted in values for these isotropic temperature factors which were similar to those of the ring carbon atoms.

Attempts to refine the I structure using multiple scale factors produced no significant improvement in either the agreement factors or changes in the model. The final residuals were $R_1 = .110$, $R_2 = .135$; indicated shifts in parameters were not greater than 0.07 of their esd's except for C(5) and C(6) which were oscillating with shifts less than 0.30 of their esd's.

The Cl(A) structure was refined on F_o^2 to give

converged values of 0.097, 0.086 and 0.154 respectively for R_1 , R_2 and R_3 . The constancy of $\sum w\Delta^2$, where $\Delta = |F_o| - |F_c|$, for various ranges of F_o indicated the weighting scheme was a good one (75). The final error in observation of unit weight was 0.906, indicating that the estimated standard deviations from experimental measurements were slightly high. Indicated shifts in parameters were less than 0.02 of the esd's for the heavy atoms, and less than 0.05 of the esd's for the light atoms.

Final difference Fourier maps were calculated for both structures. The highest 15 peaks of both maps, ranging from three-quarters to one-half the height of the last carbon atom located, were at chemically unreasonable positions less than 1.8 Å from heavy atoms. Only 4 peaks common to both maps, at less than half carbon atom heights, could be regarded as possible atomic sites. They could not be refined as hydrogen atoms because of the higher residual peaks mentioned, and it was decided that nothing more of chemical interest could result from the attempt. Similarly, although the molybdenum atoms could be refined anisotropically in both structures the models did not alter in any chemically significant fashion.

Tables 12, 13 and 14 present the final positional and thermal parameters for the Cl(A) and I structures

respectively. The root-mean-square amplitudes of vibration derived from the thermal parameters for the terminal halogens for both structures are listed in Table 15. Tables 16, 17 contain the corresponding final values of $|F_o|$ and $|F_c|$ (in electrons).

CHAPTER 5

THE X-RAY CRYSTAL STRUCTURE ANALYSIS OF A SECOND
CRYSTALLINE MODIFICATION OF $(\text{Bipyridyl H})_2((\text{Mo}_6\text{Cl}_8)\text{Cl}_6)$

5.1 Experimental Data: Bis(bipyridylium)hexachloro-
octa- μ_3 -chlorohexamolybdate(II), Cl(B)

The preparation and optical properties of this compound, Cl(B), have been detailed on page 55. All constants were obtained by the least-square procedures outlined in Chapter 4. Data were collected at 20°C, on Polaroid film with CoK α radiation ($\lambda = 1.7902 \text{ \AA}$) and on wet film with CuK α radiation ($\lambda = 1.5418 \text{ \AA}$), using a calibrated precession camera. Final dimensions were: $a = 10.275(4)$, $b = 13.071(9)$, $c = 14.07(2) \text{ \AA}$; $\beta = 92.10(3)^\circ$.

The systematic absences noted from h0l, h1l, h2l and hk0 precession photographs were: h0l when $h + 1 \neq 2n$, 0k0 when $k \neq 2n$. These absences are uniquely consistent with space group $P2_1/n$, which has a general multiplicity of four. The observed density measured in the same gradient tube as Cl(A), was 2.39 g cm^{-3} . As the calculated density for two formula units per unit cell is 2.42 g cm^{-3} , the space group requires each molecule to have a centre of symmetry. A characteristic

tabular, (-101) elongated b, crystal of approximate dimensions $0.05 \times 0.30 \times 0.20 \text{ mm}^3$ was washed free of powder and mounted with the b axis parallel to the axis of the goniometer head. The crystal shape was defined by the measurement of nine intersecting planes, to an accuracy of 0.015 mm, for making absorption corrections.

Reciprocal lattice levels h0l - h8l were collected and mechanically integrated onto multiple films using a Nonius Weissenberg camera and CuK α radiation at room temperature. All reflections up to a Bragg angle of 50.0 degrees were recorded; only reflections observed significantly above background at higher Bragg angles were measured.

The plateaux of the 1686 observed reflections, and adjacent background areas, were measured using a single beam photometer and a galvanometer calibrated to read intensities directly; initial inter-layer scaling was done on the basis of exposure times. A further 347 reflections were not measurable above background and were not included in the structure analysis.

The intensities were corrected for Lorentz, polarization and absorption effects. The linear absorption coefficient was 257.8 cm^{-1} (72c) and calculated transmission coefficients ranged from 0.092 to 0.38.

Complete details of the refinement procedures have

been given for the iodo compound, I (Chapter 4). In this case, the coefficients used for the final weighting scheme were $A = 20.2$, $B = -0.59$, $C = 0.00693$ and $D = -0.000002$.

5.2 Solution and Refinement of the Structure

Standard information relevant to this section such as the function minimized in least-squares refinements and definitions of R_1 , R_2 and R_3 are detailed at the beginning of the corresponding section (4.3) in Chapter 4.

The (Mo_6Cl_8) cluster has symmetry $m\bar{3}m$ with 24 orientations equivalent by the operations of this point group. It was considered possible that this cluster, in random orientation about a crystallographic centre of symmetry, would constitute a trial structure which could be refined as a rigid group. The computer program CUGLS, used for this special calculation has been described in detail by its originators (88,89). In this unusual application, the Mo_6Cl_8 cluster was constrained to its established geometry (pp. 2) and its centroid fixed at the origin of the unit cell. The only parameters allowed to vary were five scale factors for the different Weissenberg levels, individual isotropic temperature factors for the seven independent atoms required to define the group, and three angles (ϕ , θ and ρ) which

defined the group orientation. Initially, a limited data set consisting of 943 reflections (h01-h41) was used in refinement on F_o .

Scale factors and conventional agreement factors behaved normally during this procedure. Group parameter shifts during each cycle are detailed in Table 18. It is interesting to note the outrageous temperature factors and apparently random parameter shifts up until cycle 3. At this point one orientation angle (θ) was nearly correct and, in cycle 4, the other two angles and several temperature factors made decisive shifts towards their final correct values. Initial and final values of the variable group parameters are given in Table 19. The overall shifts in orientation angles were large and demonstrate the power of group refinement to effect much greater changes in trial atomic positions than can be achieved by conventional refinement of individual positional parameters. The value of R_1 obtained by this method was 0.34.

Tests with other random initial orientations were not encouraging. Successful alignment of the group depended, in apparently unsystematic ways, on the choice of axes for an internal group coordinate system and on the divergence of initial orientation angles from their correct values. High symmetry situations, for which

this procedure might be expected to yield correct structures, are extremely rare. A systematic mapping of those regions of $(\varnothing, \theta, \rho)$ space from which successful refinement could be achieved was not attempted. All three structures described in this thesis provide material for such an investigation of the general applicability of the method. Large amounts of computer time would be involved however, and the author is pessimistic about the value of the results.

Two successive difference Fourier syntheses and least-squares refinements located the remaining non-hydrogen atoms. These were refined using carbon scattering factors for all the bipyridylium ring atoms. The lowest resulting temperature factors indicated chemically-reasonable nitrogen atoms. Normal refinement of scale factors and individual atomic parameters led to values of 0.074 and 0.094 for R_1 and R_2 respectively.

At this point three terminal chlorine atoms had uniformly higher isotropic temperature factors than the cluster chlorine atoms. Examination of a difference Fourier map suggested that the former were vibrating anisotropically and normal to the molybdenum-chlorine bond. All other major peaks on the difference map corresponded to chemically impossible positions close to

molybdenum atoms.

The three chlorines were therefore refined with anisotropic temperature factors, resulting in values of 0.069, 0.088 for R_1 and R_2 respectively. Although inter-layer scale factors were refined, the chemical reasonableness and the resulting drop in the weighted R-factor (R_2) justified the use of this model. After correction of the weighting scheme coefficients to their final values the refinements converged so that R_1 and R_2 had values 0.061 and 0.074 respectively; all shifts in parameters were less than 0.01 of their esd's.

A difference Fourier showed that no further chemically-significant improvement could be made to the model. Of the highest 40 peaks found, ranging in height from half to one quarter of the last carbon atom located ($1.0 - 0.5 e/\text{\AA}^3$), the top 16 were less than 1.6\AA from a molybdenum atom. Of the remaining 24, only 4 were not less than 1.8\AA from the other heavy atoms and their coordinates were not those expected for hydrogen atoms, with one exception; hence no attempts were made to refine hydrogen atom parameters.

Final values of all positional and thermal parameters are presented in Tables 14 & 20. In Table 21 the final values of $|F_o|$ and $|F_c|$ (in electrons) are listed for

all measured reflections. The root-mean-square amplitudes of vibration derived from the thermal parameters of the terminal halogens are presented together with those for the I and Cl(A) structures in Table 15.

CHAPTER 6.

DESCRIPTION AND DISCUSSION OF THE THREE STRUCTURES,

(Bipyridyl H)₂((Mo₆Cl₈)X₆), (X = Cl, I)

6.1 Nomenclature.

The three salts, whose X-ray crystal structure analyses have been presented in Chapters 4 and 5, consist of discrete $((\text{Mo}_6\text{Cl}_8)\text{X}_6)^{2-}$ and $(\text{C}_{10}\text{H}_9\text{N}_2)^+$ (bipyridylium) ions. Figures I and II (opposite page 2), and VI (over) show the nomenclature and bonding in the anion and the cation (without the hydrogen atoms) respectively. Atoms related to labelled atoms by the crystallographic centre of symmetry at the centre of the anions are denoted by asterisks in the tables, all of which are collected in sequential order of reference in Appendix D.

6.2 The $((\text{Mo}_6\text{Cl}_8)\text{X}_6)^{2-}$ Anion.

All intramolecular distances within the $((\text{Mo}_6\text{Cl}_8)\text{X}_6)^{2-}$ anions of the three crystals are contained in Table 22. The structure of the (Mo_6Cl_8) cluster as originally described by Brosset (14,15) has been noted (p. 2). The Mo-X bond to each remaining X atom is perpendicular to the appropriate Cl_4 cube face (see Figure I).

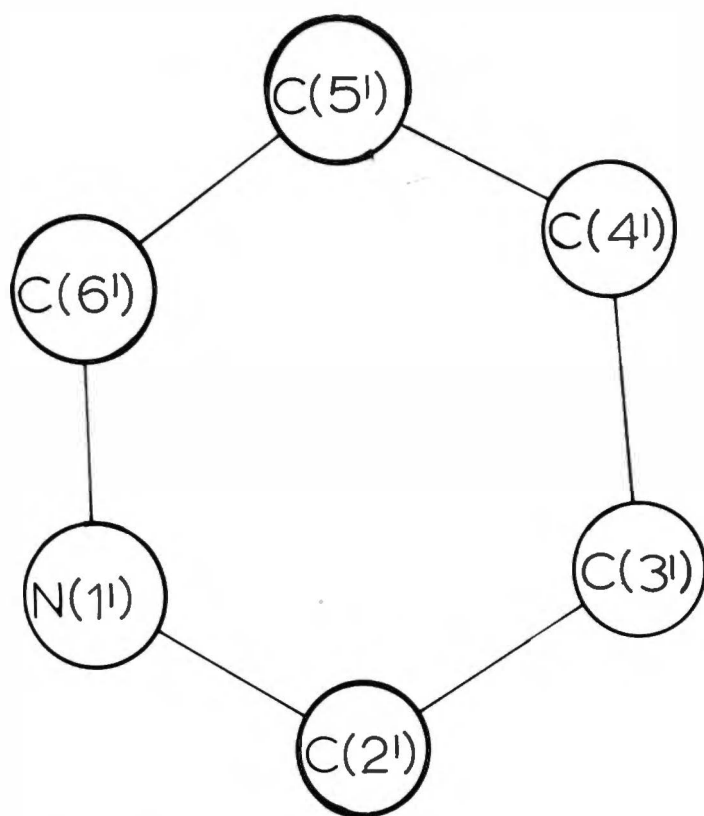
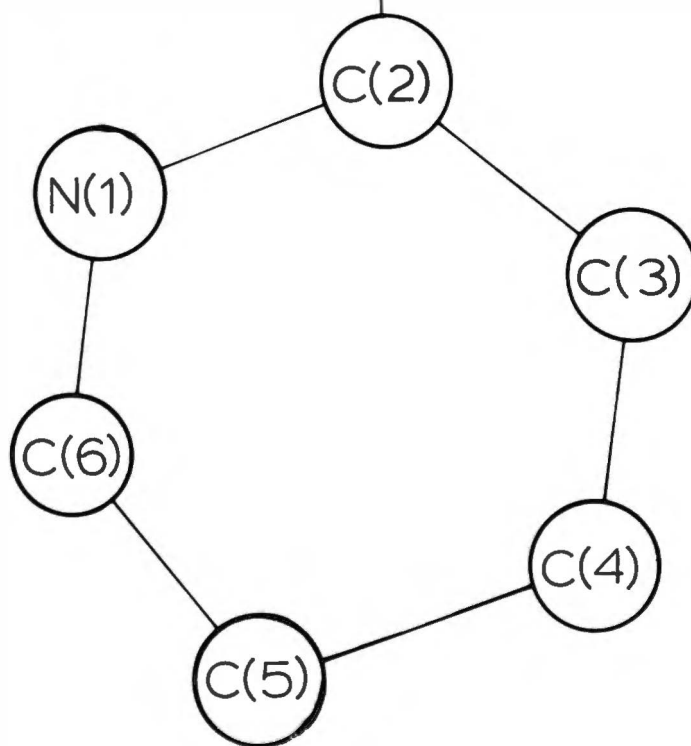


Figure VI: Atom labels for the bipyridylium cation



The weighted mean (90) distances and angles in Table 23 are those based on idealized Oh symmetry. All the corresponding distances agree within the errors quoted by Schäfer, Schnering et al. (13) for $(\text{Mo}_6\text{Cl}_8)\text{Cl}_4$, (Table 23). In particular, the Mo-Mo and Mo-X (X = Cl) bond distances are constant, with weighted means over the four structures of 2.606(1) and 2.423(1) Å respectively. The corresponding Mo-X (X = I) distance is 0.31 Å longer. This agrees well with the difference between the covalent radii (16) of iodine and chlorine atoms (0.34 Å).

The size of the idealized cube is significantly different for the $((\text{Mo}_6\text{Cl}_8)\text{Cl}_6)^{2-}$ and $((\text{Mo}_6\text{Cl}_8)\text{I}_6)^{2-}$ anions. The non-bonded Cl-Cl and the bonded Mo-Cl distances are longer for the latter compound by 0.03 (3σ) and 0.024 (6σ) Å respectively. Similarly the mean Mo-Cl-Mo angle is 0.8 (4σ) degrees smaller for the $((\text{Mo}_6\text{Cl}_8)\text{I}_6)^{2-}$ anion. It is exceedingly unlikely that such small differences will affect current interpretations of the bonding in the cluster (Section 1.6, Chapter 1). Further precise studies of the $(\text{Mo}_6\text{Cl}_8)^{4+}$ cluster, with different terminal ligands (X), would be needed to confirm that the dimensions of the cluster can be altered.

Table 24 shows that each molybdenum atom in these

structures is significantly outside the appropriate Cl_8 -cube face. Corresponding to this, the mean X-Mo-X angle for the three crystals is 92.2(1) degrees. Brosset's report (15) of this deviation from the cubic face-centered position is thus confirmed. Again, these deviations are small (0.1 Å) and of no obvious consequence to current theories of chemical bonding (p.11).

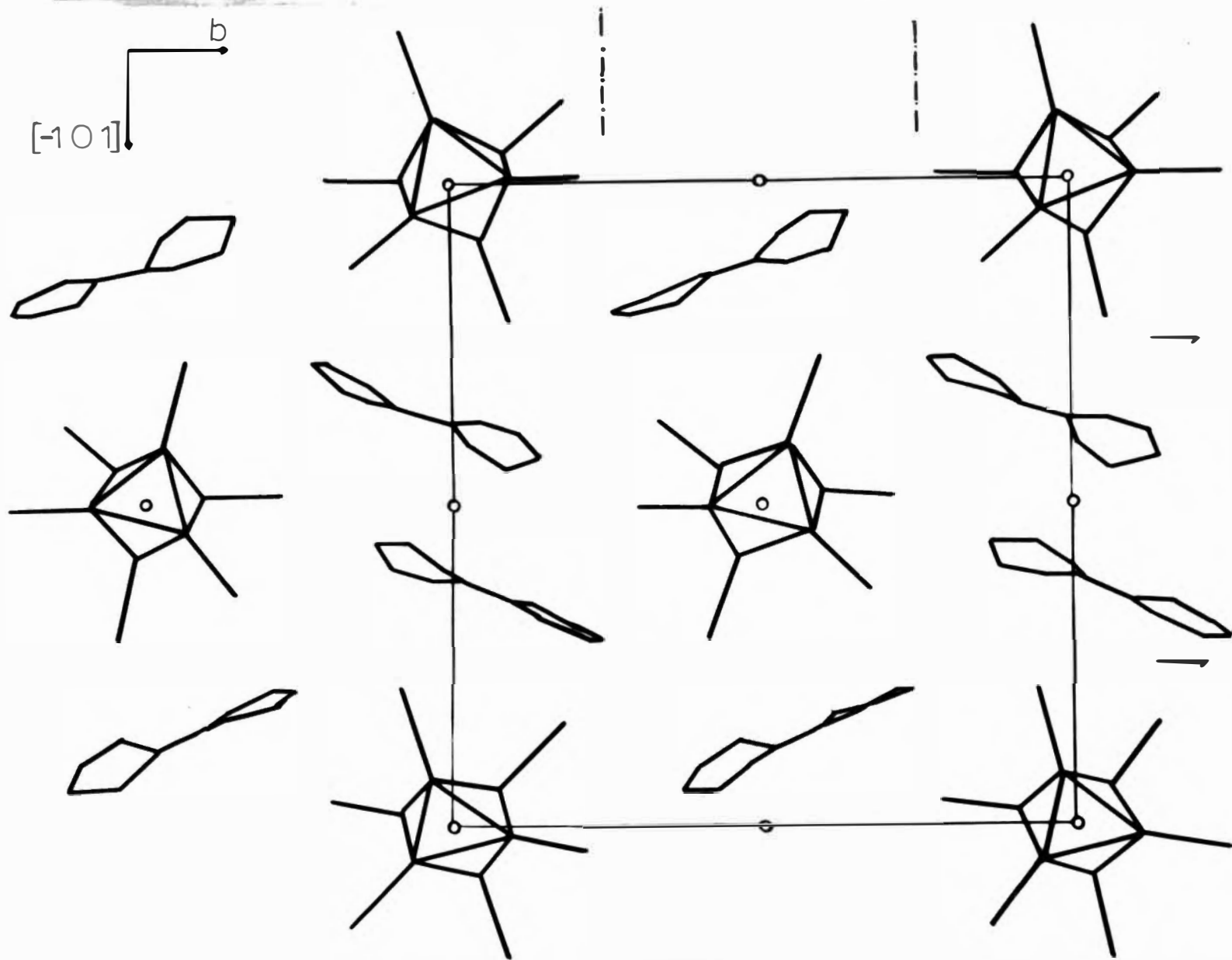
6.3 The Bipyridylium Cation, $(C_{10}H_9N_2)^+$

Tables 25 and 26 contain the intramolecular bond lengths, their weighted means, and angles in the bipyridylium cations of each structure. No symmetry is required for the independent cation in each case by the space group.

Although the weighted mean C-C and C-N distances are normal for bipyridyl (91), some individual deviations from these distances are obvious (e.g. in structure I, Table 25). Deviations of similar magnitude have been reported previously for bipyridyl in a Cu(II)-bipyridyl complex (92). The internal ring bond angles are all within one estimated standard deviation of the ideal value (120 degrees, see Table 26).

The C_5H_4N rings are not very distorted from the best calculated mean planes in the three structures (see

Figure VII: Projection showing ions centred on the (101) plane for Cl(A) and I.



Tables 27,28,29). The rings are twisted from true cis conformations by similar amounts with an average dihedral angle between the two rings of one cation of 13 degrees. Similarly, as accented in Fig. IV, the C(3)-C(2)-O(2') angles are significantly greater than the N(1)-C(2)-C(2') angles in both unprimed and primed rings in all the structures (Table 26). Thus the weighted means over the three crystals for the former and latter angles are 124.0 and 114.5 degrees respectively.

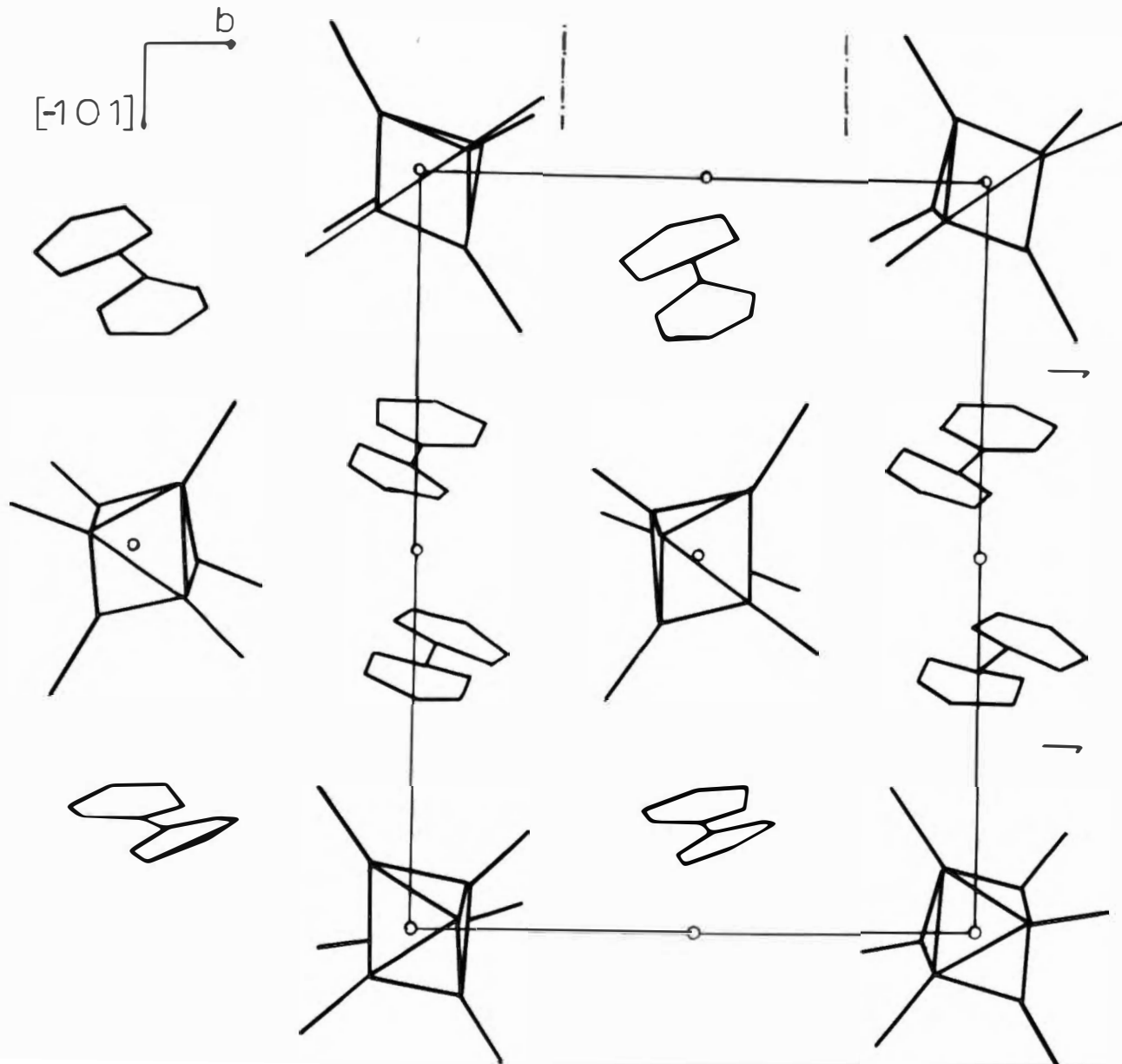
6.4 Packing of the Ions

The ionic packing appears to be dominated by the bulky anions, which are centred on the (101) planes in expanded "hexagonal close-packed" layers (see Figures VII, VIII). Packing of hexagonal layers of $(\text{Mo}_6\text{Cl}_8)\text{Cl}_6^{2-}$ anions has been reported previously (18). The cation molecules are centred on the conventional trigonal positions in these layers. Within one such layer, each bipyridylum cation is surrounded by three closest anions and each anion by six closest cations.

Examination of Figures VII, VIII indicates that the difference in the two structural forms lies in the orientation of the bipyridylum cations. The vector C(2)-C(2') for the I and Cl(A) structures is nearly coplanar with the (101) plane and approximately parallel to the b axis. Corresponding to this, the d-spacings

Figure VIII:

Projection showing ions centred on the (101) plane for Cl(B).



for the (101) planes are 6.63 and 6.93 Å for Cl(A) and I respectively.

By contrast, the C(2)-C(2') vector in the Cl(B) crystal is approximately normal to the (101) plane and perpendicular to the b axis. Obviously, the inter-layer spacing in this structure would be expected to be and is, considerably greater (8.16 Å) than for the Cl(A) structure.

The closest inter-ionic contacts for the three structures are listed in Tables 30 and 31. The number of independent contacts up to 3.8 Å is approximately the same, although a greater number of cation to cluster chlorine contacts are observed for the I and Cl(A) structures. Indeed, the cell volumes (and densities) of the two chloromolybdic(II) acid salt forms are significantly different (1875, 1900 Å³ for Cl(A), Cl(B) respectively).

From the above relationships between structures Cl(A) and Cl(B), it might be expected that the Cl(A) form would be the more stable because of its more efficient packing. However the particular preparative conditions (slow cooling of the reactants over 12 hours from 130°C, see p. 22) favoured the Cl(B) form. It is also likely that other crystalline modifications of these salts may exist corresponding to other packing arrange-

ments of cations (viz. products 3 and 4, Chapter 2).

Not many suitable contacts for hydrogen bonding between the nitrogen atoms of the cation and the cluster halogens (X or Cl) (93) are observed (e.g. N(1') and X(3) in Cl(B), Table 31). In any case such bonding to iodine atoms in structure I is unlikely. All the evidence from these three analyses suggests that the atomic arrangements are determined by the packing of the bulky anions.

APPENDIX ALABORATORY PROCEDURESA.1 Standard Preparative Methods

All compounds were stored in desiccators over phosphorus pentoxide. Both $(\text{Mo}_6\text{Cl}_8)\text{Cl}_4$ and $(\text{Mo}_6\text{Cl}_8)\text{I}_4$ were prepared by the method described by Sheldon (23).

(1) Sealed Tube Experiments The halides $(\text{Mo}_6\text{Cl}_8)\text{Cl}_4$ (0.3g) and $(\text{Mo}_6\text{Cl}_8)\text{I}_4$ (0.35g) were placed in a 12 inch long Pyrex tube of 9/16 inch bore, which was then stoppered. Just prior to the addition of the ligand(s) dissolved in 2-5 ml of dry solvent (ethanol or tetrahydrofuran), about 6-8 ml of the solvent was added to partially dissolve the $(\text{Mo}_6\text{Cl}_8)\text{Cl}_4$ or $(\text{Mo}_6\text{Cl}_8)\text{I}_4$. Immediately after the additions, dry nitrogen was flushed through above the solution for half an hour; the tube was then sealed.

During the controlled heating in an electric furnace, the tubes could be removed and inspected for completeness of reaction. After allowing them to cool (up to 8 hours), the tubes were broken open and the products washed out with further dry solvent. Excess ligand was leached from the solid using dry benzene for triphenylphosphine and triphenylarsine oxide and excess dry solvent for pyridine-N-oxide, bipyridyl and

triphenylphosphine oxide. The compounds were dried under high vacuum (10^{-4} mm Hg).

(ii) Reactions at Room Temperature (20°C) Up to 150 mg of $(Mo_6Cl_8)Cl_4$ (or $(Mo_6Cl_8)I_4$) dissolved in up to 40 ml of dry solvent (tetrahydrofuran or ethanol) was treated with excess ligand (2.5 - 3.0 molar ratio excess) dissolved in the same solvent (2-5 ml). If a precipitate did not form on standing, excess dry petroleum ether, ligroin or diethyl ether or a combination of these was added to yield solids. Filtration, removal of excess ligand and drying was achieved in the same way as (i) above.

(iii) Reactions under reflux Reaction solutions (ii) above were often heated under reflux (with a side-valve drying tube) for half to one hour (unless otherwise stated). On cooling, precipitated products were collected as above. Frequently it was necessary to assist precipitation by the addition of a less polar solvent.

A.2 Analytical Procedures

The sample to be analysed (0.03 - 0.10 g) was decomposed with ammoniacal peroxide (5-15 ml) or by fusion with sodium hydroxide (0.2 g), sodium peroxide (0.2 g) and sodium carbonate (0.5 g) in a nickel crucible.

Molybdenum Molybdenum was determined gravimetrically as the oxinate $\text{MoO}_2(\text{C}_9\text{H}_6\text{OH})_2$ (94).

Halogen (94) Halogen was determined mainly by potentiometric titration with silver nitrate using Shimadzu Type 3, Baldwin or Radiometer Copenhagen pH meter-22 potentiometers. Iodide titrations were conducted in slightly basic or neutral solutions; chloride titrations were always in dilute acid (by addition of dilute nitric acid).

Volhard and Andrews titration methods were also used. Molybdenum interferes with the more usual gravimetric method.

Carbon and Hydrogen These analyses were carried out at the Microanalytical Laboratories of Otago University, Dunedin. The reproducibility of results for a Ph_3PO complex was a satisfactory 0.3%.

A.3 Purification of Solvents and Ligands

Benzene and Ether The solvents were sodium dried.

Ethanol Ethanol was fractionally distilled. The fraction (boiling point 78 - 79°C) was stored over freshly-dried molecular sieves.

Chloroform Completely dry chloroform was prepared by Dr J. Ayers by fractionally distilling A.R. chloroform from calcium chloride, collecting the fraction at 61°C.

A.R. grade chloroform that had been kept over molecular sieves for at least 3 days was used for most work.

Dimethylformamide (95) Dimethylformamide was mixed with about 10% by volume of dry benzene. The benzene was removed with difficulty at 80°C and the dimethylformamide left over barium oxide for several days.

It was then fractionally distilled at 15-20 mm pressure and the middle fraction retained; it was stored over molecular sieves and its specific conductivity was always of the order $1.0 - 2.0 \times 10^{-7} \text{ ohm}^{-1} \text{ cm}^{-1}$.

Dimethylsulphoxide Dimethylsulphoxide was purified by Dr J.H. Hickford; it was left over phosphorus pentoxide for one day and fractionated at 20 mm pressure. The middle fraction was stored over molecular sieves, specific conductivity $\approx 3.0 \times 10^{-7} \text{ ohm}^{-1} \text{ cm}^{-1}$.

Nitrobenzene A.R. nitrobenzene was allowed to stand over molecular sieves for five days before use; specific conductivity (not measurable) $< 10^{-8} \text{ ohm}^{-1} \text{ cm}^{-1}$.

Petroleum Ether Petroleum ether (boiling point 50-70°C) was left over phosphorus pentoxide for five days and distilled.

Pyridine Pyridine (BDH A.R. grade) was kept over potassium hydroxide pellets.

Pyridine-N-oxide Pyridine-N-oxide was vacuum distilled by Dr A.M. Brodie to remove moisture.

Tetrahydrofuran Tetrahydrofuran (Light and Co.) was fractionally distilled from lithium aluminium hydride and the middle fraction, boiling point 65-66°C, was collected and stored over sodium wire.

Other Ligands All other ligands were obtained commercially in purified form: Bipyridyl (Ivor Watkins Dow, melting point 70-71°C); Triphenylarsine (Fluka AG), Triphenylarsine oxide (Koch-Light), Triphenylphosphine (Light and Co.) and Triphenylphosphine oxide (Koch-Light).

A.4 Physical Measurements

(1) Conductance Measurements The molar conductivity, Λ_m , is defined by

$$\Lambda_m = \frac{1000 (k - k_0)}{C} \quad \text{where } k \text{ and } k_0 \text{ are the specific}$$

conductivities of the electrolyte and solvent respectively ($k = \frac{\text{cell constant}}{\text{resistance}}$) and C is the concentration of the electrolyte in moles/litre. Some representative values for solvents used in this work follow ($\text{ohm}^{-1}/\text{cm}^2$) (55).

<u>Salt type</u>	<u>D.M.F.</u>	<u>DMSO.</u>	<u>PhNO₂</u>	<u>Acetone</u>	<u>Alcohol</u>
1:1	60-80	50-70	15-30	90-120	60-80
2:1	110-130	100-130	35-50	150-190	120-160
3:1	160-180		55-75	220-240	200-240

The resistances of solutions (concentration 0.1 - $1.0 \times 10^{-3} \text{M}$) and solvents were measured on a Philips

PR 9500 Conductivity bridge at 25°C using a dip-type conductivity cell with shiny platinum electrodes. The cell was calibrated with a standard potassium chloride solution at 25°C (96).

Most compounds were recovered unchanged, as indicated by X-ray powder photographs, from the conductivity solutions by the addition of excess of a mixture of approximately 90% petroleum ether and 10% diethyl ether (65). Amorphous materials were not analysed owing to the smallness of the recovered sample. Recovery from dimethylformamide is very slow, requiring, in some cases, 3 hours for sufficient sample for an X-ray powder photograph.

(11) Infra-red measurements The diagnostic value of infra-red spectra, particularly for the presence of water, has been adequately reviewed, for example by Nakamoto (63). Spectra (4000 - 400 cm^{-1}) were run on a Perkin Elmer 337 spectrophotometer using nujol and halocarbon mulls. The KBr pellet technique was also used on some samples.

Low frequency spectra (500 - 200 cm^{-1}) were recorded on a Grubb Parsons DM4 spectrophotometer. All the spectra obtained in this region were dominated by the (Mo_6Cl_8) cluster stretching frequencies and proved of little use in examining the nature of metal-

ligand bonds (35).

(iii) Ultra-violet and Visible Spectra (97) Solid state (diffuse reflectance) spectra (98) were measured on a Beckman DK2A spectrophotometer using a reflectance attachment with a magnesium oxide reference. Dilution of the sample with magnesium oxide was sometimes necessary (99).

In general, the spectra obtained were apparently not as definitive as those collected by Robinson (55) on a Hilger Uvispek with reflectance attachment. In the author's experience this latter instrument worked manually probably gives better spectral peaks for molybdenum(II) compounds although certain irreproducibility was noted (65).

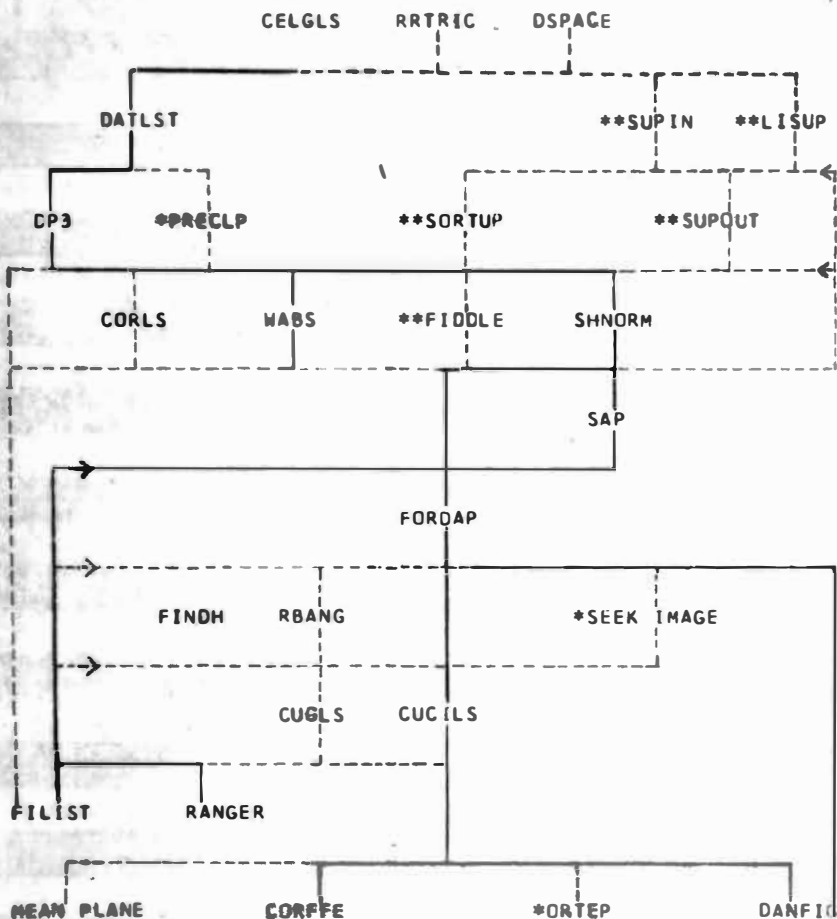
(iv) X-ray Powder Photography (100) Since the use of X-ray powder photography as a "finger-print" technique is well established (101), details of the diffraction geometry will not be presented here. Some molybdenum (II) compounds showed no diffraction pattern or very faint broad "halos". These compounds are labelled "amorphous"; the usual reasons (102) are (a) a random distribution of molecules within the unit cell such that there is no periodicity of structure or (b) small crystallite size ($< 100 \text{ \AA}$).

Two compounds are iso-structural if the relative

positions of the lines are similar. The experience of the author, as mentioned on p. 60 , is a warning against the use of X-ray powder evidence in a negative way viz. that two crystals are not isomorphous.

The compounds were ground to a fine powder and packed into either Lindemann glass or soda glass tubes, around 0.3 mm bore. The samples were then mounted firmly in the centre of a Philips Debye-Scherrer camera (radius 57.3mm) and exposed to CuK α radiation for 3-9 hours.

TABLE 32 THE UNIVERSITY OF CANTERBURY COMPUTING SYSTEM FOR X-RAY CRYSTAL STRUCTURE ANALYSIS



CALCULATIONS MAY PROCEED BY ANY SENSIBLE ROUTE WHICH DOES NOT PASS UPWARDS THROUGH A PROGRAM NAME OR AGAINST AN ARROW

** THESE PROGRAMS WERE WRITTEN BY THE AUTHOR

PRELIMINARY INVESTIGATIONS OF CELL CONSTANTS

PREPARATION OF INPUT DATA SHEETS AND CORRESPONDING CARDS (BLANKS) FOR MANC PUNCHING OBSERVED INTENSITIES

FILM FACTOR SCALING, LP AND OPTICAL ABSORPTION CORRECTIONS PREPARATION AND UPDATING FILE FOR INPUT TO L-S CALCULATIONS

WEISSENBERG ABSORPTION CORRECTIONS, CORRELATION, SCALING, SHARPENING FOR PATTERSON OR NORMALISED STRUCTURE FACTORS

DIRECT METHODS FOR PHASE DETERMINATION (SYMBOLIC ADDITION)

FOURIER SUMMATIONS INCLUDING PATTERSONS AND GENERAL PLANE

DERIVATION OF POSITIONAL COORDINATES OF ATOMS IN RIGID GROUPS AND FROM PATTERSON MAPS

FULL-MATRIX LS REFINEMENT OPTIONALLY INCLUDING RIGID GROUPS

GENERAL FILE LISTING AND ANALYSIS OF WEIGHTING SCHEMES

CRYSTAL AND MOLECULAR GEOMETRY INCLUDING TABLES OF DISTANCES AND ANGLES AND FIGURES SUITABLE FOR PUBLICATION

* THESE PROGRAMS ARE NOT YET WORKING ON THE 360/44

APPENDIX B

THE UNIVERSITY OF CANTERBURY COMPUTING SYSTEM FOR X-RAY CRYSTAL STRUCTURE ANALYSIS

B.1 Introduction

This referenced summary is presented here because this University of Canterbury Computing System has not been described previously and the author took a significant part in its construction. Table 32 opposite illustrates the flow of information through each program in the system. Those programs marked with double asterisks (**) were the sole concern of the author and are described in greater detail below.

B.2 The Computing System

Calculations are carried out on an IBM 360/44 computer with 16K words of core storage and twin 2315 disc storage drives. A comprehensive range of computer programs has been adapted to this hardware. Table 33 (over) lists the original programs and, where possible, their authors. Although many of these were originally written for 32K word machines they work in the smaller core with little reduction in capacity and speed through extensive use of phase overlay procedures.

Table 33: University of Canterbury Computer Programs in Normal Order of Use

<u>Local Name</u>	<u>Derived from</u>	<u>Authors</u>
RRTRIC	CAXR12	W. T. Robinson
DSPACE	NRC-21	M. E. Pippy
DATLST	DATLST	W. C. Hamilton (Brookhaven Laboratory)
SUPIN } LISUP }	CUXR-2	W. M. Macintyre, M. Werkema, B. R. Penfold and F. W. B. Einstein
CELGLS	ORGLS	W. R. Busing, K. O. Martin and H. A. Levy
DP3	DP3	W. C. Hamilton (Brookhaven Laboratory)
SUPOUT	-	G. J. Gainsford
WABS	GNABS	C. W. Burnham and J. A. Ibers
CORLS	-	K. Emerson
SHNORM } SAP }	NRC-4	S. R. Hall and F. R. Ahmed
FORDAP	FORDAP	A. Zalkin
CUCILS	{ ORFLS NULS4 UCILS	W. R. Busing, K. O. Martin and H. A. Levy J. A. Ibers R. J. Doedens
RANGER	RANGER	P. W. R. Corfield
RBANG	RBANG	S. F. Watkins
CUGLS	NUGLS	R. J. Doedens and J. A. Ibers
FILIST	-	P. R. Ireland
CORFFE	ORFFE-II	W. R. Busing, K. O. Martin and H. A. Levy
DANFIG	SADIAN ORTEP	W. H. Bauer C. K. Johnson
MEAN PLANE	NRC-22	M. E. Pippy and F. R. Ahmed

Most large crystallographic calculations, particularly Fourier syntheses and least-squares refinements, can be structured so that only part of the computer program need be core resident at a given time. Thus maximum storage becomes available for the variables required when handling large numbers of atoms or large cells. The overlay technique has a further advantage that program functions can be extended almost without limit, regardless of core size. For example a structure-factor least-squares program can be made to present one table analysing parameter shifts over many cycles of refinement, and another listing the final values of atomic parameters and their errors in perfectly publishable form. A Fourier program can be made to print or plot, numerically or alphanumerically or graphically, in any desired direction. The stored summation answers can be searched and interpolated for accurate coordinates of positive peaks and negative troughs. Comprehensive tables of interatomic distances and bond angles, and many rough perspective views of the trial structure, can be produced rapidly on a line printer, using output from both these calculations. Such automation ultimately saves computer time on large and small machines alike and is superior to stacking a succession of small programs which will necessarily

involve many transfers of large amounts of common information via external storage devices.

B.3 Programs Written by this Author

(i) SUPIN and LISUP These single-phase programs calculate the Weissenberg equi-inclination angle settings, γ (azimuthal) and ω (spindle rotation), for X-ray reflections in any crystal system. Outputs from SUPIN are sorted files of reflection data which facilitate rapid collection of intensities using either automatic or manual scanning modes on the Canterbury University semi-automated Supper Equi-inclination Diffractometer (CUSED, Appendix C). Files from LISUP are generated from input cards, for the collection of a specified limited data set.

(ii) SUPOUT SUPOUT is a multiple-phase program, with two main functions: (a) processing CUSED output data with optional corrections for Lorentz-polarization effects, counter drift, crystal decomposition, counter dead-time and spherical absorption, (b) averaging crystallographically equivalent reflections. Predicted agreement factors for the structure are calculated by statistical analysis of the agreement among averaged reflections. Within either of these sections, the output magnetic file can be updated; i.e. the new data can be added to

that previously written.

(iii) SORTUP This single phase program sorts standard reflection data on a magnetic file into ascending order on $\sin \theta$. This utility is only used for crystals with certain space-groups (e.g. hexagonal) to order equivalent reflections for SUPOUT (ii(b)).

(iv) FIDDLE This single-phase data-alteration program performs all minor adjustments and transfers of standard data sets.

(v) DIFPAT DIFPAT is not listed in Table 32 or 33 because it is a specialized program. It finds all reflections with common Miller indices from the two data sets of isomorphous crystals, rescales both data sets to the same absolute scale (Wilson (86)) and outputs the necessary coefficients for a difference Patterson synthesis. This program was limited to the monoclinic system geometry.

B.4 Acknowledgements

The writer wishes to thank the original authors of the adapted programs (Table 33) and his colleagues in the X-ray group at Canterbury University for their assistance. In particular, the author acknowledges the massive contribution of Robert J. Dellaca in the adaption of the major programs to this philosophy and this hardware. Thanks are also due to the staff of the Computer Laboratory of the University of Canterbury for their help.

APPENDIX C

THE CANTERBURY UNIVERSITY SUPPER EQUI-INCLINATION DIFFRACTOMETER (CUSED)

C.1 Introduction

The X-ray diffraction analyses of crystal Cl(A) (Chapter 4) was the first structure solved using reflection data collected on the Canterbury University semi-automated equi-inclination diffractometer. Since the author spent considerable time in both designing and implementing the CUSED operational procedure, some of the features of this instrument will be briefly described. Complete details are contained in the operating manual written by this author (103).

C.2 Scanning Geometry

The equi-inclination geometry has been fully described by Buerger (104,105) and therefore will not be repeated here. The total divergence of a diffracted beam from a normal crystal is around 2° , at an azimuthal angle, γ , of 140° . Since the usual counter aperture is 4° , there is a high degree of tolerance in the γ , scintillation counter arm, setting. Relatively crude stepping of the counter ($\pm 1/6^\circ$ for this instrument) is therefore allowable. Collection of data is by the

moving crystal, stationary counter technique.

C.3 The Automation

The automation consists of two programmed discs controlling the counter (γ) and crystal (ω) rotation motors. Output is printed on a KIENZLE printer. By a relay system, the following cycle is carried out through each reciprocal lattice layer (1) ω -scan, with counting, at fixed γ angle, (2) change of γ (counter arm) angle with crystal stationary and counting stopped. Machine settings allow any desired reciprocal volume to be examined. A safety stop prevents the γ motor from driving the counter over the maximum γ angle possible (146 degrees) into a collision with the X-ray tube shield.

This automation is designed to work with the Philips electronic panel containing an automatically resetting scaler and printer system. A time constant is set, usually to 60 seconds. At this interval the printer lists the accumulated counts and resets the scaler. The print-out, consequently, gives integrated intensities in the form of an histogram. That is, the sum of counts across the peaks minus the background equals the integrated intensity.

C.4 The "Dead" Time

Unfortunately the CUSED system has an approximately $\frac{1}{3}$ second "dead" time during this print-out process, when

no counting is done. An examination of prepared histograms for strong reflections showed that significant (and non-systematic) counts are lost if the print-out occurs near the time of highest counting rate. The simple empirical correction routine built into program SUPOUT (Appendix B) assumes that a plot of counting rate (counts/sec) against time for a reflection approximates to the sides of an isosceles triangle, where the base of the triangle represents the background counting level (106). Analysis of the corrections calculated on this basis, which can be up to 10% of the total count, showed they were of the right magnitude for the observed mosaic spread of the crystal under study. However, all strong reflections, in particular, should be centred within one integrated count to avoid building non-random errors into the data set.

C.5 Operating Procedure

The only manual interference required in automatic mode besides the orientation of the crystal and synchronization of the various electronic and mechanical components is (1) the setting of the equi-inclination angle and (2) the interpretation of the print-out. The former operation takes only a few minutes, usually, and the listed counts can be rapidly interpreted with the aid of a cardboard scale in conjunction with the

SUPIN lineprinter listing (Appendix B). All necessary figures are transferred directly into spaces on this listing, which also contains further information sufficient for manual dialling of the reflections.

C.6 Some Advantages of the CUSED System over Film Methods

Although the CUSED system requires more constant supervision than film methods (for example, in the regular checking of standard reflections) the data set obtained is potentially better for the following reasons:

- (1) an internally-correlated data set is obtained.
- (2) the strongest reflections are measured much more accurately.
- (3) an estimated standard deviation (σ) based on counting statistics can be calculated for each intensity measured.
- (4) a rapid check is available of the crystal centring (mounting) and the corresponding setting of all reciprocal lattice layers.
- (5) a greater volume of the reciprocal lattice sphere can be examined (ν up to 50 degrees) with one setting of the crystal.
- (6) the data collection in automatic mode is much easier physically on the operator, although the time involved is similar to film methods. Manual dialling is over three times as fast.

- (7) the crystal characteristics can be examined in detail, although crystals are always aligned approximately using film methods.
- (8) this ω -scan technique is satisfactory for highly mosaic crystals, whose intensities would be difficult to integrate onto films (107).

The CUSED system could be further improved by the use of a stepping motor to avoid the inefficient ω -scanning of empty reciprocal space, the punching of the output data onto cards or paper tape and eliminating the printer "dead" time.

C.7 Acknowledgements

The writer wishes to thank Mr C. Rowe, Mr R.L. Hooper and Mr R.H. Nokes for their personal discussions with him and maintenance of the electronic components. The assistance received from Professor T. Zoltai (57), Drs A. Cooper and K.A. Fraser (108) and Dr T.C. Furnas (82) through their respective manuals is also gratefully acknowledged.

APPENDIX D

TABLES FROM CHAPTERS 4, 5 AND 6

**Table 12 : Final Positional and Thermal Parameters for
Isotropic Atoms of Cl(A)**

<u>Atom</u>	<u>x</u>	<u>y</u>	<u>z</u>	<u>B</u>
Mo(1)	0.6159(4)	0.5838(2)	0.5673(3)	1.88(8)
Mo(2)	0.6523(4)	0.4319(2)	0.5180(3)	1.82(8)
Mo(3)	0.4770(4)	0.4689(2)	0.6418(3)	1.73(8)
Cl(1)	0.4857(11)	0.6738(6)	0.4111(9)	2.8(3)
Cl(2)	0.5512(12)	0.3856(7)	0.3198(10)	3.4(3)
Cl(3)	0.2234(11)	0.4560(7)	0.5512(9)	2.5(2)
Cl(4)	0.7327(11)	0.4833(7)	0.7161(9)	2.5(3)
N(1)	0.236(4)	0.476(2)	0.999(3)	4.7(10)
C(2)	0.159(4)	0.503(3)	0.900(4)	1.9(9)
C(3)	0.065(5)	0.447(3)	0.808(4)	4.0(11)
C(4)	0.043(5)	0.375(3)	0.840(4)	3.4(11)
C(5)	0.094(7)	0.345(3)	0.945(6)	7.5(16)
C(6)	0.193(5)	0.392(3)	1.031(4)	4.3(12)
N(1')	0.307(4)	0.620(3)	0.954(4)	4.8(10)
C(2')	0.197(4)	0.589(3)	0.878(3)	2.0(9)
C(3')	0.133(4)	0.633(3)	0.786(4)	2.5(10)
C(4')	0.175(4)	0.712(3)	0.773(3)	2.3(10)
C(5')	0.282(5)	0.747(2)	0.852(4)	2.7(10)
C(6')	0.363(5)	0.697(3)	0.939(4)	3.2(11)

Table 13 : Final Positional and Thermal Parameters for
Isotropic Atoms of I

<u>Atom</u>	<u>x</u>	<u>y</u>	<u>z</u>	<u>B</u>
Mo(1)	0.6061(4)	0.5844(3)	0.5650(3)	3.05(8)
Mo(2)	0.6491(4)	0.4358(3)	0.5169(3)	3.27(8)
Mo(3)	0.4779(4)	0.4685(3)	0.6361(3)	3.07(8)
Cl(1)	0.4787(12)	0.6700(8)	0.4155(10)	3.9(3)
Cl(2)	0.5621(12)	0.3879(8)	0.3216(10)	3.5(3)
Cl(3)	0.2282(11)	0.4517(8)	0.5518(10)	3.2(2)
Cl(4)	0.7196(12)	0.4879(8)	0.7102(10)	3.7(3)
N(1)	0.212(6)	0.485(4)	0.710(1)	7. (1)
C(2)	0.145(10)	0.510(6)	0.894(8)	10. (3)
C(3)	0.061(6)	0.459(4)	0.821(5)	6. (1)
C(4)	0.031(7)	0.387(5)	0.854(6)	7. (2)
C(5)	0.113(10)	0.362(7)	0.975(9)	11. (3)
C(6)	0.172(10)	0.426(7)	1.030(8)	10. (2)
N(1')	0.297(5)	0.615(4)	0.943(5)	7. (1)
C(2')	0.186(6)	0.583(4)	0.874(5)	5. (1)
C(3')	0.115(6)	0.629(4)	0.780(6)	6. (1)
C(4')	0.173(7)	0.710(5)	0.762(6)	7. (2)
C(5')	0.281(8)	0.738(5)	0.838(7)	8. (2)
C(6')	0.349(7)	0.687(5)	0.928(6)	7. (2)

Table 14: Final Positional and Thermal Parameters for Anisotropic Atoms in I, Cl(A) and Cl(B).

Atom	Positional			Thermal ($\times 10^3$)						
	x	y	z	β_{11}^a	β_{22}	β_{33}	β_{12}	β_{13}	β_{23}	
<u>Structure I</u>										
X(1)	0.7607(4)	0.7106(3)	0.6654(4)	14.8(6)	5.1(3)	10.4(4)	-2.0(3)	-2.7(4)	-1.4(2)	
X(2)	0.8719(5)	0.3411(3)	0.5402(4)	15.4(6)	8.5(3)	13.6(5)	4.4(4)	-0.9(4)	-1.0(3)	
X(3)	0.4422(6)	0.4221(4)	0.8378(4)	21.5(8)	9.1(4)	10.8(5)	1.2(4)	0.1(5)	0.8(3)	
<u>Structure Cl(A)</u>										
X(1)	0.7664(13)	0.6936(7)	0.6588(10)	14(2)	2.8(8)	6(1)	-2.4(9)	0.7(9)	-3.7(8)	
X(2)	0.8526(12)	0.3437(7)	0.5382(11)	8(2)	4.6(8)	10(1)	5(1)	4(1)	-0.9(7)	
X(3)	0.4437(12)	0.4251(7)	0.8286(9)	12(2)	4.3(8)	5(1)	0.2(9)	3(1)	1.6(7)	
<u>Structure Cl(B)</u>										
X(1)	0.7109(4)	0.6911(4)	0.6969(3)	12.8(5)	7.0(4)	6.1(2)	-1.4(3)	-0.8(3)	-1.9(2)	
X(2)	0.8334(4)	0.3066(3)	0.4899(3)	11.6(4)	6.5(4)	7.7(2)	3.7(3)	0.8(3)	0.3(2)	
X(3)	0.3598(4)	0.3260(3)	0.7320(2)	13.3(4)	6.5(4)	4.8(2)	-1.2(3)	1.0(2)	0.8(2)	

^a The form of the anisotropic ellipsoid is $\exp(-\beta_{11}h^2 + \beta_{22}k^2 + \beta_{33}l^2 + 2\beta_{12}hk + 2\beta_{13}hl + \beta_{23}kl)$

Table 15 : Root-Mean-Square Amplitudes of Vibration, Å,
for the terminal (X) atoms of $((\text{Mo}_6\text{Cl}_8)\text{X}_6)^{2-}$

<u>Atom</u>	<u>Axis</u>	<u>I</u>	<u>Cl(A)</u>	<u>Cl(B)</u>
X(1)	1	0.192(5)	0.05(7)	0.197(6)
	2	0.289(6)	0.26(2)	0.271(5)
	3	0.345(6)	0.28(2)	0.280(5)
X(2)	1	0.231(6)	0.05(7)	0.183(6)
	2	0.312(6)	0.26(2)	0.275(5)
	3	0.400(6)	0.30(2)	0.293(5)
X(3)	1	0.265(6)	0.14(3)	0.201(5)
	2	0.351(6)	0.24(2)	0.245(6)
	3	0.366(7)	0.26(2)	0.273(5)

Table 18: Rigid Group Refinement Shifts

<u>Parameter</u>	<u>Cycle Number</u>							
	<u>1</u>	<u>2</u>	<u>3</u>	<u>4</u>	<u>5</u>	<u>6</u>	<u>7</u>	<u>8</u>
ϕ (degrees)	0.6	2.3	-1.5	-14.5	-1.5	-0.8	-0.2	+0.3
θ (degrees)	-2.1	-6.1	-12.5	0.6	-0.4	-0.1	-0.0	0.0
ρ (degrees)	-0.3	-2.4	0.4	14.0	2.0	0.9	0.2	-0.2
B, Mo(1) \AA^2	2.11	6.8	-0.63	-13.0	1.7	1.6	1.6	1.1
B, Mo(2) \AA^2	-0.61	-0.30	0.59	0.5	1.0	0.2	0.0	0.0
B, Mo(3) \AA^2	-0.11	1.36	1.42	-5.0	1.3	1.0	0.3	0.0
B, Cl(1) \AA^2	2.26	7.20	16.52	-22.0	-3.2	0.3	-0.3	-0.2
B, Cl(2) \AA^2	2.36	6.14	-2.25	-0.81	-4.0	0.7	0.0	-0.1
B, Cl(3) \AA^2	5.6	21.81	19.21	-47.8	2.0	0.5	-0.1	-0.1
B, Cl(4) \AA^2	4.0	13.13	-7.83	-7.5	0.1	0.1	-0.1	-0.0

Table 19: Initial and Final Parameters of Rigid
Group Refinement

<u>Parameters</u>	<u>Initial</u>	<u>Final (8 Cycles)</u>	<u>Overall shift</u>
ϕ , (degrees)	133.0	118.2	14.8
θ , (degrees)	117.9	97.0	20.9
ρ , (degrees)	-79.8	-65.9	13.9
B, Mo(1) \AA^2	1.5	2.0	
B, Mo(2) \AA^2	1.5	2.8	
B, Mo(3) \AA^2	1.5	1.9	
B, Cl(1) \AA^2	1.5	2.0	
B, Cl(2) \AA^2	1.5	3.7	
B, Cl(3) \AA^2	1.5	3.6	
B, Cl(4) \AA^2	1.5	3.4	

**Table 20: Final Positional and Thermal Parameters for
Isotropic Atoms of Cl(B)**

<u>Atom</u>	<u>x</u>	<u>y</u>	<u>z</u>	<u>B</u>
Mo(1)	0.5910(1)	0.5836(1)	0.5850(1)	3.28(2)
Mo(2)	0.6427(1)	0.4152(1)	0.4949(1)	3.28(2)
Mo(3)	0.4391(1)	0.4250(1)	0.5998(1)	3.20(2)
Cl(1)	0.5090(3)	0.7323(3)	0.4897(2)	4.22(7)
Cl(2)	0.6066(3)	0.4114(3)	0.3199(2)	4.05(7)
Cl(3)	0.2214(3)	0.4295(3)	0.5193(2)	4.06(7)
Cl(4)	0.6620(3)	0.4263(3)	0.6696(2)	3.90(6)
N(1)	0.219(1)	0.124(1)	0.564(1)	5.7(3)
C(2)	0.274(2)	0.030(1)	0.564(1)	4.4(3)
C(3)	0.248(2)	-0.040(2)	0.491(1)	6.8(5)
C(4)	0.158(2)	-0.010(2)	0.417(2)	7.8(5)
C(5)	0.105(2)	0.083(2)	0.421(1)	7.0(5)
C(6)	0.132(2)	0.152(2)	0.494(1)	6.4(4)
N(1')	0.390(1)	0.86(1)	0.702(1)	5.1(3)
C(2')	0.361(1)	0.004(1)	0.645(1)	4.1(3)
C(3')	0.408(2)	-0.092(2)	0.670(1)	5.3(4)
C(4')	0.487(2)	-0.105(2)	0.750(1)	6.7(4)
C(5')	0.513(2)	-0.018(2)	0.809(1)	5.6(1)
C(6')	0.467(2)	0.077(1)	0.784(1)	4.7(3)

Table 21: Final Values of F_o and F_c for Structure Cl(B)

Table with multiple columns (M, L, OBS, CALC) and rows of numerical data, organized into sections labeled with 'K' values (e.g., K=0, K=1, K=2, etc.). Each section contains a grid of values corresponding to different parameters and observations.

Table 22 : Intramolecular Distances (\AA) in $((\text{Mo}_6\text{Cl}_8)_2\text{X}_6)^{2-}$

<u>Atoms</u>	<u>I</u>	<u>Cl(A)</u>	<u>Cl(B)</u>
Mo(1)-X(1)	2.759(8)	2.416(11)	2.414(4)
Mo(2)-X(2)	2.737(7)	2.412(11)	2.422(4)
Mo(3)-X(3)	2.716(8)	2.450(11)	2.430(4)
Mo(1)-Mo(3 [*])	2.592(7)	2.598(6)	2.614(2)
Mo(1)-Mo(2 [*])	2.597(7)	2.603(5)	2.610(3)
Mo(1)-Mo(3)	2.606(8)	2.607(6)	2.608(2)
Mo(1)-Mo(2)	2.619(11)	2.600(5)	2.605(2)
Mo(2)-Mo(3 [*])	2.589(8)	2.595(5)	2.601(2)
Mo(2)-Mo(3)	2.595(7)	2.609(6)	2.607(2)
Mo(1)-Cl(1)	2.462(14)	2.480(11)	2.491(4)
Mo(1)-Cl(4)	2.494(14)	2.492(11)	2.472(4)
Mo(1)-Cl(2 [*])	2.501(14)	2.425(14)	2.472(4)
Mo(1)-Cl(3 [*])	2.540(13)	2.459(13)	2.472(4)
Mo(2)-Cl(1 [*])	2.460(15)	2.476(12)	2.494(4)
Mo(2)-Cl(4)	2.490(14)	2.463(11)	2.463(4)
Mo(2)-Cl(2)	2.505(13)	2.462(12)	2.477(4)
Mo(2)-Cl(3 [*])	2.517(14)	2.459(12)	2.476(4)
Mo(3)-Cl(4)	2.454(13)	2.470(12)	2.459(4)
Mo(3)-Cl(1 [*])	2.472(16)	2.471(12)	2.479(4)
Mo(3)-Cl(2 [*])	2.515(16)	2.453(13)	2.472(4)
Mo(3)-Cl(3)	2.543(12)	2.479(11)	2.471(4)
Cl(1)...Cl(2 [*])	3.51(2)	3.47(2)	3.514(6)
...Cl(3 [*])	3.57(2)	3.51(2)	3.491(5)
...Cl(4 [*])	3.47(2)	3.46(1)	3.481(6)
Cl(2)...Cl(4 [*])	3.50(2)	3.47(2)	3.489(5)
...Cl(3 [*])	3.57(2)	3.52(2)	3.503(5)
Cl(3)...Cl(4 [*])	3.55(2)	3.48(2)	3.505(6)

Table 23 : Weighted Mean Distances (\AA) and Angles (degrees)
of $(\text{Mo}_6\text{Cl}_8\text{X}_6)^{2-}$ for Idealized Oh Symmetry

(a) Distances

<u>Atoms</u>	<u>I</u>	<u>Cl(A)</u>	<u>Cl(B)</u>	<u>Mo₆Cl₁₂</u> ^a
Mo-Mo	2.598(3)	2.602(2)	2.607(1)	2.61 ± 1
Mo-X	2.737(4)	2.426(6)	2.422(2)	2.38 ± 3
Mo-Cl	2.498(4)	2.463(4)	2.475(1)	2.47 ± 3
Cl...Cl	3.53(1)	3.49(1)	3.497(4)	3.42 - 3.52

(b) Angles

Mo-Cl-Mo	62.8(2)	63.5(2)	63.6(1)	63.9
X-Mo-Cl	91.7(3)	92.3(2)	92.2(1)	
Mo-Mo-Cl	58.6(2)	58.2(2)	58.2(1)	
Cl-Mo-Cl	89.9(2)	89.9(2)	89.9(1)	

^a Schäfer et al. (13)

**Table 24 : Distances to Mean Planes^a through Faces of
Idealized Cl₈ Cube**

Atoms in Plane	Target Atom	I		Cl(A)		Cl(B)	
		P ^b	P/ σ (P) ^c	P	P/ σ (P)	P	P/ σ (P)
Cl(4), Cl(1*) Cl(3), Cl(2*)	Mo(3)	0.063	15.3	0.102	28.9	0.086	79.8
Cl(2), Cl(3*) Cl(4), Cl(1*)	Mo(2)	0.071	16.3	0.096	27.2	0.097	84.4
Cl(3*), Cl(4) Cl(2*), Cl(1)	Mo(1)	0.088	20.6	0.096	26.5	0.102	91.2

^a Mean planes calculated using program Mean Plane (Appendix B)

^b P, Distance of Target atom from the mean plane, in Å.

^c σ (P) = estimated standard deviation in P.

Table 25: Bond and Weighted Mean Lengths in the Bipyridylum Cations, $(C_{10}H_9N_2)^+$, Å

<u>Atoms</u>	<u>I</u>	<u>Cl(A)</u>	<u>Cl(B)</u>	
N(1)-C(2)	1.32(10)	1.33(4)	1.35(2)	
C(2)-C(3)	1.39(10)	1.56(5)	1.39(2)	
C(3)-C(4)	1.34(9)	1.28(5)	1.43(2)	
C(4)-C(5)	1.60(11)	1.34(7)	1.33(3)	
C(5)-C(6)	1.35(12)	1.46(6)	1.39(3)	
C(6)-N(1)	1.21(10)	1.50(5)	1.36(2)	
N(1')-C(2')	1.37(7)	1.33(5)	1.36(3)	
C(2')-C(3')	1.45(8)	1.34(5)	1.39(2)	
C(3')-C(4')	1.53(9)	1.38(5)	1.36(2)	
C(4')-C(5')	1.35(9)	1.36(5)	1.43(3)	
C(5')-C(6')	1.45(9)	1.41(5)	1.37(3)	
C(6')-N(1')	1.35(8)	1.40(5)	1.38(3)	
<u>Weighted Means</u>	<u>I</u>	<u>Cl(A)</u>	<u>Cl(B)</u>	<u>Bipyridyl^a</u>
C - C (within C_5H_4N rings)	1.43(3)	1.39(2)	1.38(1)	1.39
C - N	1.33(4)	1.38(2)	1.36(1)	1.36
C(2) - C(2') ^b	1.33(10)	1.49(5)	1.47(2)	1.50

^a Unweighted averages (Merritt and Schroeder (91)).

^b Only one independent measurement.

**Table 26 : Bond Angles in the Bipyridylum Cations,
(C₁₀H₉N₂)⁺, (in degrees)**

<u>Defining Atoms</u>	<u>I</u>	<u>Cl(A)</u>	<u>Cl(B)</u>
C(2)-N(1)-C(6)	117(8)	113(4)	120(1)
C(3)-C(2)-N(1)	122(9)	123(4)	123(1)
C(4)-C(3)-C(2)	120(7)	117(4)	117(1)
C(5)-C(4)-C(3)	115(7)	125(5)	119(2)
C(6)-C(5)-C(4)	110(8)	120(5)	123(2)
N(1)-C(6)-C(5)	128(10)	120(4)	118(2)
C(2')-N(1')-C(6')	125(6)	122(4)	123(2)
C(3')-C(2')-N(1')	119(6)	120(4)	120(1)
C(4')-C(3')-C(2')	117(6)	120(4)	120(1)
C(5')-C(4')-C(3')	120(7)	121(4)	119(2)
C(6')-C(5')-C(4')	120(7)	118(4)	121(2)
N(1')-C(6')-C(5')	120(6)	117(4)	118(2)
N(1)-C(2)-C(2')	109(8)	112(4)	116(1)
C(3)-C(2)-C(2')	128(9)	124(4)	121(1)
N(1')-C(2')-C(2)	120(6)	116(4)	113(1)
C(3')-C(2')-C(2)	121(7)	124(4)	127(1)

Table 27 : Analysis of Planarity in the Bipyridylum Cations, $(C_{10}H_9N_2)^+$, in Cl(B).

Equation of the plane referred to orthogonal axes^c is
 $m_1X + m_2Y + m_3Z = d$

Weighted Mean plane through

<u>(a)</u> All atoms in unprimed C_5H_4N ring		<u>(b)</u> All atoms in primed C_5H_4N ring	
m_1	0.7729	m_1	0.8359
m_2	0.3687	m_2	0.1772
m_3	-0.5164	m_3	-0.5195
$d, \text{\AA}$	-1.9906	$d, \text{\AA}$	1.8839

<u>Atom</u>	<u>Deviation, P^d</u>	<u>P/$\sigma(P)$^e</u>	<u>Atom</u>	<u>Deviation P</u>	<u>P/$\sigma(P)$^e</u>
N(1)	0.008 \AA	0.6	N(1)	-0.002 \AA	0.2
C(2)	-0.007	0.5	C(2')	0.005	0.4
C(3)	0.002	0.1	C(3')	-0.014	0.8
C(4)	0.007	0.3	C(4')	0.021	1.1
C(5)	-0.002	0.1	C(5')	-0.014	0.8
C(6)	-0.008	0.4	C(6')	0.006	0.4

χ^2 - squared = 0.820, 2.923, respectively

Dihedral angle between planes (a) and (b) = 11.6 degrees.

^c The orthogonal system of axes has X(\AA) along the a-axis, Y(\AA) in the (a, b) plane and Z(\AA) along the c* axis.

^d From the Mean plane.

^e $\sigma(P)$ is the estimated standard deviation in P, in \AA .

Table 28: Analysis of Planarity in the Bipyridylium Cations,**Weighted mean plane through**

(a) All atoms in unprimed C ₅ H ₄ N ring	(b) All atoms in primed C ₅ H ₄ N ring
m ₁ 0.8712	m ₁ 0.7633
m ₂ -0.3439	m ₂ -0.3467
m ₃ -0.3504	m ₃ -0.5451
d -7.3370	d -9.3608

<u>Atom</u>	<u>Deviation, P</u>	<u>P/σ(P)</u> ^c	<u>Atom</u>	<u>Deviation, P</u>	<u>P/σ(P)</u>
N(1)	0.070 Å	1.8	N(1')	-0.028 Å	0.7
C(2)	-0.087	2.0	C(2')	-0.025	0.6
C(3)	0.033	0.7	C(3')	0.039	0.9
C(4)	0.040	0.8	C(4')	0.012	0.3
C(5)	-0.059	0.9	C(5')	-0.063	1.4
C(6)	-0.039	0.7	C(6')	0.090	1.9

χ^2 -squared = 9.477, 7.489 respectively

Dihedral angle between planes (a) and (b) = 12.8
degrees.

^c For symbols used, see Table 27

Table 29 : Analysis of Planarity in the Bipyridylium
Cations, $(C_{10}H_9N_2)^+$, in I

Weighted mean plane through

(a) All atoms in unprimed C_5H_4N ring	(b) All atoms in primed C_5H_4N ring
m_1^c 0.8708	m_1 0.7245
m_2 -0.3673	m_2 -0.4041
m_3 -0.3269	m_3 -0.5584
d -7.5503	m_4 -10.2374

<u>Atom</u>	<u>Deviation, P^c</u>	<u>P/σ(P)^c</u>	<u>Atom</u>	<u>Deviation, P</u>	<u>P/σ(P)</u>
N(1)	0.088	1.4	N(1')	-0.008	0.1
C(2)	0.007	0.1	C(2')	-0.001	0.02
C(3)	-0.028	0.3	C(3')	-0.004	0.1
C(4)	-0.025	0.3	C(4')	0.020	0.3
C(5)	0.076	0.7	C(5')	-0.029	0.3
C(6)	-0.116	1.0	C(6')	0.022	0.3

χ^2 - squared = 3.745, 0.312 respectively.

Dihedral angle between planes (a) and (b) = 15.9 degrees

^c For symbols, see Table 27

Table 30: Shortest Inter-ionic Contacts (\AA) around one
 $(\text{Mo}_6\text{Cl}_8)\text{X}_6^{2-}$ Anion in I and Cl(A).

<u>Atom</u>	<u>I</u>	<u>Cl(A)</u>	<u>Ring Number^a</u>
X(1) ... C(6')	3.68(7)	3.51(5)	1
X(3) ... N(1)	3.52(6)	3.33(4)	2
X(3) ... C(2)	3.59(10)	3.37(5)	2
X(3) ... N(1')	3.40(5)	3.21(4)	3
X(3) ... C(6')	3.67(7)	3.58(5)	3
Cl(1) ... C(5)	3.68(11)	3.47(5)	4
Cl(1) ... C(4')	3.64(8)	3.35(4)	1
Cl(1) ... C(5')	3.77(8)	3.42(5)	1
Cl(2) ... C(4')	3.53(7)	3.54(4)	5
Cl(2) ... C(5')	3.52(8)	3.65(4)	5
Cl(4) ... N(1)	3.61(9)	3.42(5)	3
Cl(4) ... C(3)	3.47(7)	3.25(5)	6
Cl(4) ... C(4)	3.68(8)	3.54(5)	6
Cl(4) ... C(6)	3.46(10)	3.58(5)	1

^a Independent bipyridyl rings are numbered sequentially; for each of these contacts, there is a centrosymmetrically related similar contact.

Table 31 : Shortest Inter-ionic Contacts (\AA) Around one
 $(\text{Mo}_6\text{Cl}_8)\text{Cl}_6^{2-}$ Anion of Cl(B)

<u>Atoms</u>	<u>Distance</u>	<u>Independent Ring^a</u>
X(1) ... C(4')	3.62 (2)	1
X(1) ... C(6')	3.63 (2)	2
X(2) ... C(3)	3.59 (2)	3
X(2) ... C(6)	3.68 (2)	4
X(2) ... C(6')	3.58 (2)	5
X(3) ... N(1')	3.19 (2)	1
X(3) ... C(3')	3.30 (1)	5
X(3) ... C(4')	3.69 (2)	5
Cl(3) ... C(6')	3.50 (2)	1
Cl(1) ... N(1)	3.47 (1)	3
Cl(1) ... C(3')	3.61 (2)	1
Cl(2) ... N(1')	3.40 (2)	5
Cl(3) ... C(5')	3.54 (2)	6
Cl(4) ... C(5')	3.42 (2)	7

^a The numbering of the bipyridylium rings is to indicate the number of independent rings making close contacts; each of these contacts has an exactly similar contact related by the centre of symmetry at the centre of the anion.

REFERENCES

1. C.W. Blomstrand; J. prakt. Chem., 71, 449 (1857);
77, 96 (1859); 82, 423 (1861).
2. K. Lindner, E.H. Heller and H. Helwig; Z. anorg. Chem.,
130, 209 (1923).
3. K. Lindner; Ber. dt. chem. Ges., 55, 1458 (1922).
4. K. Lindner and A. Köhler; Z. anorg. Chem., 140, 357 (1924).
5. K. Lindner; Z. anorg. Chem., 162, 203 (1927).
6. K. Lindner and H. Helwig; Z. anorg. Chem., 142, 180
(1925).
7. J. Atterburg; Bull. Soc. Chim., 18, 21 (1872).
8. A. Rosenheim and F. Kohn; Z. anorg. Chem., 66, 1 (1910).
9. W. Muthmann and W. Nagel, Ber. dt. chem. Ges., 31,
2009 (1898).
10. D.E. Couch and A. Brenner; J. Res. natn. Bur. Stand.,
63A, 185 (1959).
11. W. Hellriegel; German Patent 703, 895 (1941).
12. S. Senderoff and A. Brenner, J. electrochem. Soc., 101,
28 (1954).
13. Von H. Schäfer, H.-G.v. Schering, J. Tillack, F. Kuhnen,
H. Wöhrle and H. Baumann; Z. anorg. allgem. Chem.,
353, 281 (1967).
14. C. Brosset; Arkiv. Kemi. Miner. Geol., 20A, No. 7 (1945).
15. C. Brosset; Arkiv. Kemi. Miner. Geol., 22A, No. 11 (1946).
16. L. Pauling; "Nature of the Chemical Bond", Cornell
Univ. Press, 3rd Ed. (1960).
17. Interatomic distances, Chemical Soc. publication No.11
(1958).
18. P.A. Vaughan; Proc. natn. Acad. Sci. U.S.A., 36, 461
(1950).
19. C. Brosset; Arkiv. Kemi, 1, 353 (1950).

20. P.A. Vaughan, J.H. Sturdivant and L. Pauling; *J. Am. chem. Soc.*, 72, 5477 (1950).
21. J.C. Sheldon; *J. chem. Soc.*, 3106 (1960).
22. J.C. Sheldon; *Nature, Lond.* 184, 1210 (1959).
23. J.C. Sheldon; *J. chem. Soc.*, 1007 (1960).
24. J.C. Sheldon; *J. chem. Soc.*, 410 (1962).
25. J.C. Sheldon; *J. chem. Soc.*, 4183 (1963).
26. J.C. Sheldon; *J. chem. Soc.*, 750 (1961).
27. J.C. Sheldon; *Chem. Ind.*, 323 (1961).
28. J.C. Sheldon; *J. chem. Soc.*, 1287 (1964).
29. D.A. Edwards; *J. less-common Metals*, 7, 159 (1964).
30. F.A. Cotton and N.F. Curtis; *Inorg. Chem.*, 4, 241 (1965).
31. W.M. Carmichael and D.A. Edwards; *J. inorg. nucl. Chem.*, 1535 (1967).
32. J. Lewis, D.J. Machin, R.S. Nyholm, P. Pauling and P.W. Smith; *Chem. Ind.*, 259 (1960).
33. J.E. Fergusson, B.H. Robinson, and C.J. Wilkins; *J. chem. Soc (A)*, 486 (1967).
34. R.J.H. Clark, D.L. Kepert, R.S. Nyholm and G.A. Rodley; *Spectrochim. Acta*, 22, 1697 (1966).
35. F.A. Cotton, R.M. Wing and R.A. Zimmerman; *Inorg. Chem.*, 6, 11 (1967).
36. C. Durand, R. Schaal, and P. Souchay; *C.r.hebd. Seanc. Acad. Sci., Paris*, 248, 979 (1959).
37. D.L. Kepert and K. Vrieze; "Halides Containing Multi-centred Metal-Metal Bonds" in "Halogen Chemistry" Vol. III, Edited by V. Gutmann, Academic Press, London & New York (1967).
38. Von. H. Schäfer and H.-G.v. Schnering; *Angew. Chem.*, 76, 833 (1964).
39. B.T. Tjabbes; *Proc. K. med. Acad. Amst.*, 35, 696 (1932).

40. W. Klemm and H. Steinberg; Z. anorg. Chem., 227, 193 (1936).
 41. F. Klanberg and H.W. Kohlschütter; Z. Naturf., 15b, 616 (1960).
 42. P.F. Snowden; M.Sc. Thesis, University of Canterbury (1967).
 43. P. Nannelli and B.F. Block; Inorg. Chem., 7, 2423 (1968).
 44. D.P. Craig and E.A. Magnusson; Disc. Farad. Soc., 26, 116 (1958).
 45. R.J. Gillespie; Can. J. Chem., 39, 2336 (1961).
 46. J.E. Fergusson; "Halide Chemistry of Chromium, Molybdenum and Tungsten" in "Halogen Chemistry", Vol.III (see Reference 37).
 47. D.L. Kepert; J. chem. Soc., 4736 (1965).
 48. L.D. Crossman, D.P. Olsen and G.H. Duffey; J. Chem. Phys., 38, 73 (1963).
 49. G.H. Duffey; J. chem. Phys., 19, 963 (1951).
 50. F.A. Cotton and T.E. Haas; Inorg. Chem., 3, 10 (1964).
 51. J.F.A. Kettle; Theoret. chim. Acta, 3, 211 (1965).
 52. J.F.A. Kettle; Nature, Lond., 207, 1384 (1965).
 53. R.D. Burbank; Inorg. Chem., 5, 1491 (1966).
 54. W.F. Libby; J. chem. Phys., 46, 399 (1967).
 55. B.H. Robinson, Ph.D. Thesis, University of Canterbury (1964).
 56. A.M. Brodie; B.Sc. (Hons) Report, University of Canterbury (1965).
 57. T. Zoltai; "An Inexpensive Automation of the Buerger Single Crystal Diffractometer", Dept. of Geology and Geophysics, University of Minnesota (1963).
 58. I.U.P.A.C. Report, J. Am. chem. Soc., 82, 1202 (1960).
 59. G.J. Gainsford; B.Sc. (Hons) Report, University of Canterbury (1965).
-

60. M. Elder; Ph.D. Thesis, University of Canterbury (1967).
61. A.A. Schilt and R.C. Taylor; J. inorg. nucl. Chem., 9, 211 (1959).
62. H. Jagodzinski; "Diffuse Disorder Scattering by Crystals" in "Advanced Methods of Crystallography", Ed. G.N. Ramachandran, Academic Press, London (1964).
63. K. Nakamoto; "Infra-red Spectra of Inorganic and Coordination Compounds", Wiley, New York (1963).
64. D.L. Kepert; University of Western Australia, Nedlands, Western Australia, private communication.
65. G.J. Gainsford; Ph.D. Interim Report, University of Canterbury (1967).
66. R.H. Lee, E. Griswold and J. Kleinberg; Inorg. Chem., 3, 1278 (1964).
67. G.W. Parshall; J. Am. chem. Soc., 90: 6, 1669 (1969).
68. L. Vaska; Chemy Ind., 1402 (1961).
69. J. Chatt and B.L. Shaw; J. Am. chem. Soc., 82, 1263 (1960).
70. L.N. Swink and C.B. Carpenter; Acta Cryst., 22, 602 (1967).
71. H. Jagodzinski; "On Disorder Phenomena in Crystals" in "Crystallography and Crystal Perfection", Ed. by G.N. Ramachandran, Academic Press, London (1963).
72. International Tables for X-ray Crystallography, Kynoch Press, Birmingham, England (1962).
 - (a) Volume I, Section 4.3
 - (b) Volume III, pp. 17, Section 1.3.2.1
 - (c) Volume III, Section 3.2.1.1, Equation (6); Table 3.2.2B; pp.157
 - (d) Volume III, Table 3.3.1A, pp.204; Table 3.3.1B, pp.210
 - (e) Volume II, Section 6.1.2, p. 318.
73. K.A. Jensen and P.H. Nielsen; Acta. Chem. Scand., 17, 1875 (1963).

74. F.A. Cotton, R.D. Barnes and E. Bannister; *J. chem. Soc.*, 2199 (1960).
 75. "Computing Methods in Crystallography", Ed. by J.S. Rollett, Pergamon Press, London (1965), pp.113.
 76. C.J. Wilkins and H.M. Haendler; *J. chem. Soc.*, 3174 (1965).
 77. S.M. Hunter, V.M. Langford, G.A. Rodley and C.J. Wilkins; *J. chem. Soc. (A)*, 305 (1968).
 78. G.B. Deacon and J.H.S. Green; *Chem. Ind.*, 1031 (1965).
 79. S. Glasstone; "Textbook of Physical Chemistry", 2nd Edition, Nostrand & Co., New York (1947), pp.693.
 80. S. Kida, J.V. Quagliano, S.Y. Tyree and J.A. Walmsley; *Spectr. Acta*, 19, 189 (1966).
 81. N.N. Greenwood and K. Wade; *J. chem. Soc.*, 1130 (1960).
 82. T.C. Furnas; "Single Crystal Orienter Instruction Manual", General Electric Co., Milwaukee, Wisconsin, U.S.A., (1966).
 83. P.W.R. Corfield, R.J. Doedens and J.A. Ibers; *Inorg. Chem.*, 6, 197 (1967).
 84. W.C. Hamilton and J.A. Ibers; *Acta Cryst.*, 17, 781 (1964).
 85. D.T. Cromer; *Acta Cryst.*, 18, 17 (1965).
 86. A.J.C. Wilson; *Nature, Lond.*, 150, 152 (1942).
 87. W.C. Hamilton; *Acta Cryst.*, 18, 502 (1965).
 88. R. Eisenberg and J.A. Ibers; *Inorg. Chem.*, 4, 773 (1965).
 89. S.J. La Placa and J.A. Ibers; *Acta Cryst.*, 18, 511 (1965).
 90. W.C. Hamilton; "Statistics in Physical Science", Ronald Press Co., New York (1964), pp.43.
 91. L.L. Merritt, Jr. and E.D. Schroeder; *Acta Cryst.*, 2, 801 (1956).
 92. G.A. Barclay, B.F. Hoskins and C.H.L. Kennard; *J.chem. Soc.*, 5691 (1963).
 93. G.C. Pimentel, A.L. McClellan; "The Hydrogen Bond", Freeman, San Francisco (1960).
-

94. A.I. Vogel; "Quantitative Inorganic Analysis", Longmans, 3rd Edition, London (1961).
95. A.B. Thomas and E.G. Rochow; J. Am. chem. Soc., 79, 1843 (1957).
96. "Handbook of Chemistry and Physics", The Chemical Rubber Co., Cleveland, Ohio (1962), 47th Edition.
97. T.M. Dunn; "The Visible and Ultra-Violet Spectra of Complex Compounds" in "Modern Coordination Chemistry", Ed. by J. Lewis and R.G. Wilkins, Interscience, London (1960).
98. G. Kortüm; Trans. Farad. Soc., 58, 1624 (1962).
99. T.R. Griffiths, K.A.K. Lott and M.C.R. Symons; Anal. Chem., 31, 1338 (1959).
100. H. Lipson and W. Cochran; "The Determination of Crystal Structures", 3rd Edition, Bell, London (1966).
101. L.V. Azaroff and M.J. Buerger; "The Powder Method in X-ray Crystallography", McGraw-Hill, New York (1958).
102. C.W. Bunn; "Chemical Crystallography", Clarendon Press, Oxford (1961).
103. G.J. Gainsford; "Canterbury University Supper Equi-inclination Diffractometer Manual (CUSED)", University of Canterbury (1968).
104. M.J. Buerger; "Crystal Structure Analysis", Wiley and Sons, New York (1960), pp.118.
105. M.J. Buerger; "X-ray Crystallography", Wiley and Sons, New York (1942), pp.252.
106. G.J. Gainsford; Appendix to program SUPOUT, University of Canterbury Program Write-ups (1968).
107. L.E. Alexander and G.S. Smith; Acta Cryst., 17, 1195 (1964).
108. "Operation Manual for the Sydney University Supper Diffractometer", Sydney University (1967).